Development of parabolic-elliptic formulations for bending edge waves on thin elastic plates

Saad Althobaiti

Ph.D

Submitted in partial fulfilment of the requirements of the degree of

Doctor of Philosophy

School of Computing and Mathematics, Keele University.

June 2019

Declaration

I certify that this thesis submitted for the degree of Doctor of Philosophy is the result of my own research, except where otherwise acknowledged, and that this thesis (or any part of the same) has not been submitted for a higher degree to any other university or institution.

Signed: (Saad Althobaiti) . . .

Date: . . . .

Contents

List of Figures

Acknowledgements

I would like to express my deepest gratitude to my supervisor Dr Danila Prikazchikov, his wisdom and knowledge has been invaluable to me. I am very thankful for the time that he has taken to help me throughout this process, I am truly grateful. Without his continual support and guidance, this thesis would not have been possible.

I would also like to thank Professor Julius Kaplunov, for his encouragement has been a great source of strength to me and made these four years far more bearable than it would have been without him. There have been many times that I have struggled and his support has always been constant and unwavering.

Finally, I am forever indebted to my wife, for managing the rest of my life for me whilst I was engrossed in applied mathematics. I cannot imagine that this has been an easy process, so please receive my heartfelt gratitude.

Abstract

The project is concerned with the analysis of bending edge waves propagating in thin elastic orthotropic plates, and aims at the derivation of explicit formulations for bending edge waves, generalising recent results for isotropic plates. The derived parabolic-elliptic formulations provide significant simplification in analysis and allow efficient approximate solutions to a number of dynamic problems, where the contribution of the edge wave is dominant. The effect of the Winkler-Fuss foundation, supporting the plate is also studied.

First, the eigensolutions in terms of a single plane harmonic function are obtained, serving as a basis for further derivations of asymptotic models oriented to extraction of the contribution of the studied localized waves to the overall dynamic response. The proposed models are obtained through a multi-scale perturbation scheme, also employing properties of plane harmonic functions. The approximate formulations for the bending edge wave field include elliptic partial differential equations, describing the decay away

from the edge, along with the parabolic equations on the edge associated with wave propagation. Model examples for excitation of the studied waves are investigated, in particular, including impulse edge loading, internal sources and moving loads. Finally, the effect of inhomogeneity arising from a Winkler-Fuss foundation with periodic stiffness is addressed, revealing novel resonant phenomena.

Introduction

Dynamic phenomena in thin walled elastic solids, in particular, plates and shells, have attracted significant interest from researchers within the framework of applied mathematics, as well as civil and structural engineering. Numerous application areas of thin walled bodies include, for example, architectural structures, bridges, hydraulic structures, pavements, containers, air and space-crafts, marine vessels and structures, machine parts and solar panels.

Mathematical modelling of thin elastic plates typically relies on reduction of the original three-dimensional problem in elasticity to lower dimensional structural theories, exemplified by the classical contribution of Kirchhoff (1851), followed by a considerable number of refining attempts, see e.g. Timoshenko (1938), Mindlin (1955) and Reissner (1964), followed by numerous studies, e.g. Kienzler (2002). It is worth mentioning that many of the refined theories are not asymptotically justified, see the reasoning in Goldenveiser et al. (1993), and also Kaplunov et al. (1998). We also mention a recent review by

Elishakoff et al. (2015), revisiting the Timoshenko's shear deformation theory.

Asymptotic analysis of dispersive behaviour in thin-walled elastic structures may be classified into four distinct scenarios, including long-wave low-frequency, long-wave high-frequency, short-wave low-frequency, and short-wave high-frequency approximations, for more details see Kaplunov et al. (1998). Generally, for short-wave theories a typical wave length is of order of the thickness, whereas the long-wave approximation is associated with the wave length being much greater than the thickness. A number of contributions, extending this approach to incorporate the effects of anisotropy, pre-stress and incompressibility constraint, include Kaplunov et al. (2000), Kaplunov et al. (2002), Kaplunov and Nolde (2002), Pichugin and Rogerson (2002), Nolde et al. (2004) and Rogerson and Prikazchikova (2009). Typically, asymptotic theories in the long-wave low-frequency limit generalise the corresponding static formulations, see e.g. Goldenveiser et al. (1993). High-frequency theories, characterised by sinusoidal variation across the thickness, find applications, in particular, in wave scattering, see Kaplunov and Markushevich (1993). Long-wave high-frequency models have been studied in Kaplunov et al. (2000), Pichugin and Rogerson (2001), Kaplunov et al. (2002) and L. Aghalovyan and M. Aghalovyan (2016), also being important for structures with clamped faces see e.g. Kaplunov (1995) and Kaplunov and Nolde (2002), layered structure studied by Lutianov and Rogerson (2010), Ryazantseva and Antonov (2012), Craster et al. (2014), and Kaplunov et al.

(2017). Localisation effects for long-wave high-frequency modes were investigated by Kaplunov et al. (2000), Gridin et al. (2005) and Kaplunov et al. (2005). The approximation in the short wave high-frequency limit is useful for analysis of non-stationary wave phenomena see Kossovich (1986), e.g Kaplunov et al. (2002) and Rogerson et al. (2004). Throughout this thesis we will be operating within the long-wave low-frequency region.

Most of the previously mentioned studies are related to thin plates, infinite in the in-plane directions. Studies of dynamics in the near-edge vicinity of a semi-infinite thin elastic plate are equally important, motivated, in particular, by applications in non-destructive testing, e.g for aircraft wings, submarine hulls and floating platforms. We mention here a fundamental contribution of Friedrichs and Dressler (1961), in which the approximate boundary conditions at the free edge of the Kirchhoff plate were derived. The near-edge dynamic phenomena include edge vibrations and edge waves. As for edge vibrations, one of the main focuses of studies has been on the edge resonant effects, starting from works of Shaw (1956), Torvik (1967), Roitberg and Weidl (1998), and including more recent results of Kaplunov et al. (2004), Pagneux (2011), and Gulgazaryan and Srapionyan (2012), also a review by Lawrie and Kaplunov (2012).

It is known that the edge waves on elastic plates are related to surface waves, discovered by Lord Rayleigh (1885). Edge waves occurring in elastic structures, can be divided into two main subcategories, namely, into flexural and extensional edge waves. As known since early 20^{th} century, a thin layer in generalised plane stress state is described approximately by equations, that are formally equivalent to those of plane strain elasticity, see e.g. Filon (1903). Therefore, a semi-infinite plate in plane stress state possesses an analogue of surface waves, which are usually referred to as extensional edge waves, seemingly first exposed in Oliver et al. (1954), see also Lawrie and Kaplunov (2012). The effect of pre-stress on the propagation of extensional edge waves have been recently investigated by Pichugin and Rogerson (2012) for incompressible elastic plates, focusing on the long-wave low-frequency limiting behaviour of extensional edge waves propagating along the free edge of such a layer, and revealing a possibility of a non-unique edge wave solution. From a physical point of view, edge waves are similar to Rayleigh waves, because they are both localized near the edge/surface. However, there is a considerable difference between them. Indeed, the bending edge waves are dispersive, whereas extensional edge waves and Rayleigh waves have constant phase velocities.

The interesting history of the discovery of bending edge waves is reported by Norris et al. (2000). These waves were discovered by Konenkov (1960) within the framework of Kirchhoff plate theory. However, the knowledge of his findings was limited by the scarcity of Soviet literature available at that time, and this result was not widely known in western scientific circles. The wave was rediscovered independently by Sinha (1974) and Thurston and McKenna (1974). In recent years it has been found that some preliminary results related to the work of Konenkov were obtained by Ishlinskii (1954) who studied stability of elastic plates. A detailed review of the existing state of art on edge waves is presented in Lawrie and Kaplunov (2012).

Over recent years, intensive research has been conducted on flexural edge waves with much emphasis placed on layering, refined plate models and the effects of fluid loading etc., see e.g. Norris and Abrahams (2000) and Zakharov (2002, 2004). Zilbergleit and Suslova (1983) have investigated the Stoneley-type flexural interfacial wave propagating at the junction of two plates. Edge waves for the case of a circular disc were investigated by Destrade and Fu (2008). Flexural edge waves on an arbitrarily curved plate edge have been studied by Cherednichenko (2007). Edge waves may also arise in elastic shells, see Kaplunov et al. (2000), Kaplunov and Wilde (2001) and also Fu and Kaplunov (2012). We also mention contributions of Kaplunov et al. (2005), Zernov and Kaplunov (2008), Krushynska (2011) and Feng et al. (2017), considering edge waves within exact 3D formulation of elasticity. Other recent developments in the area of edge waves phenomena in metamaterials were reported by Pal et al (2017), Yanget al (2018) and Yu et al (2018). One more direction of development of the research field of flexural edge waves theory is associated with anisotropic plates, see Norris (1994), Thompson et al. (2002), Zakharov and Becker (2003), Fu (2003), also Fu and Brookes (2006), Lu et al. (2007), and Piliposian et al. (2010). The consideration of bending edge waves in orthotropic Kirchhoff plates was first performed by Norris (1994). More recently, Thompson et al. (2002) studied the speed of edge wave on a thin orthotropic plate in a more general case, for an arbitrary angle between the principle direction of anisotropy and the edge. In addition, a review of other relevant contributions may be found in, Norris et al. (2000).

Furthermore, the effect of an elastic foundation on bending edge waves has been considered recently by Kaplunov et al. (2014), Kaplunov et al. (2016) and Althobaiti et al. (2017). Extension of the analysis to more sophisticated foundation models have been considered by Kaplunov and Nobili (2015). Further progress is possible along with consideration of variable elastic characteristics similarly to Aghalovyan and Adamyan (1986).

In a recent work, Kaplunov and Prikazchikov (2013) have discussed both surface and edge waves within the framework of explicit asymptotic models oriented towards extraction of the contribution of the wave in question to the overall dynamics response. These models combine simplified formulations with enhanced physical understanding.

In the case of surface waves, the decay over the interior is described by elliptic equations, and the propagation along the surface is governed by a hyperbolic equation in terms of elastic potentials. The model was first proposed by Kaplunov and Kossovitch (2004) and then developed further in Kaplunov et al. (2006), Dai et al. (2010), Erbas et al.

(2013), and Ege et al. (2015). The results were also successfully implemented for moving load problems, see Kaplunov et al. (2010), Kaplunov et al. (2013) and also Erbas et al. (2017). The effects of anisotropy have been investigated in Prikazchikov (2013), Parker(2013), and Nobili and Prikazchikov (2018). The methodology have recently been summarized in Kaplunov and Prikazchikov (2017), with some further development for pre-stressed incompressible elastic material appearing in Khajiyeva et al. (2018).

In the case of bending edge waves the decay away from the edge is also governed by an elliptic equation for deflection of the plate, whereas the propagation along the edge is represented by a beam-type parabolic equation. For isotropic Kirchhoff plate, Kaplunov and Prikazchikov (2013) have constructed a bending edge wave of arbitrary profile, mirroring the result of Chadwick (1976) for surface and interfacial waves, and then used it as a basis of a perturbation scheme resulting in the parabolic-elliptic formulation for the bending edge wave. The parabolic-elliptic model, for an isotropic Kirchhoff plate resting on a Winkler-Fuss foundation, has been derived in Kaplunov et al. (2016).

This thesis aims at extending the results for bending edge wave on a Kirchhoff plate supported by a Winkler-Fuss foundation in order to account for the effects of anisotropy and inhomogeneity.

The layout of the thesis is as follows. The opening Chapter covers all preliminary knowledge and background for Kirchhoff plate theory, which is used throughout this thesis.

Chapter 2 describes the explicit model for bending edge wave in an isotropic plate, containing a parabolic equation at the edge and an elliptic equation over the interior. We consider a model example, illustrating the proposed approach, in particular, for an internal source embedded in a plate.

In Chapter 3, we extend the previous results of Kaplunov et al. (2014), to the bending edge wave on an orthotropic elastic plate supported by the Winkler-Fuss foundation, subject to free edge boundary conditions, assuming the principle direction of anisotropy coincides with the coordinate axis. The analysis of the dispersion relation reveals a cut-off frequency and a local minimum of the phase velocity. Also, the conventional eigensolution of the sinusoidal profile is extended to a more general form, with the deflection expressed in terms of a single plane harmonic function.

Chapter 4 contains derivation of an explicit formulation for the bending edge wave on a thin orthotropic plate resting on a Winkler-Fuss foundation. The procedure relies on a slow-time perturbation of the eigensolution obtained in the previous Chapter. The formulation includes an elliptic equation associated with decay away from the edge, and a parabolic beam-like equation governing edge wave propagation for both sub-cases of boundary conditions, forcing moment and shear forcing. The model is oriented at extracting the contribution of the bending edge wave to the overall dynamic response. Several model examples are considered, illustrating the proposed approach.

The final Chapter extends the results for homogeneous bending edge waves on a plate supported by a foundation, to the case of an inhomogeneous foundation, namely for the Winkler-Fuss foundation with a periodically varying stiffness. This allows a perturbation procedure. In addition to the expected Bragg-type resonances, some novel resonant frequencies are revealed. The analysis is carried out for both isotropic and orthotropic plates.

Chapter 1

Basic equations

This chapter contains the fundamental concepts, equations and techniques, used throughout this thesis. We start from a brief description of the Euler-Bernoulli beam. Then, we derive the equation of flexural motion in a thin Kirchhoff plate, within both orthotropic and isotropic materials, and discuss various boundary conditions imposed on the edge of a semi-infinite Kirchhoff plate. Then, the Fourier and Laplace integral transforms are introduced. Finally, we present the Winkler-Fuss model of elastic foundation and comment briefly on more advanced models.

1.1 Euler-Bernoulli beam

Consider the bending of a homogeneous elastic beam of small thickness $2h$, infinite in the longitudinal direction. An element of the beam under the action of a distributed force $P(x,t)$ is shown in Fig 1.1.

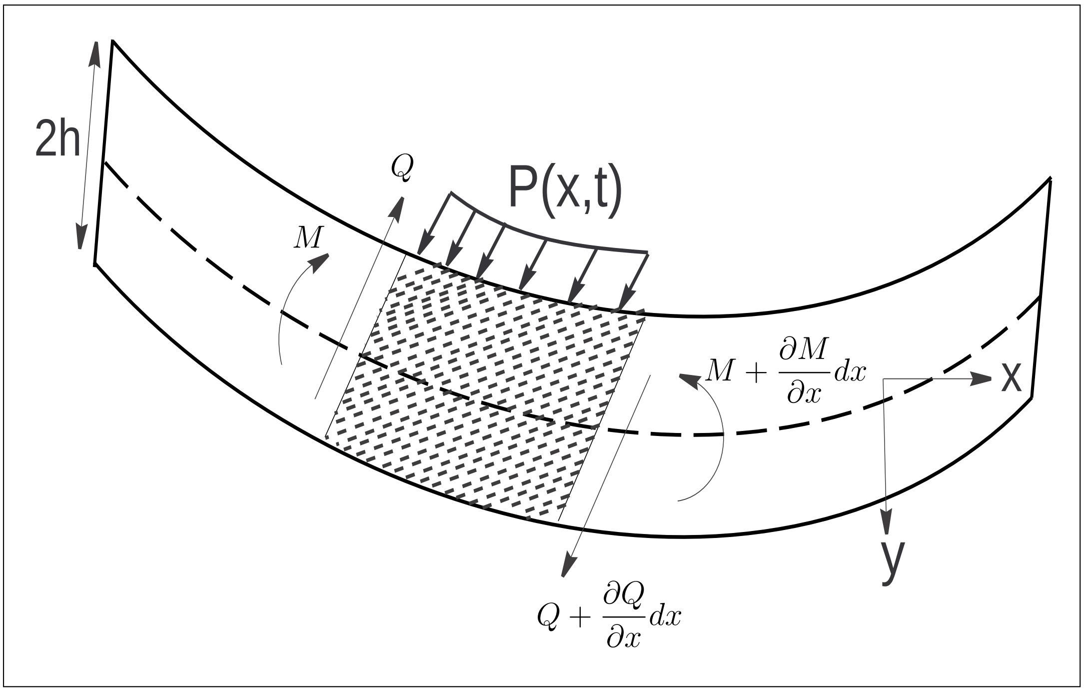

Figure 1.1: Element of a beam

In Fig.1.1 above, the bending moment and shear force are denoted by M and Q, respectively. We rely on the hypothesis of the Euler-Bernoulli beam, namely, that the plane cross-section that is initially perpendicular to the axis of the beam remains plane and perpendicular to the neutral axis during bending.

In other words, the vertical deflection is nearly constant through the thickness, see Graff (1991).

The relationship between bending moment and curvature is given by

$$\frac{\partial^2 W}{\partial x^2} = -M/EI, \tag{1.1}$$

where W is the coordinate of the neutral surface of the beam, E is the Young's modulus, and I is second moment of area of the beam's cross-section.

Projecting the second Newton's law on the vertical direction, we have

$$-Q + (Q + \frac{\partial Q}{\partial x}\ dx) + P\ dx = \rho A \frac{\partial^2 W}{\partial t^2}\ dx, \tag{1.2}$$

where A and ρ denote the cross-section area of the beam and volume mass density, respectively. The last equation reduces to

$$\frac{\partial Q}{\partial x} + P = \rho A \frac{\partial^2 W}{\partial t^2}, \tag{1.3}$$

Provided that the effects of rotational inertia of the elements are neglected, the moment equation can be written as

$$Q = \frac{\partial M_x}{\partial x}, \tag{1.4}$$

for more details see e.g. Graff (1991).

Therefore, in view of (1.3) and (1.4), equation (1.3) may be rearranged in terms of the deflection W of the beam as

$$-EI \frac{\partial^4 W}{\partial x^4} + P = \rho A \frac{\partial^2 W}{\partial t^2}. \tag{1.5}$$

By combining formula (1.3) and (1.5), we obtain the equation of transverse motion of the beam in the following form

$$EI\frac{\partial^4 W}{\partial x^4} + \rho A\frac{\partial^2 W}{\partial t^2} = 0, \tag{1.6}$$

in absence of loading $P(x,t) = 0$.

We note that this $1D$ equation of bending of an elastic beam may also be derived through asymptotic methods, applied to $3D$ problem of elasticity, see e.g. Goldenveizer et al. (1993), and also Aghalovyan (2015).

1.2 Kirchhoff plate

In this section, we expand our consideration in the previous section, focusing on bending of a thin elastic plate. The classical Kirchhoff plate theory (1850) is an extension of the Euler-Bernoulli beam theory.

Consider an element of a thin elastic plate of thickness $2h$, subjected to forces and moments, as shown in Fig.1.2.

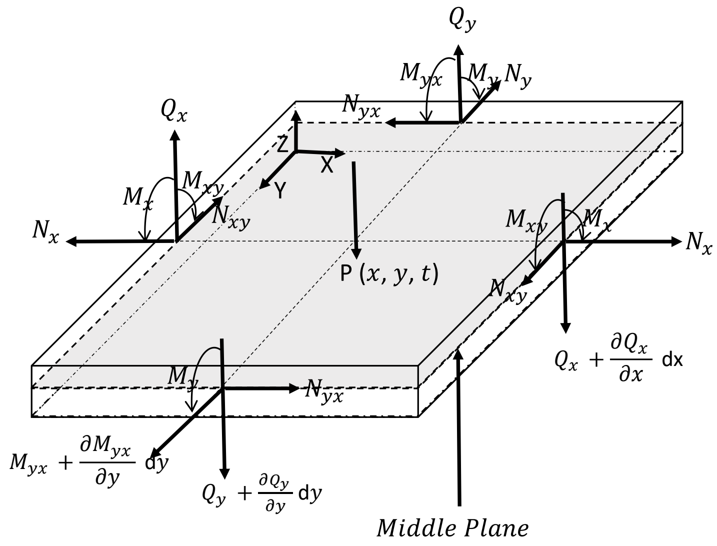

Figure 1.2: Effective resultants from Kirchhoff theory acting on the plate

Here M_x, M_y and M_{xy} are bending moments, Q_x and Q_y are shearing forces in the z direction, N_x, N_y, N_{xy}, and N_{yx} are shearing forces in the x and y directions, and $P = P(x, y, t)$ is an external force.

The following classical hypotheses of Kirchhoff, see Kaplunov et al. (1998), are adopted:

a. the straight lines normal to the mid plane remain straight after bending;

b. the straight lines normal to the mid plane remain normal after deformation;

c. the thickness of the plate does not change under dynamic conditions during the deformation.

The force equation of motion in z direction is written as

$$Q_x\, dy + \left(Q_x + \frac{\partial Q_x}{\partial x}\, dx\right) dy - Q_y dx + \left(Q_y + \frac{\partial Q_y}{\partial y} dy\right) dx + P dx dy = 2\rho h\, dx dy \frac{\partial^2 W}{\partial t^2}, \tag{1.7}$$

along with the two moment equations around x and y axis given by

$$\left(M_x + \frac{\partial M_x}{\partial x}\, dx\right) dy - M_x dy - M_{yx} dx - \left(M_{yx} + \frac{\partial M_{yx}}{\partial y} dy\right) dx - Q_x dy dx = 0, \tag{1.8}$$

and

$$\left(M_y + \frac{\partial M_y}{\partial y}\, dy\right) dx - M_y dx + M_{xy} dy - \left(M_{xy} + \frac{\partial M_{xy}}{\partial x} dx\right) dy - Q_y dx dy = 0, \tag{1.9}$$

see Graff (1991). Note that rotary-inertia effects have been neglected in (1.8) and (1.9). Expressing the forces Q_x and Q_y from (1.8) and (1.9), respectively, and substituting the results into (1.7), we obtain the following equation of vertical motion

$$\frac{\partial^2 M_x}{\partial x^2} + \frac{\partial^2 M_y}{\partial y^2} - 2\frac{\partial^2 M_{xy}}{\partial x \partial y} = 2\rho h \frac{\partial^2 W}{\partial t^2}. \tag{1.10}$$

It is worth mentioning that the bending equation for a thin elastic plate can be asymptotically justified from $3D$ elasticity, see Goldenveizer et al. (1993) and Kaplunov et al. (1998).

Below, we will express the bending and twisting moments in terms of the deflection for the cases of orthotropic and isotropic plates.

1.2.1 Orthotropic plate

In case of orthotropy, we assume that the material has three planes of symmetry, e.g. see Courtney (1990). The bending moments M_x, M_y and M_{xy} arising in equation (1.10) are now expressed in terms of the deflection W as

$$M_x = -\left(D_x \frac{\partial^2 W}{\partial x^2} + D_1 \frac{\partial^2 W}{\partial y^2} \right), \tag{1.11}$$

$$M_y = -\left(D_y \frac{\partial^2 W}{\partial y^2} + D_1 \frac{\partial^2 W}{\partial x^2} \right), \tag{1.12}$$

and

$$M_{xy} = 2D_{xy} \frac{\partial^2 W}{\partial xy}, \tag{1.13}$$

where D_x and D_y are the bending stiffness in the x, y directions respectively, see e.g. Norris (1994).

The material constants D_x, D_y, D_1 and D_{xy} appearing in (1.11-1.12) can be expressed in terms of the engineering constants as

$$D_x = \frac{2h^3}{3} \frac{E_1}{1 - \nu_1 \nu_2} \ , \quad D_y = \frac{\nu_2}{\nu_1} D_x$$

and

$$D_1 = \nu_2 D_x \ , \quad D_{xy} = \frac{2}{3} h^3 G_{12},$$

where E_1, E_2 are the Young's moduli, with suffixes 1 and 2 referring to the x and y directions, G_{12} is the shear modulus in the $x-y$ plane, and ν_1, ν_2 are the Poisson's ratios, for more details on the technical constants see e.g. Jones (1999).

Note that the material parameters must satisfy the following conditions ensuring positive definiteness of the strain energy density

$$D_x > 0,\ D_y > 0\ ,\ D_{xy} > 0\ ,\ D_x D_y > D_1^2,$$

see Norris (1994).

Substituting (1.11)-(1.13) into the governing equation (1.10), we obtain the equation of motion for an orthotropic plate in the form

$$D_x \frac{\partial^4 W}{\partial x^4} + 2(D_1 + 2D_{xy}) \frac{\partial^4 W}{\partial x^2 \partial y^2} + D_y \frac{\partial^4 W}{\partial y^4} + 2\rho h \frac{\partial^2 W}{\partial t^2} = 0. \tag{1.14}$$

In terms of the scaling

$$\xi = \frac{x}{\sqrt[4]{D_x}} \quad , \quad \zeta = \frac{y}{\sqrt[4]{D_y}},$$

the governing equation (1.14) becomes

$$\frac{\partial^4 W}{\partial \xi^4} + 2\alpha \frac{\partial^4 W}{\partial \xi^2 \partial \zeta^2} + \frac{\partial^4 W}{\partial \zeta^4} + 2\rho h \frac{\partial^2 W}{\partial t^2} = 0, \tag{1.15}$$

where

$$\alpha = \frac{D_1 + 2D_{xy}}{\sqrt{D_x D_y}}. \tag{1.16}$$

1.2.2 Isotropic material

In case of an isotropic plate, the number of material parameters is reduced, since

$$D_x = D_y = D \ , \ D_{xy} = \frac{D}{2}(1 - \nu) \text{ and } D_1 = \nu D$$

where D is the flexural stiffness of the plate specified by

$$D = \frac{2Eh^3}{3(1 - \nu^2)},$$

with E and ν denoting the Young modulus and Poisson's ratio, respectively.

In this case, the moments M_x, M_y and M_{xy} are expressed through the deflection W as

$$M_x = -D\left(\frac{\partial^2 W}{\partial x^2} + \nu\frac{\partial^2 W}{\partial y^2}\right), \tag{1.17}$$

$$M_y = -D\left(\frac{\partial^2 W}{\partial y^2} + \nu\frac{\partial^2 W}{\partial x^2}\right), \tag{1.18}$$

and

$$M_{xy} = D(1 - \nu)\frac{\partial^2 W}{\partial x \partial y}. \tag{1.19}$$

Note that for isotropic material $\alpha = 1$, see (1.16). Then, the governing equation of motion (1.15) takes the form

$$D\left(\frac{\partial^4 W}{\partial x^4} + 2\frac{\partial^4 W}{\partial x^2 \partial y^2} + \frac{\partial^4 W}{\partial y^4}\right) + 2\rho h\frac{\partial^2 W}{\partial t^2} = 0, \tag{1.20}$$

or

$$D\Delta^2 W + 2\rho h \frac{\partial^2 W}{\partial t^2} = 0, \tag{1.21}$$

where

$$\Delta = \frac{\partial^2}{\partial x^2} + \frac{\partial^2}{\partial y^2}$$

is the Laplace operator.

1.3 Boundary conditions

Consider a semi-infinite orthotropic elastic plate, occupying the region $-\infty < x < \infty$, $0 \leqslant y < \infty$, $-h \leqslant z \leqslant h$, see Fig.1.3.

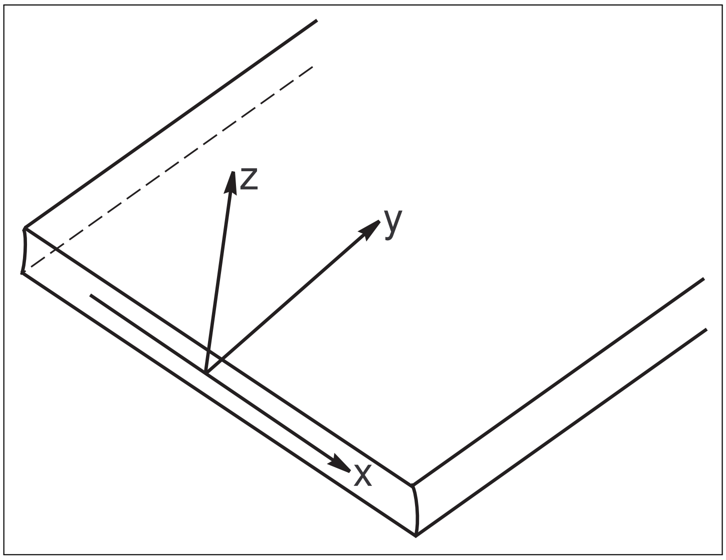

Figure 1.3: A semi-infinite thin elastic plate.

In order to formulate the appropriate boundary conditions at a free edge of an orthotropic Kirchhoff plate, we introduce the so-called modified shear force, see Graff (1991), namely, Q_x and Q_y can be expressed in terms of the deflection W as

$$Q_x = -\left(D_y \frac{\partial^3 W}{\partial x^3} + (D_1 + 4D_{xy})\frac{\partial^3 W}{\partial y^2 \partial x}\right),$$

and

$$Q_y = -\left(D_y \frac{\partial^3 W}{\partial y^3} + (D_1 + 4D_{xy})\frac{\partial^3 W}{\partial x^2 \partial y}\right).$$

Thus, the free edge boundary conditions at $y = 0$ are expressed in terms of vanishing bending moment M_y and modified shear force Q_y

$$M_y = 0, \;\; Q_y = 0, \tag{1.22}$$

or, in terms of the deflection W

$$\begin{aligned} &D_1 \frac{\partial^2 W}{\partial x^2} + D_y \frac{\partial^2 W}{\partial y^2} = 0, \\ &(D_1 + 4D_{xy})\frac{\partial^3 W}{\partial x^2 \partial y} + D_y \frac{\partial^3 W}{\partial y^3} = 0. \end{aligned} \tag{1.23}$$

In the case of an isotropic plate, the modified shear force is given by

$$Q_x = -D\left(\frac{\partial^3 W}{\partial x^3} + (2-\nu)\frac{\partial^3 W}{\partial y^2 \partial x}\right),$$

and

$$Q_y = -D\left(\frac{\partial^3 W}{\partial y^3} + (2-\nu)\frac{\partial^3 W}{\partial x^2 \partial y}\right).$$

The free edge boundary conditions (1.22) take the form

$$\begin{aligned} &\frac{\partial^2 W}{\partial y^2} + \nu \frac{\partial^2 W}{\partial x^2} = 0, \\ &\frac{\partial^3 W}{\partial y^3} + (2-\nu)\frac{\partial^3 W}{\partial x^2 \partial y} = 0. \end{aligned} \tag{1.24}$$

In the case of a prescribed edge loading, it could be a combination of given bending moment and modified shear force. Due to the linearity of the problem, this may be decomposed into two separate sub-problems, involving a bending moment or shear force only.

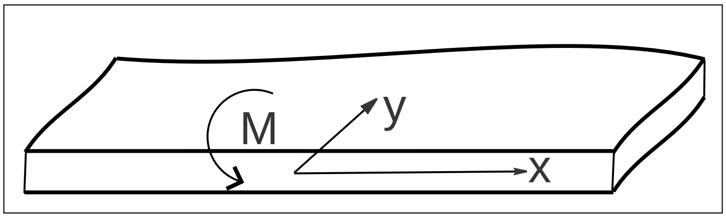

Figure 1.4: Bending moment at the plate edge.

For a prescribed bending moment $M_y = M(x,t)$ at the plate edge $y = 0$, as shown in Fig.1.4, the boundary conditions become

$$M_y = M(x,t)\ ,\ Q_y = 0. \tag{1.25}$$

For an orthotropic case, (1.25) is written in terms of the deflection W as

$$
\begin{aligned}
&D_1 \frac{\partial^2 W}{\partial x^2} + D_y \frac{\partial^2 W}{\partial y^2} = -M(x,t), \\
&(D_1 + 4D_{xy}) \frac{\partial^3 W}{\partial x^2 \partial y} + D_y \frac{\partial^3 W}{\partial y^3} = 0,
\end{aligned}
\tag{1.26}
$$

whereas for an isotropic plate these take the form

$$
\begin{aligned}
&\frac{\partial^2 W}{\partial y^2} + \nu \frac{\partial^2 W}{\partial x^2} = -M(x,t), \\
&\frac{\partial^3 W}{\partial y^3} + (2-\nu) \frac{\partial^3 W}{\partial x^2 \partial y} = 0.
\end{aligned}
\tag{1.27}
$$

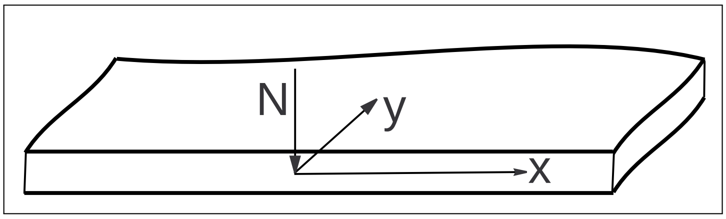

Figure 1.5: Transverse shear force at the plate edge

For the case of a prescribed shear force $N_y = N(x,t)$ applied at the edge $y = 0$, as shown in Fig.1.5, the boundary conditions become

$$
M_y = 0 \ , \ Q_y = N(x,t),
$$

or

$$
\begin{aligned}
&D_1 \frac{\partial^2 W}{\partial x^2} + D_y \frac{\partial^2 W}{\partial y^2} = 0, \\
&(D_1 + 4D_{xy}) \frac{\partial^3 W}{\partial x^2 \partial y} + D_y \frac{\partial^3 W}{\partial y^3} = -N(x,t),
\end{aligned}
\tag{1.28}
$$

for an orthotropic plate, and

$$\begin{aligned}
&\frac{\partial^2 W}{\partial y^2} + \nu \frac{\partial^2 W}{\partial x^2} = 0, \\
&\frac{\partial^3 W}{\partial y^3} + (2-\nu)\frac{\partial^2 W}{\partial x^2 \partial y} = -N(x,t),
\end{aligned} \tag{1.29}$$

for an isotropic plate.

1.4 Integral transforms

In the subsequent analysis we intend to give a brief description of two integral transforms which will be applied later in the thesis, namely the Fourier and the Laplace transforms.

1.4.1 Fourier integral transform

The Fourier integral transform of an integrable function $W(x)$, is defined by

$$F\left(W(x)\right) = W^F(\alpha) = \frac{1}{\sqrt{2\pi}} \int_{-\infty}^{\infty} e^{-ix\alpha} W(x) dx, \tag{1.30}$$

with the inverse Fourier transform given by

$$W(x) = F^{-1}\left(W^F(\alpha)\right) = \frac{1}{\sqrt{2\pi}} \int_{-\infty}^{\infty} e^{ix\alpha} W^F(\alpha) d\alpha, \tag{1.31}$$

where $\alpha \in R$ is the Fourier parameter.

One of the most important properties of the Fourier transform is the derivative property, which is

$$\frac{d^n W(x)}{dx^n} = (i\alpha)^n W^F(\alpha). \tag{1.32}$$

Another useful property is the convolution theorem, given by

$$[W_1(x) * W_2(x)]^F = W_1^F(\alpha) W_2^F(\alpha), \tag{1.33}$$

where the convolution operation is defined as follows

$$W_1(x) * W_2(x) = \int_{-\infty}^{+\infty} W_1(x-y) W_2(y)\, dy.$$

1.4.2 Laplace integral transform

The Laplace integral transform of a function $W(t)$ is defined by

$$W^L(s) = \int_0^{\infty} e^{-st} W(t) dt, \tag{1.34}$$

where s is the Laplace parameter.

The inverse Laplace transform is given by

$$W(t) = \frac{1}{2\pi i} \int_{a_o+i\infty}^{a_o-i\infty} e^{st} W^L(s) ds, \tag{1.35}$$

where a_o is a real constant, satisfying $a_o = s$.

The Laplace integral transform, similar to that of Fourier, has the derivative property given by the following expression

$$\left[\frac{d^n W(t)}{dt^n}\right]^L = (s)^n W^L(s), \tag{1.36}$$

for zero initial data.

1.5 Elastic foundation

1.5.1 Winkler-Fuss foundation

The simplest structural model of an elastic foundation, the Winkler-Fuss foundation associated with a system of elastic springs, was proposed by Winkler (1867) who assumed that the deflection at any point within the foundation depends only on the local pressure at that point, see Fig.1.6. Winkler supposed the behaviour of foundation in the following form

$$P = \beta W, \tag{1.37}$$

where P is the force on the foundation, β is the coefficient of the foundation and W is the the vertical displacement of the foundation.

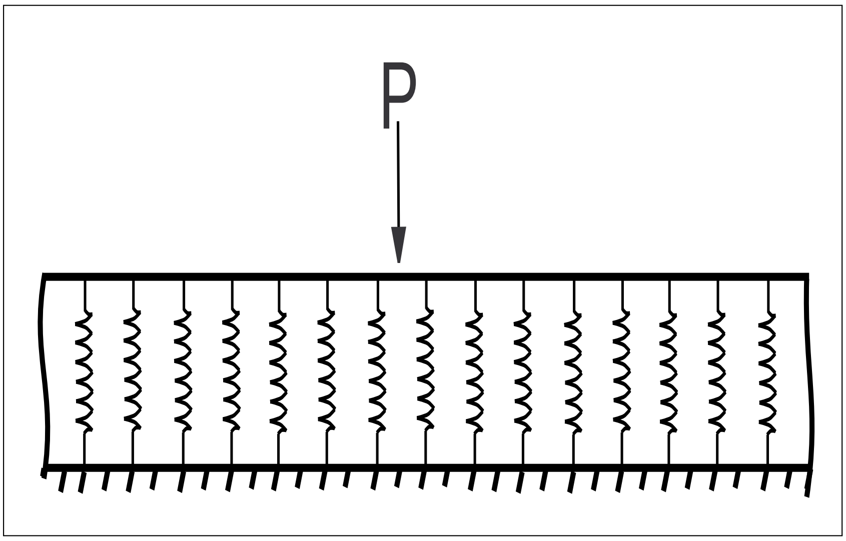

Figure 1.6: Winkler-Fuss foundation

In fact, Fuss (1801) considered an elastic beam floating on the surface of an incompressible fluid, see Borodich (2014), and also Borodich et al. (2015). This simplest model of elastic foundation, often referred to as Winkler-Fuss foundation, is widely used in civil engineering, for example in railway dynamics and contact mechanics, see e.g. Yim and Chopra (1984), Nikolaou et al. (2001), Dutta and Roy (2002), Liyanapathirana and Poulos (2005), and Wang et al. (2005). Two-parametric asymptotic analysis of mechanical response of a coated half-space, leading to Winkler-Fuss behaviour, involving geometric and material parameters is considered by Alexandrov (2010) and Kaplunov et al. (2018). For further historical remarks on the Winkler-Fuss model the reader is referred to Fryba (1995).

1.5.2 More advanced models

The Winkler-Fuss foundation is the simplest example of one-parametric foundation. More advaned approaches include two-parametric models such as Hetenyi (1946), Pasternak (1954) and Vlasov's (1966) foundation, for more details see Muravskii 2001. Furthermore, one can find reviews of foundation models in Kuznetsov (1952) and Kerr (1964). Recently, considerable amount of research has focused on more advanced Winkler-Fuss type models, taking in account inhomogeneity and non-linearity, for example see Martynyak et al. (2015). In Chapter 5 we consider an inhomogeneous Winkler-Fuss foundation, assuming the coefficient of Winkler-Fuss foundation $\beta(x)$ having a periodically varying stiffness. This may have potential engineering applications, involving in particular inhomogeneity/roughness in railway tracks, pipelines, buried structures, floating structures, etc., see for example Hunt (2008).

Chapter 2

Explicit models for bending edge waves on an isotropic elastic plate

This chapter contains brief results on parabolic-elliptic models for bending edge waves in case of an isotropic elastic semi-infinite plate.

The chapter is organized as follows. First, we consider a homogeneous bending edge wave of sinusoidal profile and derive its dispersion relation, following the classical work of Konenkov (1960). Then we discus generalisation in terms of an arbitrary plane harmonic function. Next, we formulate an explicit model for the Konenkov wave, including both types of excitation, namely the case of the bending moment and the modified transverse shear forces. Finally, we implement this model to the problem of an internal source, embedded in the plate.

2.1 Homogeneous bending edge wave

Consider a thin semi-infinite elastic isotropic plate of thickness $2h$ occupying the domain $-\infty < x < \infty$, $0 \leqslant y < \infty$, $-h \leqslant z \leqslant h$, see Fig.2.1.

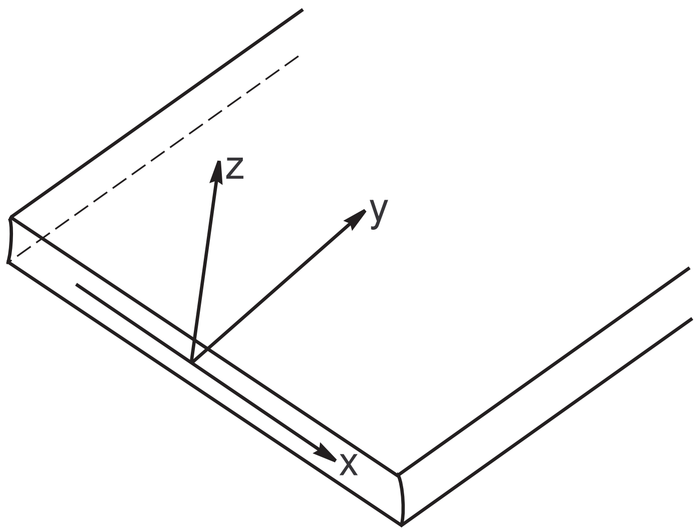

Figure 2.1: Thin isotropic elastic plate

The governing equation for transverse displacement W is (1.20). The free edge boundary conditions (1.24) are imposed, assuming the absence of bending moment and modified transverse shear force at the edge $y = 0$.

2.1.1 Bending edge wave of a sinusoidal profile

Let us derive the dispersion relation for the bending edge wave, following the original contribution of Konenkov (1960). The solution of the plate equation (1.20) is sought in the form of a travelling harmonic wave as

$$W(x, y, t) = Ae^{i(kx-wt)-k\lambda y}, \tag{2.1}$$

where A is an arbitrary constant, ω is the frequency, $k > 0$ is wave number, and the condition Re $\lambda > 0$ ensures decay away from the edge $y = 0$.

Substituting (2.1) into (1.20), we arrive at a bi-quadratic equation for λ, namely

$$Dk^4 \left(\lambda^4 - 2\lambda^2 + 1\right) - 2\rho h\omega^2 = 0. \tag{2.2}$$

It may be shown that there exist two roots λ_1 and λ_2 satisfying the decay condition Re $\lambda > 0$, namely

$$\lambda_j = \sqrt{1 + (-1)^j \sqrt{\frac{2\rho h}{D}} \frac{\omega}{k^2}}, \qquad (j = 1, 2).$$

Therefore the deflection may be presented as

$$W(x, y, t) = \sum_{j=1}^{2} A_j e^{i(kx-wt)-k\lambda_j y}, \tag{2.3}$$

where A_1 and A_2 are arbitrary constants.

Substituting (2.3) into the boundary conditions (1.24) leads to a system of order two

$$\begin{pmatrix} \lambda_1^2 - \nu & \lambda_2^2 - \nu \\ \lambda_1^3 - (2-\nu)\lambda_1 & \lambda_2^3 - (2-\nu)\lambda_2 \end{pmatrix} \begin{pmatrix} A_1 \\ A_2 \end{pmatrix} = \begin{pmatrix} 0 \\ 0 \end{pmatrix}, \tag{2.4}$$

which has nontrivial solutions provided that the determinant of the matrix in the left-hand side equals zero. As a result, we get

$$(\lambda_1^2 - \nu)(\lambda_2^3 - (2-\nu)\lambda_2) - (\lambda_2^2 - \nu)(\lambda_1^3 - (2-\nu)\lambda_1) = 0,$$

or

$$\frac{\lambda_1^2 - \nu}{\lambda_2^2 - \nu} = \frac{\lambda_1^3 - (2-\nu)\lambda_1}{\lambda_2^3 - (2-\nu)\lambda_2}, \tag{2.5}$$

which may be simplified as

$$(\lambda_2 - \lambda_1)[\lambda_1^2\lambda_2^2 - \nu(\lambda_2^2 + \lambda_1\lambda_2 + \lambda_1^2) + \lambda_1\lambda_2(2-\nu) - \nu(\nu-2)] = 0.$$

Using the fact that

$$\lambda_1^2 + \lambda_2^2 = 2,$$

we obtain

$$\lambda_1^2\lambda_2^2 - 2(\nu-1)\lambda_1\lambda_2 - \nu^2 = 0.$$

After some transformations we deduce

$$\lambda_1\lambda_2 = \nu - 1 + \sqrt{2\nu^2 - 2\nu + 1},$$

leading to

$$\lambda_1^2\lambda_2^2 = 1 - c^4, \tag{2.6}$$

where c is a well-known coefficient first presented by Konenkov (1960),

$$c = \left[(1-\nu)\left(3\nu - 1 + 2\sqrt{2\nu^2 - 2\nu + 1}\right)\right]^{\frac{1}{4}}, \tag{2.7}$$

note this depends on the Poisson ratio only, see Fig 2.2.

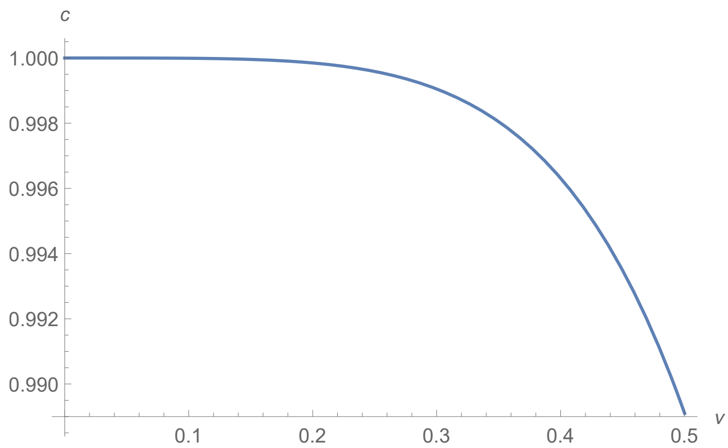

Figure 2.2: The coefficient c versus the Poisson's ratio .

Since the coefficient c is close to unity, one of the attenuation orders is almost zero. This corresponds physically to known effect of a relatively slow decay of the bending edge waves.

Using (2.7), the dispersion relation between the frequency and wave number is obtained in the form

$$Dk^4c^4 = 2\rho h\omega^2. \tag{2.8}$$

In view of the boundary conditions (1.24), the eigensolution for displacement is given by

$$W(x, y, t) = A\left(e^{-k\lambda_1 y} - \frac{\nu - \lambda_1^2}{\nu - \lambda_2^2} e^{-k\lambda_2 y}\right) e^{i(kx - \omega t)}. \tag{2.9}$$

This conventional derivation presented for the bending edge wave is not general and explicit enough, since it is restricted to free harmonic waves of sinusoidal profile only. Arguments of the same nature presented see Chadwick (1976) for the Rayleigh wave led to contraction of an explicit asymptotic model derived by Kaplunov and Prikazchikov (2013). Similar consideration will now be made for the bending edge wave. However, this is not a trivial extension from surface waves in view of the dispersive nature of the bending edge wave. Below we generalise it to that of arbitrary profile, following the consideration of Kaplunov and Prikazchikov (2013).

2.1.2 Bending edge wave of arbitrary profile

We begin by rewriting the equation of motion in terms of the dimensionless variables,

$$\xi = \frac{x}{h}, \qquad \zeta = \frac{y}{h}, \qquad \tau = \frac{t}{h}\sqrt{\frac{E}{3\rho(1 - \nu^2)}}. \tag{2.10}$$

The governing equation (1.20) becomes

$$\Delta^2 W + \frac{\partial^2 W}{\partial \tau^2} = 0, \tag{2.11}$$

where

$$\Delta = \frac{\partial^2}{\partial \xi^2} + \frac{\partial^2}{\partial \zeta^2}$$

denotes the 2D Laplace operator in the dimensionless variables ξ and ζ.

Next we adopt the beam-like assumption, see Kaplunov and Prikazchikov (2013),

$$\gamma^4 \frac{\partial^4 W}{\partial \xi^4} + \frac{\partial^2 W}{\partial \tau^2} = 0, \tag{2.12}$$

where γ is a coefficient to be determined.

Physically, this assumption corresponds to beam-like behaviour. It has been observed that a string is a basic object for the classical Rayleigh wave (Kaplunov et al, 2010), since the propagation on the surface is described by a 1D wave equation. However, the bending edge wave is dispersive, therefore the solution of the form $f(x-ct)$ employed by Chadwick (1976) for surface waves, would not work for the bending edge wave. It may be guessed that the corresponding object for Konenkov wave would be a beam, associated with assumption (2.12). Another interpretation of (2.12) will be presented below.

It should be emphasized that this assumption is key, leading below to transformation of the parabolic equation (2.11) to the following elliptic equation

$$\left(1-\gamma^4\right) \frac{\partial^4 W}{\partial \xi^4} + 2\frac{\partial^4 W}{\partial \xi^2 \partial \zeta^2} + \frac{\partial^4 W}{\partial \zeta^4} = 0. \tag{2.13}$$

The above equation may also be expressed in operator form as

$$\Delta_1 \Delta_2 W = 0, \tag{2.14}$$

where

$$\Delta_j = \frac{\partial^2}{\partial \zeta^2} + \lambda_j^2 \frac{\partial^2}{\partial \xi^2}, \qquad j = 1, 2$$

and

$$\lambda_j^2 = 1 + (-1)^j \gamma^2.$$

The solution of (2.14) is then written as a sum of two arbitrary plane harmonic functions decaying as $\zeta \to \infty$, namely

$$W = \sum_{j=1}^{2} W_j(\xi, \lambda_j \zeta, \tau). \tag{2.15}$$

Employing the Cauchy-Riemann identities for a plane harmonic function W_j

$$\frac{\partial W_j}{\partial \xi} = \frac{1}{\lambda_j} \frac{\partial W_j}{\partial \zeta}, \quad \texttt{and} \quad \frac{\partial W_j}{\partial \zeta} = -\lambda_j \frac{\partial W_j}{\partial \xi}, \tag{2.16}$$

and substituting this result into the homogeneous edge boundary conditions and requiring the related determinant to vanish, we have (2.6), leading once again to the dispersion relation in (2.8), implying $\gamma = c$, with c denoted by (2.7).

Since $\gamma = c$, the physically intuitive guess for beam-like assumption (2.12) is confirmed. In other words, the assumption (2.12) corresponds to an effective beam, with a bending stiffness chosen so that the dispersion relation of this beam is identical to that of a bending edge wave on a semi-infinite plate.

Consequently, using the boundary conditions (1.24), the deflection profile (2.15) may be expressed through a single harmonic function, say W_1, as

$$W = W_1(\xi, \lambda_1 \zeta, \tau) - \frac{\nu - \lambda_1^2}{\nu - \lambda_2^2} W_1\left(\xi, \lambda_2 \zeta, \tau\right). \tag{2.17}$$

Clearly, the previously obtained eigensolution (2.9) is a particular case of (2.17).

It is worth noting that the representation (2.17) involves only the harmonic function, not its conjugate, as was the case for the Rayleigh wave, obtained by Chadwick (1976).

2.2 Model formulation

In this section we present briefly the results for a parabolic-elliptic model for the bending edge wave on an isotropic Kirchhoff plate, associated with that obtained see Kaplunov and Prikazchikov (2013).

The aim of this model is extracting the contribution of the bending edge wave to the overall dynamic response.

Consider the non-homogeneous boundary conditions at the edge $y = 0$

$$\begin{aligned} \frac{\partial^2 W}{\partial y^2} + \nu \frac{\partial^2 W}{\partial x^2} &= -M, \\ \frac{\partial^3 W}{\partial y^3} + (2-\nu) \frac{\partial^3 W}{\partial x^2 \partial y} &= -N, \end{aligned} \tag{2.18}$$

where M and N are the prescribed bending moment and modified shear force, respectively.

For convenience we treat them separately as two sub-problems. Let us first consider the case of edge bending moment, that is when $N = 0$, $M \neq 0$.

The model below relies on the representation of the eigensolution in terms of a single plane harmonic function (2.17).

Perturbation of this eigensolution in slow time, leads to a beam-like equation along the edge $y = 0$ which can be written as

$$D\gamma^4 \frac{\partial^4 W}{\partial x^4} + 2\rho h \frac{\partial^2 W}{\partial t^2} = Q \frac{\partial^2 M}{\partial x^2}, \tag{2.19}$$

where Q is the material constant

$$Q = \frac{\chi\,(\chi + \nu)}{1 - \nu + \chi}, \tag{2.20}$$

with

$$\chi = \sqrt{1 - \gamma^4}, \tag{2.21}$$

depending on the Poisson's ratio only. The variation of the constant Q on the Poisson's ratio ν is shown on the following Fig.2.3,

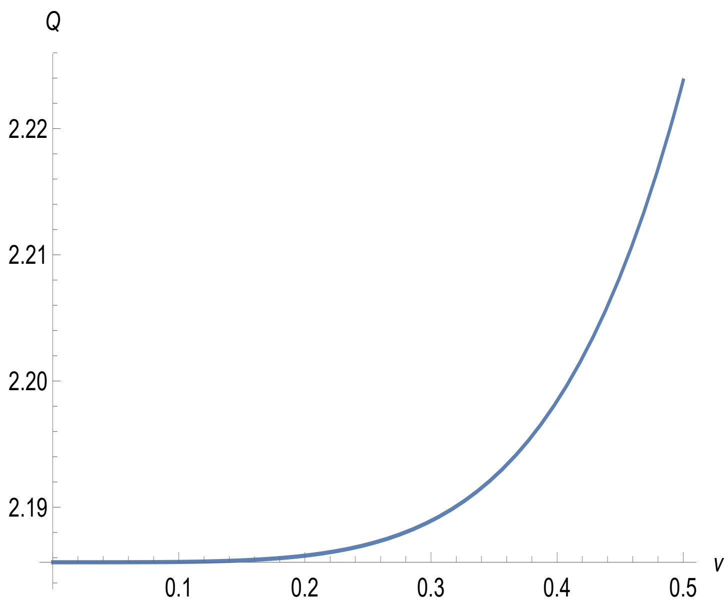

Figure 2.3: The coefficient Q versus the Poisson's ratio .

Solution of (2.18) on the edge $y = 0$ serves as a Dirichlet-type boundary condition for the elliptic equation

$$\frac{\partial^2 W_1}{\partial y^2} + \lambda_1^2 \frac{\partial^2 W_1}{\partial x^2} = 0, \tag{2.22}$$

with the resulting deflection W expressed through the plane harmonic function W_1 as (2.16).

A similar formulation may be derived for the second sub-problems where $N \neq 0$ and $M = 0$.

This corresponds to excitation by means of a prescribed shear force, for which

$$\begin{aligned} &\frac{\partial^2 W}{\partial y^2} + \nu \frac{\partial^2 W}{\partial x^2} = 0, \\ &\frac{\partial^3 W}{\partial y^3} + (2 - \nu) \frac{\partial^3 W}{\partial x^2 \partial y} = -N. \end{aligned} \tag{2.23}$$

Now, the slow time perturbation procedure leads to a parabolic equation for the rotation angle $\theta = \dfrac{\partial W}{\partial y}$ evaluated at the edge $y = 0$, namely,

$$D\gamma^4 \frac{\partial^4 \theta}{\partial x^4} + 2\rho h \frac{\partial^2 \theta}{\partial t^2} = -Q \frac{\partial^2 N}{\partial x^2}, \tag{2.24}$$

with Q defined in (2.20).

Similarly, the elliptic equation over the interior is given by

$$\frac{\partial^2 \theta}{\partial y^2} + \lambda_1^2 \frac{\partial^2 \theta}{\partial x^2} = 0, \tag{2.25}$$

with the eigensolution following from (2.17).

Thus, for the case of a prescribed edge shear force, the bending edge wave field is again described by a parabolic beam-like equation (2.24) on the edge, together with the elliptic equation (2.25) , governing the decay away from the edge .

2.3 Excitation due to internal source

In this section, we consider an example illustrating the implementation of the asymptotic model for an internal source embedded in the plate.

Below we implement the superposition principle, decomposing the solution in two steps:

1 The problem for an infinite plate with an embedded source.

2 The problem for a semi-infinite plate with the discrepancy taken care of due to appropriate non-homogeneous boundary conditions on the edge.

The governing equation for an infinte Kirchhoff isotropic plate with an embedded point time harmonic source is given by

$$D\Delta^2 W + 2\rho h \frac{\partial^2 W}{\partial t^2} = P\delta(x)\delta(y - y_0)\, e^{i\omega t}, \tag{2.26}$$

where $\delta(.)$ is the Dirac's delta function and P is the magnitude of the load and the source has coordinates $x = 0$, $y = y_0$, see the Figure 2.4.

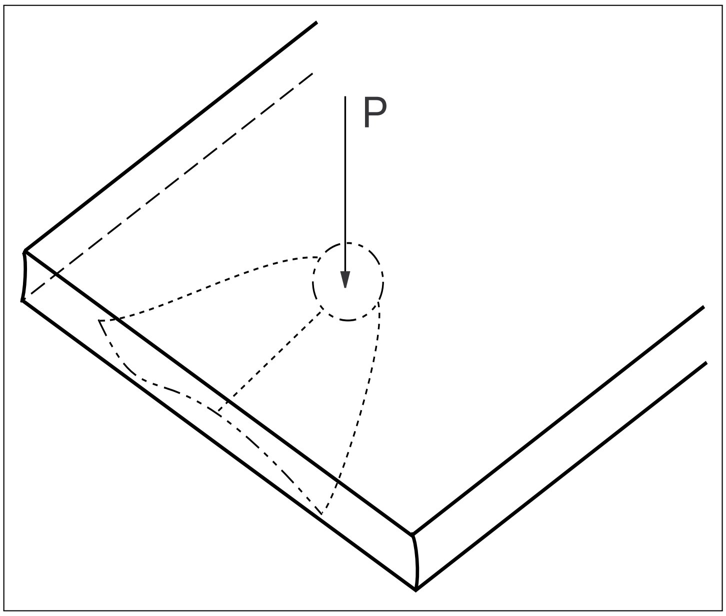

Figure 2.4: Embedded source

In fact, the deflection produced by the source is the Green's function, see e.g. Gunda et al. (1998)

$$W^* = \frac{i}{8k^2 D}\left[H_0^1(kr) - H_0^1(ikr)\right], \tag{2.27}$$

where r is distance of the observation point from the source location, H_0^1 is the zero order Hankel function of the first kind and k is wave number, related to frequency ω through the dispersion relation

$$Dk^4 = 2\rho h \omega^2.$$

Using the superposition principle, we can formulate a problem for a semi-infinite homogeneous plate governed by

$$D\Delta^2 W + 2\rho h \frac{\partial^2 W}{\partial t^2} = 0, \tag{2.28}$$

with the effect of source modelled by the following boundary conditions

$$\begin{aligned} &\frac{\partial^2 W}{\partial y^2} + \nu \frac{\partial^2 W}{\partial x^2} = M^*, \\ &\frac{\partial^3 W}{\partial y^3} + (2-\nu)\frac{\partial^2 W}{\partial x^2 \partial y} = N^*, \end{aligned} \tag{2.29}$$

where M^* and N^* are the bending moment and modified shear force at $y = 0$ defined by

$$M^* = \frac{\partial^2 W^*}{\partial y^2} + \nu \frac{\partial^2 W^*}{\partial x^2}, \tag{2.30}$$

and

$$N^* = \frac{\partial^3 W^*}{\partial y^3} + (2-\nu)\frac{\partial^2 W^*}{\partial x^2 \partial y}. \tag{2.31}$$

As before, the problem may be decomposed into two sub-problems. Let us begin with the bending moment excitation. After some transformation the effective bending edge moment is represented as

$$\begin{aligned} M^* = &\frac{1}{8Dk\left(x^2+y_0^2\right)^{3/2}} \left[-ik\sqrt{x^2+y_0^2}\left(\nu x^2+y_0^2\right) H_0^{(1)}\left(ik\sqrt{x^2+y_0^2}\right) - \right. \\ &k\sqrt{x^2+y_0^2}\left(\nu x^2+y_0^2\right) H_0^{(1)}\left(k\sqrt{x^2+y_0^2}\right) + \\ &\left.(\nu-1)\left(x^2-y_0^2\right)\left(H_1^{(1)}\left(ik\sqrt{x^2+y_0^2}\right) + iH_1^{(1)}\left(k\sqrt{x^2+y_0^2}\right)\right)\right]. \end{aligned} \tag{2.32}$$

Now applying the parabolic-elliptic model, we have

$$D\gamma^4 \frac{\partial^4 W}{\partial x^4} - 2\rho h \omega^2 W = Q\frac{\partial^2 M^*}{\partial x^2}, \tag{2.33}$$

where Q is defined in (2.20).

Applying the Fourier transform to (2.33) along the edge , we have

$$W^F = \frac{-Qh^2k^2M^{*F}}{Dk^4\gamma^4 - 2\rho h \omega^2}. \tag{2.34}$$

where k denotes the parameter of the Fourier transforms. The solution for the function W may be expressed as

$$W = \frac{1}{2\pi}\int\limits_{-\infty}^{\infty} e^{ikx}\frac{h^2 M^{*F} k^2 \chi\,(\chi+\nu)}{(1-\nu+\chi)(\gamma^4-1)Dk^4}\,dk. \tag{2.35}$$

The graphical illustration of a real part of W^F is shown in Fig. 2.5.

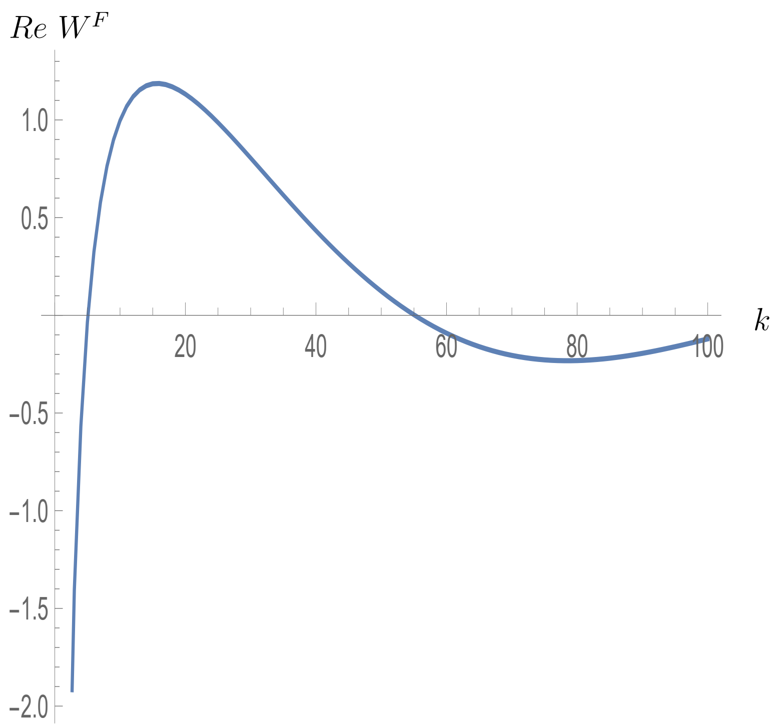

Figure 2.5: Real part of W^F for $E = 2.3GPa$, $\nu = 0.3$ and $h = 0.1$

The case of shear force excitation may be treated similarly.

Thus, we have presented an example of implementation of the parbolic-elliptic model for the bending edge waves to the problem of a time-harmonic internal source. Similar approach could be realised for transient internal sources.

Chapter 3

Edge bending wave on an othotropic elastic plate resting on the Winkler-Fuss foundation.

This chapter is concerned with the propagation of bending edge waves on an orthotropic plate supported by the Winkler-Fuss foundation, subject to free edge boundary conditions. First, the dispersion relation is derived. Then, the general profile of the wave is constructed in terms of an arbitrary plane harmonic function.

Finally, several illustrative examples are considered including that of a conventional sinusoidal profile, together with a less trivial form of the eigensolution arising for a given initial data. An example of initial conditions corresponding to a point load demonstrates a more localized distribution along the longitudinal variable occurring with an increase in the transverse variable moving away from the edge.

Some of the results of this chapter have been published in Althobaiti and Prikazchikov (2016) and Althobaiti et al. (2017).

3.1 Bending edge waves of sinusoidal profile on an orthotropic elastic plate

3.1.1 Problem statement

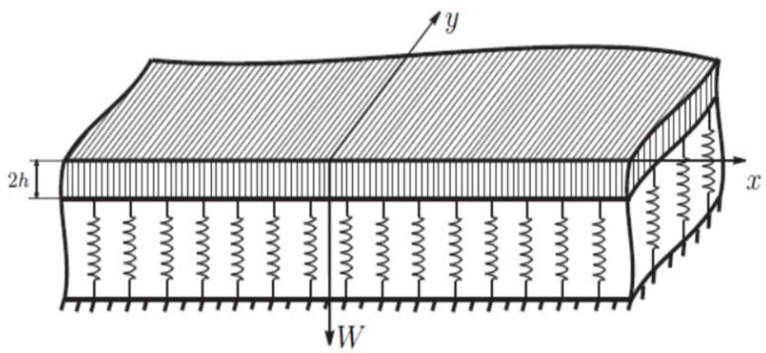

Figure 3.1: Elastic plate on the Winkler-Fuss foundation.

Consider an orthotropic elastic plate of thickness $2h$ supported by a Winkler-Fuss foundation, see Figure 3.1. Let the plate occupy the region $-\infty < x < \infty, 0 \leq y < \infty$, $0 \leq z \leq 2h$, with the foundation domain given by $-\infty < x < \infty, 0 < y < \infty$, $2h \leqslant z < \infty$.

The governing equation for the flexural displacement W of an orthotropic, homogeneous, thin elastic plate is

$$D_x \frac{\partial^4 W}{\partial x^4} + 2H \frac{\partial^4 W}{\partial x^2 \partial y^2} + D_y \frac{\partial^4 W}{\partial y^4} + 2\rho h \frac{\partial^2 W}{\partial t^2} + \beta W = 0, \tag{3.1}$$

where $H = D_1 + 2D_{xy}$, and β is the Winkler coefficient. Clearly, when $\beta = 0$ this corresponds to a free Kirchhoff plate, see Norris (1994).

In the absence of prescribed moment and modified shear force on the edge $y = 0$, the boundary conditions are expressed as (1.23).

3.1.2 Dispersion equation

Let us derive the dispersion equation for the bending edge wave. The solution of the plate equation (3.1) is sought in the form of a travelling harmonic wave as (2.1).

Substitution of (2.1) into (3.1) results in the following bi-quadratic equation

$$\lambda^4 - \frac{2D_1 + 4D_{xy}}{D_y} \lambda^2 + \frac{D_x k^4 + \beta - 2\rho h \omega^2}{D_y k^4} = 0, \tag{3.2}$$

which may be shown to have two roots satisfying the decay condition $Re\lambda > 0$. Therefore, the deflection is expressed in the form

$$W(x, y, t) = \sum_{j=1}^{2} A_j e^{i(kx-\omega t)-k\lambda_j y}, \tag{3.3}$$

with

$$\lambda_1^2 + \lambda_2^2 = \frac{2D_1 + 4D_{xy}}{D_y}, \quad \lambda_1^2\lambda_2^2 = \frac{D_x k^4 + \beta - 2\rho h\omega^2}{D_y k^4}, \ (Re\lambda_j > 0), \tag{3.4}$$

implying the associated attenuation orders, λ_1 and λ_2 given by

$$\lambda_j = \sqrt{\frac{H}{D_y} + (-1)^j \frac{\kappa}{2}}, \qquad j = 1, 2, \tag{3.5}$$

where

$$\kappa = 2\sqrt{\frac{H^2}{D_y^2} - \left(\frac{D_x}{D_y} - \gamma^4\right)}. \tag{3.6}$$

Now, substituting (3.3) into boundary conditions, we have

$$\begin{pmatrix} D_1 - \lambda_1^2 D_y & D_1 - \lambda_2^2 D_y \\ \lambda_1^3 D_y - \lambda_1(D_1 + 4D_{xy}) & \lambda_1^3 D_y - \lambda_2(D_1 + 4D_{xy}) \end{pmatrix} \begin{pmatrix} A_1 \\ A_2 \end{pmatrix} = \begin{pmatrix} 0 \\ 0 \end{pmatrix}. \tag{3.7}$$

The above set of linear equations possesses non-trivial solutions provided the related determinant vanishes, i.e.

$$\begin{vmatrix} D_1 - \lambda_1^2 D_y & D_1 - \lambda_2^2 D_y \\ \lambda_1^3 D_y - \lambda_1(D_1 + 4D_{xy}) & \lambda_1^3 D_y - \lambda_2(D_1 + 4D_{xy}) \end{vmatrix} = 0. \tag{3.8}$$

As a result we get

$$\lambda_2 \left(\lambda_2^2 D_y - (D_1 + 4D_{xy})\right) \left(\lambda_1^2 D_y - D_1\right) - \\ \lambda_1 \left(\lambda_1^2 D_y - (D_1 + 4D_{xy})\right) \left(\lambda_2^2 D_y - D_1\right) = 0. \tag{3.9}$$

Factorising the last equation and using the relation (3.4), it is possible to establish that

$$D_y^2 \lambda_1^2 \lambda_2^2 + 4D_y D_{xy} \lambda_1 \lambda_2 - D_1^2 = 0, \tag{3.10}$$

which implies

$$\frac{D_x k^4 + \beta - 2\rho h \omega^2}{D_y k^4} = \frac{\left(\sqrt{D_1^2 + 4D_{xy}^2} - 2D_{xy}\right)^2}{D_y^2}. \tag{3.11}$$

The dispersion relation may then be re-cast as

$$D_x c^4 k^4 = 2\rho h \omega^2 - \beta, \tag{3.12}$$

where

$$c^4 = 1 - \frac{\left(\sqrt{4D_{xy}^2 + D_1^2} - 2D_{xy}\right)^2}{D_x D_y}, \tag{3.13}$$

is a constant, arising for the bending edge wave on an orthotropic elastic plate, first obtained by Norris (1994).

It is well-known that typical value of the coefficient c^4 is close to 1, see Norris (1994) and generalises the well-known Konenkov constant for isotropic plate, see (2.7).

In other words, foundation adds stiffening to the structure, and waves can only propagate starting from a certain frequency value. From (3.12) we have

$$\omega^2 \geqslant \frac{\beta}{2\rho h} \tag{3.14}$$

hence the cut-off frequency

$$\omega_0 = \sqrt{\frac{\beta}{2\rho h}}. \tag{3.15}$$

Similarly to Kaplunov et al. (2014), the presence of elastic foundation causes a cut-off frequency. It should be noted that the value of the cut-off frequency is identical to that of the isotropic case due to the fact that the principal anisotropy directions coincide with the coordinate axis.

The dispersion relation (3.12) may be represented in dimensionless form as

$$K^4 = \Omega^2 - 1, \tag{3.16}$$

where

$$K = k\gamma\sqrt[4]{\frac{D_x}{\beta}}, \quad \Omega = \omega\sqrt{\frac{2\rho h}{\beta}}, \tag{3.17}$$

hence $\Omega = 1$ is the dimensionless cut-off frequency, similarly to the isotropic case examined in Kaplunov et al. (2014), see Fig.3.2

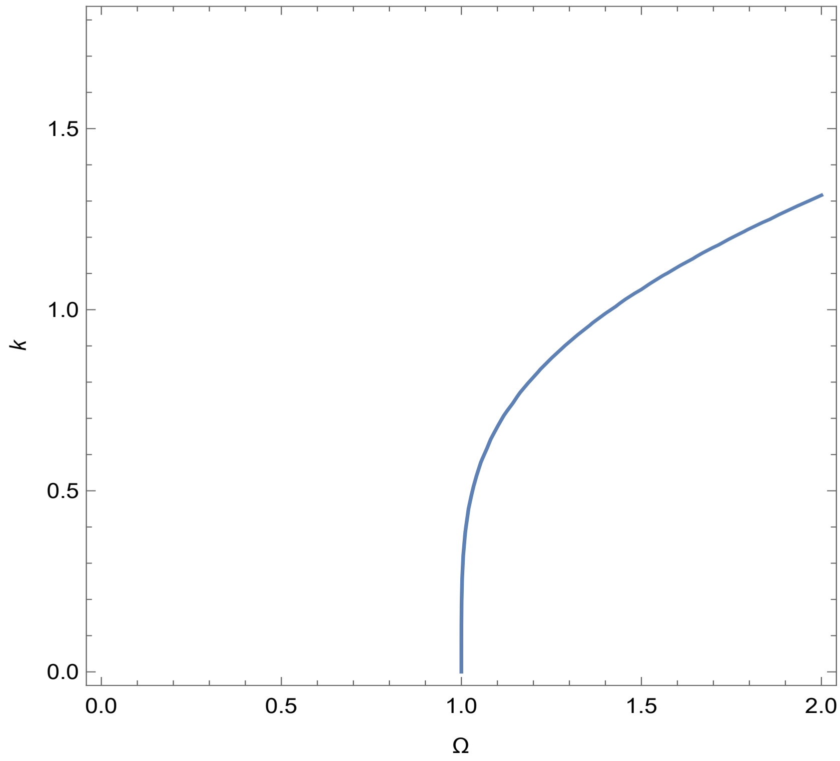

Figure 3.2: Dispersion curve for edge wave.

Following the aforementioned publication, we note that the phase velocity normalized by $\dfrac{\sqrt{2\rho h}}{\gamma\sqrt[4]{\beta D_x}}$,

$$V^{ph} = \frac{\Omega}{K} = \frac{\Omega}{\sqrt[4]{\Omega^2 - 1}}, \tag{3.18}$$

has the local minimum $V^{ph} = \sqrt{2}$ at $\Omega = \sqrt{2}$, corresponding to $K = 1$.

Moreover, at this point V^{ph} coincides with the group velocity

$$V^g = \frac{d\Omega}{dK} = \frac{2\sqrt[4]{(\Omega^2 - 1)^3}}{\Omega}, \tag{3.19}$$

see Fig.3.3, which is in fact almost identical to Fig. 3 of Kaplunov et al. (2014).

It is also worth mentioning that the minimum value $V^{ph} = V^g = \sqrt{2}$, associated with the dispersion relation implies the critical speed of a moving load problem, corresponding to the local minimum of the phase velocity, as noticed previously to the classical 1D problem for a beam on a Winkler foundation, see Timoshenko (1926).

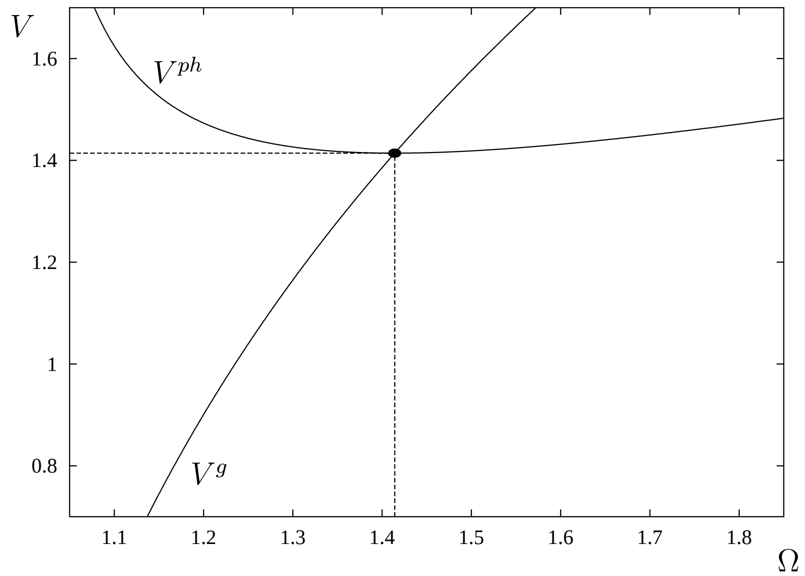

Figure 3.3: The phase and group velocities V^{ph} and V^{g} vs. frequency.

Therefore, we may expect the same resonant effect of an edge moving load on an elastically supported plate. Thus, the effects of the cut-off frequency and local minimum of phase velocity corresponding to the critical regime of the moving edge load, observed for isotropic Kirchhoff plate on Winkler foundation, are also confirmed for an orthotropic plate.

In view of the boundary conditions (1.23) the deflection profile may be written as

$$W = A\left(e^{-k\lambda_1 y} - \frac{D_1 - \lambda_1^2 D_y}{D_1 - \lambda_2^2 D_y} e^{-k\lambda_2 y}\right) e^{i(kx - \omega t)}. \tag{3.20}$$

Let us now generalise this profile to arbitrary shape, following the procedure in subsection 2.1.2.

3.2 Homogeneous bending edge wave of arbitrary profile

In this subsection we generalise the profile (3.20) to that expressed in terms of an arbitrary single plane harmonic function. Some of the results have been reported already in Althobaiti and Prikazchikov (2016).

Let us introduce the following dimensionless quantities

$$\xi = \frac{x}{h}, \qquad \eta = \frac{y}{h}, \qquad \tau = t\sqrt{\frac{D_x}{2\rho h^5}}. \tag{3.21}$$

The governing equation (3.1) becomes

$$D_x \frac{\partial^4 W}{\partial \xi^4} + 2H \frac{\partial^4 W}{\partial \xi^2 \partial \eta^2} + D_y \frac{\partial^4 W}{\partial \eta^4} + D_x \frac{\partial^2 W}{\partial \tau^2} + \beta h^4 W = 0. \tag{3.22}$$

Next, we adopt the beam-like assumption, similarly to that in Kaplunov et al. (2016), thus

$$\gamma^4 \frac{\partial^4 W}{\partial \xi^4} + \frac{\partial^2 W}{\partial \tau^2} + \beta^* W = 0, \tag{3.23}$$

where $\beta^* = \dfrac{\beta h^4}{D_x}$ and presenting an analogue of the string-like assumption for the Rayleigh wave, see Kaplunov and Prikazchikov (2017).

As will be shown later, the assumption (3.23) is additionally justified by the fact that the associated dispersion relation of this effective beam on the Winkler foundation coincides with the dispersion relation (3.12) of the bending edge wave. As before, γ is a constant which will be determined later.

In view of (3.23), we can exclude explicit time dependence from (3.22), resulting in

$$\frac{\partial^4 W}{\partial \eta^4} + 2H\frac{\partial^4 W}{\partial \xi^2 \partial \eta^2} + \frac{D_x}{D_y}\left(1-\gamma^4\right)\frac{\partial^4 W}{\partial \xi^4} = 0. \tag{3.24}$$

It may be shown that the obtained equation (3.24) is elliptic, therefore it may be represented as

$$\Delta_1 \Delta_2 W = 0,$$

where

$$\Delta_j = \partial_\eta^2 + \lambda_\xi^2 \partial_1^2,$$

with

$$\lambda_1^2 + \lambda_2^2 = \frac{2H}{D_y} \quad \text{and} \quad \lambda_1^2 \lambda_2^2 = \frac{D_x}{D_y}\left(1-\gamma^4\right). \tag{3.25}$$

The solution is therefore expressed as a sum of two arbitrary plane harmonic functions

$$W = \sum_{j=1}^{2} W_j(\xi, \lambda_j \eta, \tau), \tag{3.26}$$

satisfying the decay condition $(W \to 0 \ \text{ as } \ y \to \infty)$.

Here and below we restrict our contribution to the case of real λ_1 and λ_2.

In terms of the scaling (3.21), the boundary conditions (1.23) take the form

$$
\begin{aligned}
&D_x \frac{\partial^2 W}{\partial \xi^2} + D_y \frac{\partial^2 W}{\partial \eta^2} = 0, \\
&(D_1 + 4D_{xy}) \frac{\partial^3 W}{\partial \xi^2 \partial \eta} + D_y \frac{\partial^3 W}{\partial \eta^3} = 0.
\end{aligned}
\tag{3.27}
$$

Employing the Cauchy-Riemann identities (2.16) for a plane harmonic function $W_j(\zeta, \lambda\xi)$, substituting (3.25) into the boundary conditions (1.23) and taking conjugate of the second equation, we get

$$
\begin{aligned}
&(D_1 - \lambda_1^2 D_y) \frac{\partial^2 W_1}{\partial \xi^2} + (D_1 - \lambda_2^2 D_y) \frac{\partial^2 W_2}{\partial \xi^2} = 0 \\
&(\lambda_1^3 D_y - \lambda_1(D_1 + 4D_{xy}))\frac{\partial^3 W_1}{\partial \xi^3} + (\lambda_2^3 D_y - \lambda_2(D_1 + 4D_{xy}))\frac{\partial^3 W_2}{\partial \xi^3} = 0,
\end{aligned}
\tag{3.28}
$$

which possesses non-trivial solutions provided that the associated determinant vanishes, which yields precisely (3.8). Hence, we deduce

$$
D_1 D_y(\lambda_1^2 + \lambda_2^2) + D_y^2 \lambda_1^2 \lambda_2^2 + 4D_y D_{xy} \lambda_1 \lambda_2 + D_1^2 + 4D_1 D_{xy} = 0. \tag{3.29}
$$

Using (3.25), the last equation may be rearranged to the form

$$
(D_y \lambda_1 \lambda_2 + 2D_{xy})^2 = 4D_{xy}^2 + D_1^2. \tag{3.30}
$$

After some algebraic manipulations we have

$$
\frac{D_x}{D_y} - \gamma^4 = \left(\frac{\sqrt{4D_{xy}^2 + D_1^2} - 2D_y}{D_y} \right)^2. \tag{3.31}
$$

Similarly to the previous subsection, only a positive root is of interest, leading to

$$
\gamma^4 = 1 - \frac{\left(\sqrt{4D_{xy}^2 + D_1^2} - 2D_{xy}\right)^2}{D_x D_y}, \tag{3.32}
$$

which coincides exactly with the (3.13), hence,

$$\gamma = c.$$

In Figs. 3.5-3.7, we investigate the behaviour of the coefficient γ for the varying values of the material constants, E_1, E_2, ν_1 and ν_2. The values of material parameters are given in figure captions.

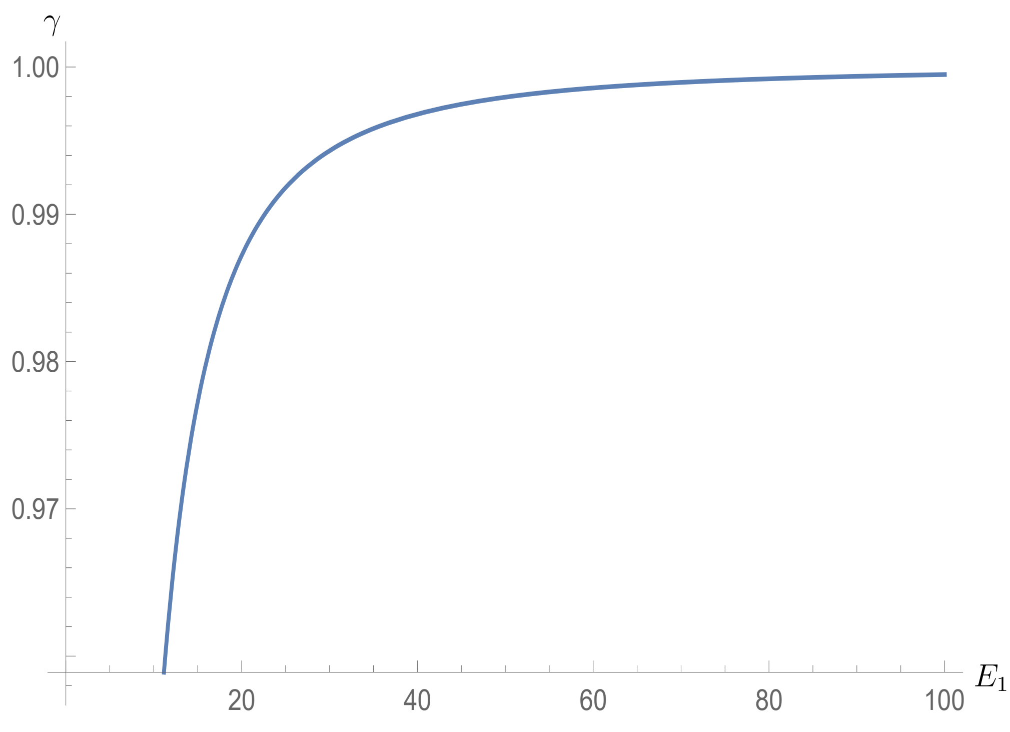

Figure 3.4: The coefficient γ vs. parameter E_1, GPa for $E_2 = 18.1GPa$ and $\nu_1 = \nu_2 = 0.25$.

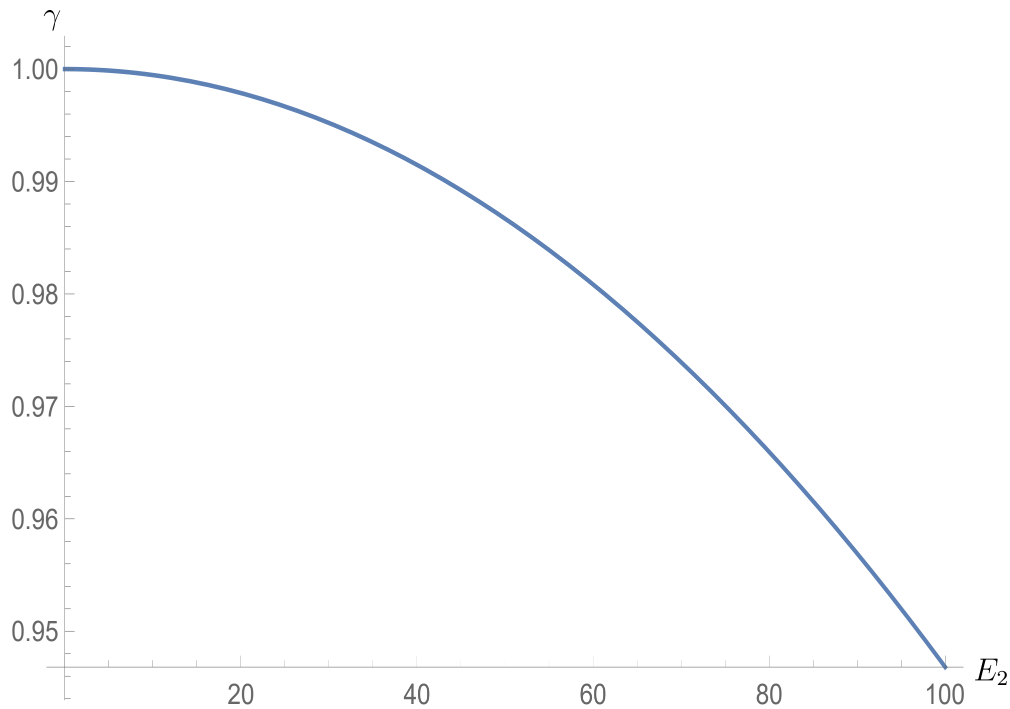

Figure 3.5: The coefficient γ vs. constant E_2, GPa with $E_1 = 54.2GPa$ and $\nu_1 = \nu_2 = 0.25$.

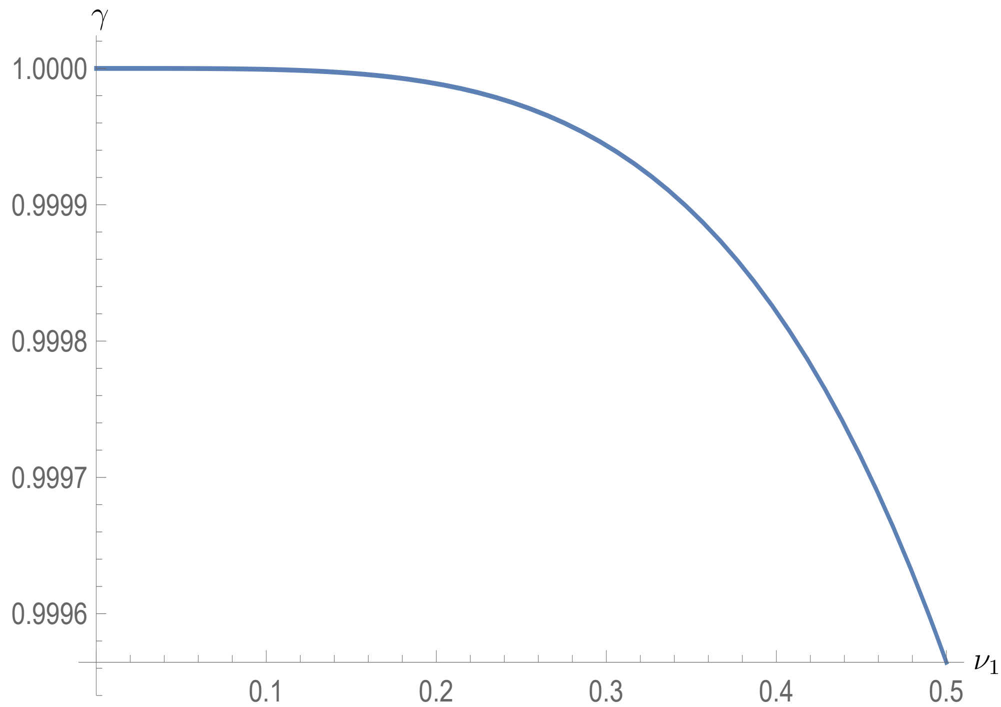

Figure 3.6: The coefficient γ vs. Poisson's ratio ν, for $E_1 = 54.1GPa$ and $E_2 = 18.1GPa$.

Dependence of γ on ν_2 looks pretty similar to Fig. 3.7 and is therefore not presented here. Also, we observe that Fig. 3.7 is similar to Fig. 2.2 for isotropic case.

Now let us present an additional clarification of the assumption (3.23). Indeed, if we re-write it in the original x and t variables, we get

$$D_x c^4 \frac{\partial^4 W}{\partial x^4} + 2\rho h \frac{\partial^2 W}{\partial t^2} + \beta = 0,$$

which corresponds to a beam on a Winkler-Fuss foundation. The associated dispersion relation is

$$D_x c^4 k^4 - \beta - 2\rho h \omega^2 = 0,$$

coinciding with (3.12), providing an additional confirmation of the assumption, complementing the physically intuitive guess described earlier.

Thus, the physical meaning of the parameter γ introduced in the assumption (3.23) is the coefficient in the dispersion relation (3.12), correcting the bending stiffness.

Note that from the boundary conditions (1.23), the harmonic functions W_1 and W_2 are related to each other through

$$W_2\left(\xi, 0, t\right) = -\frac{D_1 - \lambda_1^2 D_y}{D_1 - \lambda_2^2 D_y} W_1\left(\xi, 0, t\right). \tag{3.33}$$

Consequently, we can represent the deflection of the plate W in terms of a single plane harmonic function as

$$W = W_1(x, \lambda_1 y, \tau) - \frac{D_1 - \lambda_1^2 D_y}{D_1 - \lambda_2^2 D_y} W_1\left(x, \lambda_2 y, t\right), \tag{3.34}$$

generalising the result in Kaplunov et al. (2016) to the orthotropic plate.

3.3 Illustrative examples

Let us now present several numerical examples, assuming

$$W_1\left(\xi, \lambda_1 \eta, \tau\right) = A \cos \xi \; e^{-\lambda_1 \eta - i\omega\tau}, \tag{3.35}$$

where the frequency ω is determined from the assumption (3.23).

The dependence on time is omitted in this example, with the curves on Fig. 3.9. showing the variation of the dimensionless quantity

$$W_0\left(\xi, \lambda_1 \eta\right) = \cos \xi \left(e^{-\lambda_1 \eta} - \frac{D_1 - \lambda_1^2 D_y}{D_1 - \lambda_2^2 D_y} e^{-\lambda_2 \eta} \right), \tag{3.36}$$

on the longitudinal coordinate ξ for several values of the transverse coordinate η, namely

$$\eta = 0 \;,\; 1 \;,\; 10 \;,\; \text{and } 50$$

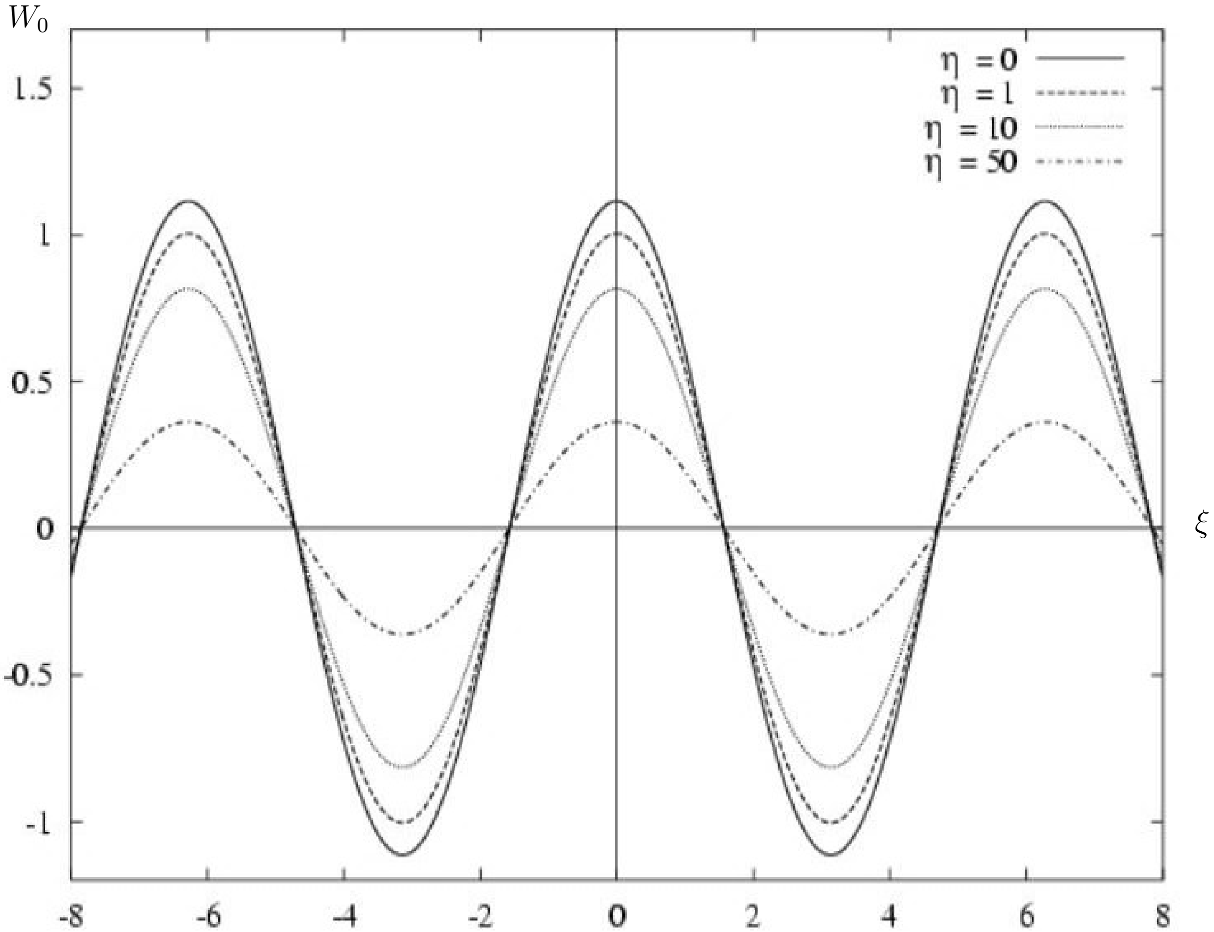

Figure 3.7: Displacement of sinusoidal profile.

The calculations are performed for the following values of material parameters

$$E_1 = 54.2\text{GPa}, \quad E_2 = 18.1\text{GPa}, \quad G_{xy} = 8.96\text{GPa}, \nu_1 = \nu_2 = 0.25, h = 0.1m,$$

corresponding to a thin epoxy/glass plate, see Norris (1994).

Typically for edge bending waves, one of the attenuation parameters λ_1, λ_2 is close to zero, therefore the exponential decay away from the edge is rather slow, which is clearly confirmed by Fig.3.9.

In addition to this expected behaviour, the obtained representation (3.34) may allow other, non-sinusoidal types of eigensolutions. Let us investigate the wave profile caused by arbitrary initial conditions.

According to (3.1) the deflection may be expressed in terms of the function $W_1(\xi, \lambda_1\eta, \tau)$, being harmonic in the first two arguments, satisfying

$$\frac{\partial^2 W_1}{\partial \eta^2} + \lambda_1^2 \frac{\partial^2 W_1}{\partial \xi^2} = 0, \tag{3.37}$$

along with the beam-like assumption

$$\gamma^4 \frac{\partial^4 W_1}{\partial \xi^4} + \frac{\partial^2 W_1}{\partial \tau^2} + \beta W_1 = 0, \tag{3.38}$$

subject to the following initial conditions

$$W_1|_{\tau=0} = A(\xi, \lambda_1\eta), \qquad \frac{\partial W_1}{\partial \tau}|_{\tau=0} = B(\xi, \lambda_1\eta). \tag{3.39}$$

It is clear from (3.37) that $A(\xi, \lambda_1\eta)$and $B(\xi, \lambda_1\eta)$ are harmonic functions.

Applying the Fourier integral transform with respect to longitudinal variable ξ with parameter k, we deduce

$$W_1^F = W_1(k, \tau)\, e^{-\lambda_1\eta|k|}, \tag{3.40}$$

where W_1^F denotes the Fourier transform

$$W_1^F = \int_{-\infty}^{\infty} W_1(\xi, \lambda_1\eta, \tau)\, e^{-ik\xi} d\xi.$$

Using (3.38), we have the following initial value problem for $W_1(k, \tau)$

$$\frac{\partial^2 W_1^F}{\partial \tau^2} + \left(\gamma^4 k^4 + \beta\right) W_1^F = 0, \tag{3.41}$$

subject to

$$W_1^F\,|_{\tau=0}\; = a\left(k\right), \qquad \frac{\partial W_1^F}{\partial \tau}\,|_{\tau=0}\; = b\left(k\right), \tag{3.42}$$

where $a(k)$, $b(k)$ are the initial conditions for the quantity W_1.

Therefore, the solution is given by

$$W_1\left(\xi,\lambda_1\eta,\tau\right) = \frac{1}{2\pi}\int_{-\infty}^{\infty}\left[\frac{b\left(k\right)}{\gamma_1}\sin\left(\gamma_1\tau\right) + a\left(k\right)\cos\left(\gamma_1\tau\right)\right]e^{-\lambda_1\eta|k|+ik\xi}dk, \tag{3.43}$$

where

$$\gamma_1 = \sqrt{\gamma^4k^4+\beta_1}.$$

Let us specify, for example,

$$A\left(\xi,\lambda_1\eta\right) = \frac{A\lambda_1\eta}{\lambda_1^2\eta^2+\xi^2}, \qquad B\left(\xi,\lambda_1\eta\right) = 0, \tag{3.44}$$

corresponding to point load at the edge

$$W_1\,|_{\tau=\eta=0}\; = A\delta\left(\xi\right), \qquad \frac{\partial W_1}{\partial \tau}\,|_{\tau=\eta=0}\; = 0. \tag{3.45}$$

The function W_1 is therefore given by

$$W_1\left(\xi,\lambda_1\eta,\tau\right) = \frac{A}{\pi}\int_0^{\infty}\cos\left(\gamma_1\tau\right)\cos\left(k\xi\right)e^{-\lambda_1\eta k}dk, \tag{3.46}$$

with the deflection following from (3.34).

In case of absence of the foundation ($\beta = 0$) the last formula (3.46) may be simplified to

$$W_1\left(\xi,\lambda_1\eta,\tau\right) = \frac{A}{2\pi}\sum_{m=1}^{2} Re\int_0^{\infty}\exp\left[i\gamma^2\tau k^2 - \left(\lambda_1\eta + (-1)^m i\xi\right)k\right]dk, \tag{3.47}$$

which may be evaluated explicitly through a standard integral, see Prudnikov (1986), yielding

$$\int_0^{\infty} \exp\left(-px^2 - qx\right) dx = \frac{1}{2}\sqrt{\frac{\pi}{p}} \exp\left(\frac{q^2}{4p}\right) \operatorname{erfc}\left(\frac{q}{2\sqrt{p}}\right), \tag{3.48}$$

where

$$\operatorname{Re} p = 0, \; \operatorname{Im} p \neq 0 \;\text{ and } Re\; q > 0.$$

Using the formula (3.48), it is possible to obtain

$$W_s = \frac{4\gamma\sqrt{\pi\tau}}{A} W\left(\xi, \eta, \tau\right), \tag{3.49}$$

where W_s is a scaled deflection and

$$W_s\left(\xi, \eta, \tau\right) = Re\left[e^{i\pi/4} \sum_{m=1}^{2} \left(f\left(\lambda_1\zeta + (-1)^m i\chi\right) - \frac{D_1 - \lambda_1^2 D_y}{D_1 - \lambda_2^2 D_y} f\left(\lambda_2\zeta + (-1)^m i\chi\right)\right)\right], \tag{3.50}$$

with

$$f(z) = e^{z^2}\;, \;\xi = 2\gamma\sqrt{\tau}\chi \;\text{ and }\; \eta = 2\gamma\sqrt{\tau}\zeta.$$

The dependence of the function W_s given by formula (3.50) is shown on the next Fig.3.8, for relative depth of ζ

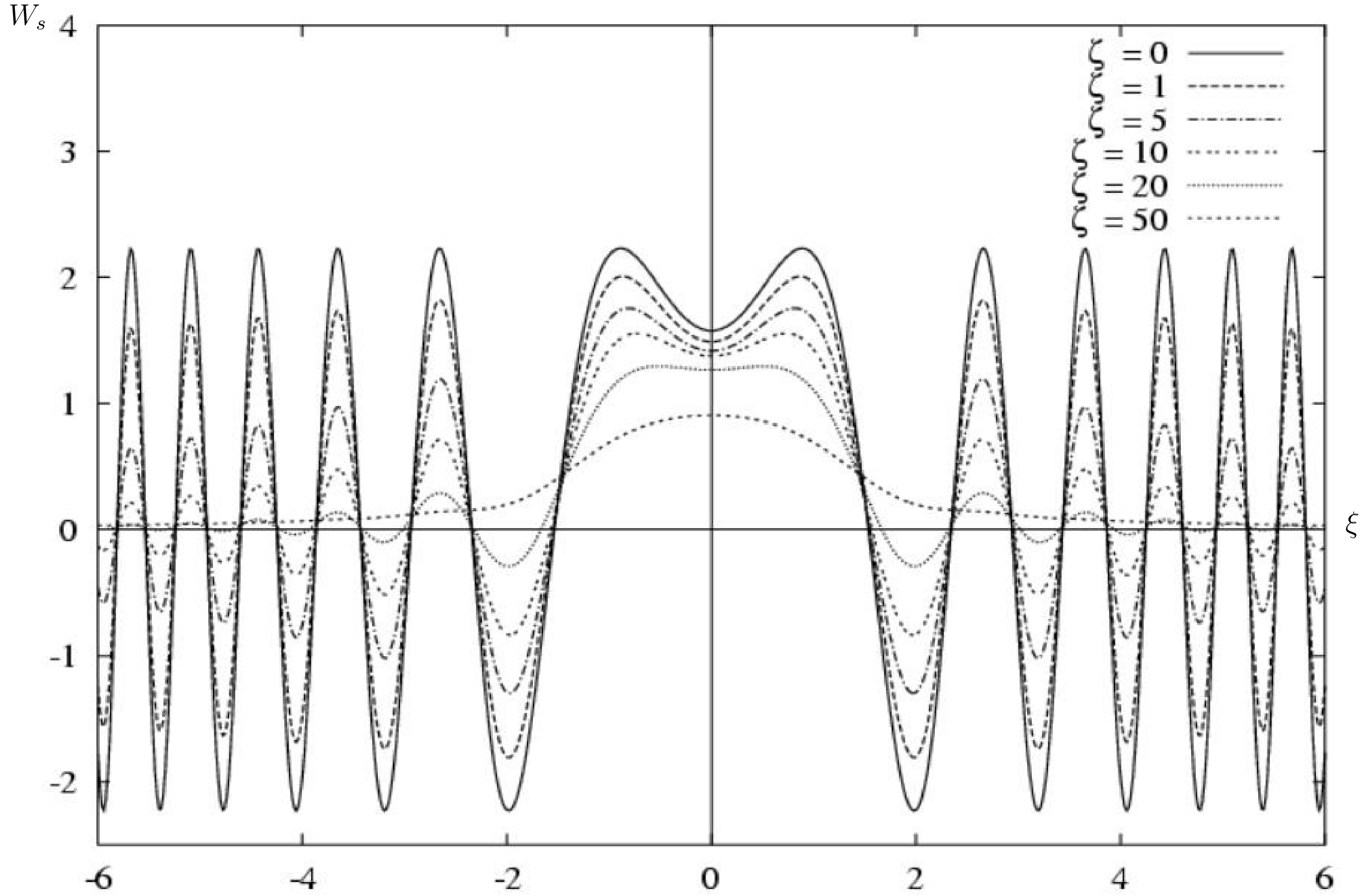

Figure 3.8: Non-sinusoidal profile.

clearly showing a very different type of behaviour compared to Fig. 3.8.

Similarly, the calculations are performed for epoxy glass, with the values of material parameters the same as for Figure 3.9. Indeed, the curves show a more localized type of distribution of deflection along the longitudinal coordinate. Remarkably, the localisation effect increases as we move away from the edge, see for example the curve for $\zeta = 50$. One more observation, from Fig. 3.9, for most of the curves the deflection amplitude decays away from the centre, except for one at the edge $\zeta = 0$.

This may be readily explained, since at $\eta = 0$ the integral (3.47) becomes

$$\int_0^\infty \cos\left(\alpha k^2\right)\cos\left(\beta k\right) dk = \frac{1}{2}\sqrt{\frac{\pi}{\alpha}}\sin\left(\frac{\pi}{4} + \frac{\beta^2}{4\alpha}\right), \tag{3.51}$$

see Prudnikov et al. (1986).

In view of the last formulation (3.51), we deduce for the scaled deflection at the edge $\zeta = 0$ that

$$W_s\left(\chi, 0, \tau\right) = \frac{2D_y\left(\lambda_1^2 - \lambda_2^2\right)}{D_1 - \lambda_2^2 D_y}\sin\left(\frac{\pi}{4} + \chi^2\right). \tag{3.52}$$

Thus, it has been established that the displacement eigensolution for bending edge wave on an orthotropic elastic plate supported by the Winkler-Fuss elastic foundation may be represented in terms of an arbitrary plane harmonic function. The dispersion relation has been analysed, revealing similar features to that of the isotropic Kirchhoff plate considered in Kaplunov et al. (2014). Finally, the presented examples illustrate theoretical possibilities of not only sinusoidal, but also localized profiles.

Chapter 4

Asymptotic model for the bending edge wave on an orthotropic elastic plate resting on the Winkler-Fuss foundation

In this chapter, a derivation of an explicit formulation for the bending edge wave on a thin orthotropic elastic plate resting on a Winkler-Fuss foundation is performed, generalising the results in Kaplunov et al. (2016) for isotropic plates to orthotropic ones. The previously obtained eigensolution, in terms of an arbitrary plane harmonic function see.e.g. (3.34), will serve as a basis for further derivations of asymptotic models oriented at extraction of the contribution of the studied localized waves from the overall dynamic response. The derived model is expected to provide efficient approximate solutions to a number of dynamic problems (including those for moving loads) where the contribution of edge wave is dominant over that bulk waves.

The proposed models are obtained through a multi-scale perturbation scheme, also employing properties of plane harmonic functions, in particular the Cauchy-Riemann identities. The resulting formulation for the bending edge wave field includes elliptic partial differential equations, describing the decay away from the edge, along with the parabolic equations on the edge associated with wave propagation. Then, we analyse steady motion of a point moment along the edge of the plate, observing the resonant regime. In addition, a beam-like behaviour on the edge is revealed, which might be expected from the derived parabolic-elliptic formulation for the bending edge wave.

4.1 Explicit model formulation

In this section, we derive an asymptotic model for the bending edge wave on an orthotropic elastic plate resting on the Winkler-Fuss foundation. First, a multi-scale slow time perturbation of the eigensolution is performed. Then, in both cases of boundary conditions at the edge, namely, the case of forcing moment and shear forcing, the elliptic behaviour over the interior is complemented by a parabolic beam-like equation on the edge, corresponding to propagation of the wave.

4.1.1 Perturbation scheme

Now that the results in section 3.2, expressing the wave field in terms of a single plane harmonic function, have been established, we proceed with the development of an explicit model for the bending edge wave. In parallel with Kaplunov et al. (2016), our starting point is a multiple scale procedure.

Let us perturb equation (3.1) around the edge wave eigensolution.

We introduce fast ($\tau_f = \tau$) and slow ($\tau_s = \epsilon\tau$) time variables accordingly, where $\epsilon \ll 1$ is a small parameter, therefore

$$\frac{\partial^2}{\partial \tau^2} = \frac{\partial^2}{\partial \tau_f^2} + 2\epsilon \frac{\partial^2}{\partial \tau_f \partial \tau_s} + \epsilon^2 \frac{\partial^2}{\partial \tau_s^2}. \tag{4.1}$$

We remark that the slow time perturbation scheme my be interpreted from a physical point of view as a focus on frequencies which are close to those frequencies of the homogeneous bending edge wave. In other words it means that the deviation of the phase speed of the analysed motion from that of the homogeneous edge wave is small.

The deflection W is then expanded in an asymptotic series as

$$W = \frac{h^2 p}{\epsilon D_x}\left(W^{(0)} + \epsilon W^{(1)} + ...\right), \tag{4.2}$$

where

$$p = \max_{x,t}\,[M(x,t), hN(x,t)].$$

Next, we substitute (4.2) into (3.1) having at leading order

$$\left(\frac{\partial^4}{\partial\zeta^4} + \frac{2H}{D_y}\frac{\partial^4}{\partial\xi^2\partial\zeta^2}\right)W^{(0)} + \frac{D_x}{D_y}\left(\frac{\partial^4}{\partial\xi^4} + \beta^*\right)W^{(0)} + \frac{\partial^2 W^{(0)}}{\partial\tau_f^2} = 0. \tag{4.3}$$

Using the beam-like assumption,

$$\gamma^4\frac{\partial^4 W^{(0)}}{\partial\xi^4} + \frac{\partial^2 W^{(0)}}{\partial\tau_f^2} + \beta^* W^{(0)} = 0, \tag{4.4}$$

equation (4.3) may then be rewritten in an operator form as

$$\Delta_1\Delta_2 W^{(0)} = 0, \tag{4.5}$$

where

$$\Delta_j = \partial_\zeta^2 + \lambda_j^2\partial_\xi^2, \qquad j = 1, 2, \quad \lambda_j^2 = \frac{H}{D_y} + (-1)^j\frac{\kappa}{2}$$

and

$$\kappa = 2\sqrt{\frac{H^2}{D_y^2} - \left(\frac{D_x}{D_y} - \gamma^4\right)}.$$

The solution of (4.3) is then given by

$$W^{(0)} = \sum_{j=1}^{2} W_j^{(0)}(\xi, \lambda_j\zeta, \tau_f, \tau_s), \tag{4.6}$$

where W_j, $(j = 1, 2)$ are harmonic in the first two arguments, and the decay as $\zeta \to \infty$ is supposed.

At the next order we obtain from (4.1)

$$\left(\frac{\partial^4}{\partial\zeta^4} + \frac{2H}{D_y}\frac{\partial^4}{\partial\xi^2\zeta^2}\right)W^{(1)} + \frac{D_x}{D_y}\left(\frac{\partial^4}{\partial\xi^4} + \beta^*\right)W^{(1)} + \frac{\partial^2 W^{(1)}}{\partial\tau_f^2} + 2\frac{\partial^2 W^{(0)}}{\partial\tau_f\partial\tau_s} = 0, \qquad (4.7)$$

which, in view of the beam like assumption, may be re-written as

$$\Delta_1\Delta_2 W^{(1)} = -2\frac{\partial^2 W_j^{(0)}}{\partial\tau_f\partial\tau_s} \qquad (j = 1, 2). \qquad (4.8)$$

The next order solution is then given by a combination of harmonic functions, yielding

$$W^{(1)} = W_1^{(1)} + W_2^{(1)}. \qquad (4.9)$$

Further analysis of (4.8) requires separate consideration for both functions $W_j^{(1)}$, $j = 1, 2$. Using the properties of harmonic functions, we deduce an auxiliary relation for the first function

$$\Delta_2 W_1^{(0)} = \left[\frac{\partial^2}{\partial\xi^2} + \lambda_2^2\frac{\partial^2}{\partial\xi^2}\right]W_1^{(0)} = (\lambda_2^2 - \lambda_1^2)\frac{\partial^2 W_1^{(0)}}{\partial\xi^2} = -\kappa\frac{\partial^2 W_1^{(0)}}{\partial\xi^2}, \qquad (4.10)$$

and

$$\Delta_1 W_2^{(0)} = -\kappa\frac{\partial^2 W_2^{(0)}}{\partial\xi^2}. \qquad (4.11)$$

In view of assumption (4.4), differentiating equation (4.8) twice with respect to ξ, we deduce

$$\Delta_1\Delta_2\frac{\partial^2 W_1^{(1)}}{\partial\xi^2} = -\frac{1}{\gamma^2}\Delta_2\frac{\partial^2 W_1^{(0)}}{\partial\tau_f\partial\tau_s}, \qquad (4.12)$$

from which

$$\Delta_1 \frac{\partial^3 W_1^{(1)}}{\partial \xi^2 \partial \zeta} = -\frac{1}{\gamma^2} \frac{\partial^3 W_1^{(0)}}{\partial \tau_f \partial \tau_s \partial \zeta}. \tag{4.13}$$

It is convenient to continue the process for the derivative $\Phi_j^{(1)} = \dfrac{\partial W_j^{(1)}}{\partial \zeta}$, resulting in

$$\frac{\partial W_j^{(1)}}{\partial \xi} = \Phi_j^{(1,0)} + \zeta \Phi_j^{(1,1)}. \tag{4.14}$$

Then equation (4.13) is rewritten as

$$\Delta_1 \Phi_j^{(1)} = -\frac{1}{\gamma^2} \frac{\partial^3 W_j^{(0)}}{\partial \tau_f \partial \tau_s \partial \zeta}. \tag{4.15}$$

Following Kaplunov et. al (2016), the solution of (4.12) is sought in the form

$$\frac{\partial^3 W_1^{(1)}}{\partial \xi^2 \partial \zeta} = \frac{\partial^3 \Phi_j^{(1,0)}}{\partial \xi^2 \partial \zeta} - \frac{\zeta}{\kappa} \frac{\partial^2 W_1^{(0)}}{\partial \tau_s \partial \tau_f}, \tag{4.16}$$

where $\Phi_1 = \Phi_1\left(\xi, \lambda_1 \zeta, \tau_f, \tau_s\right)$.

Similarly, for the second function, $W_2^{(0)}$, we have

$$\Delta_2 \frac{\partial^3 W_2^{(1)}}{\partial \xi^2 \partial \zeta} = -\frac{1}{\gamma^2} \frac{\partial^2 W_2^{(0)}}{\partial \tau_f \partial \tau_s \partial \zeta}, \tag{4.17}$$

hence

$$\frac{\partial^3 W_2^{(1)}}{\partial \xi^2 \partial \zeta} = \frac{\partial^3 \Phi_2^{(1,0)}}{\partial \xi^2 \partial \zeta} - \frac{\zeta}{\kappa} \frac{\partial^2 W_2^{(0)}}{\partial \tau \partial \tau_f}, \tag{4.18}$$

where $\Phi_2 = \Phi_2\left(\xi, \lambda_1 \zeta, \tau_f, \tau_s\right)$ is also an arbitrary harmonic function.

Finally, we obtain

$$\frac{\partial^3 W}{\partial \xi^2 \partial \zeta} = \frac{h^2 P}{D_x} \left[\frac{\partial^3}{\partial \xi^2 \partial \zeta} \left(\frac{1}{\epsilon} (W_1^{(0)} + W_2^{(0)}) + (\Phi_1^{(1,0)} + \Phi_2^{(1,0)}) \right) - \frac{\zeta}{\kappa} \frac{\partial^2}{\partial \tau_s \partial \tau_f} (W_1^{(0)} - W_2^{(0)}) + ... \right]. \tag{4.19}$$

4.1.2 Parabolic equation on the edge

Now we are in position to consider the non-homogeneous boundary conditions (1.24) as

$$\begin{aligned} D_1 \frac{\partial^2 W}{\partial \xi^2} + D_y \frac{\partial^2 W}{\partial \zeta^2} &= \frac{h^2 D_x}{P} M, \\ (D_1 + 4D_{xy}) \frac{\partial^3 W}{\partial \xi^2 \partial \zeta} + D_y \frac{\partial^3 W}{\partial \zeta^3} &= \frac{h^3 D_x}{p} \frac{\partial^2 N}{\partial \xi^2}, \end{aligned} \tag{4.20}$$

where M and N are the prescribed bending moment and shear force respectively.

Now, due to the linearity of the problem, the problem may be split into the two separate sub-problems presented below

(a) Bending moment

We consider the case of an edge bending moment applied at the edge of an orthotropic plate, that is when $N = 0$, $M \neq 0$.

On substituting the asymptotic expansion (4.19) into the boundary conditions (3.27) we have at leading order

$$\begin{aligned} &(D_1 - \lambda_1^2 D_y) \frac{\partial^2 W_1^{(0)}}{\partial \xi^2} + (D_1 - \lambda_2^2 D_y) \frac{\partial^2 W_2^{(0)}}{\partial \xi^2} = 0 \\ &(\lambda_1^3 D_y - \lambda_1 (D_1 + 4D_{xy})) \frac{\partial^3 W_1^{(0)}}{\partial \xi^3} + (\lambda_2^3 D_y - \lambda_2 (D_1 + 4D_{xy})) \frac{\partial^3 W_2^{(0)}}{\partial \xi^3} = 0, \end{aligned} \tag{4.21}$$

which leads, after some transformation, to a dispersion relation in the form

$$\lambda_1 \lambda_2 = \left(\frac{4D_{xy}^2 + D_1^2 - 2D_{xy}}{D_y} \right), \tag{4.22}$$

as a condition for existence of non-trivial solutions.

At next order, the boundary conditions (1.23) are given by

$$
\begin{aligned}
&D_1 \frac{\partial^2 W_1^{(1)}}{\partial \xi^2} + D_1 \frac{\partial^2 W_2^{(1)}}{\partial \xi^2} + D_y \frac{\partial^2 W_1^{(1)}}{\partial \zeta^2} + D_y \frac{\partial^2 W_2^{(1)}}{\partial \zeta^2} = \frac{h^2 D_x}{P} M, \\
&(D_1 + 4D_{xy}) \frac{\partial^3 W_1^{(1)}}{\partial \xi^2 \partial \zeta} + (D_1 + 4D_{xy}) \frac{\partial^3 W_2^{(1)}}{\partial \xi^2 \partial \zeta} \\
&+ D_y \frac{\partial^3 W_1^{(1)}}{\partial \zeta^3} + D_y \frac{\partial^3 W_2^{(1)}}{\partial \zeta^3} = 0.
\end{aligned}
\tag{4.23}
$$

It may be deduced from the relations (4.13) and (4.17) that

$$
\frac{\partial^4 W_1^{(1)}}{\partial \xi^4} = \frac{1}{\lambda_1^2} \left(-\frac{1}{\gamma^2} \frac{\partial^2 W_1^{(0)}}{\partial \tau_f \partial \tau_s} - \frac{\partial^4 W_1^{(1)}}{\partial \xi^2 \partial \zeta^2} \right). \tag{4.24}
$$

Similarly,

$$
\frac{\partial^4 W_2^{(1)}}{\partial \xi^4} = \frac{1}{\lambda_2^2} \left(\frac{1}{\gamma^2} \frac{\partial^2 W_2^{(0)}}{\partial \tau_f \partial \tau_s} - \frac{\partial^4 W_2^{(1)}}{\partial \xi^2 \partial \zeta^2} \right). \tag{4.25}
$$

Using (4.19), we may rewrite the boundary conditions (4.23) as

$$
\begin{aligned}
&D_1 \left[\frac{\partial^4}{\partial \xi^4} \left(W_1^{(1)} + W_2^{(1)} \right) \right] + D_y \left[\frac{\partial^4}{\partial \xi^2 \partial \zeta^2} \left(\Phi_1^{(1,0)} + \Phi_2^{(1,0)} \right) \right] = \frac{D_x}{p} \frac{\partial^2 M}{\partial \xi^2}, \\
&(D_1 + 4D_{xy}) \left[\frac{\partial^5}{\partial \xi^4 \partial \zeta} \left(\Phi_1^{(1,0)} + \Phi_2^{(1,0)} \right) - \frac{1}{\gamma^2} \frac{\partial^3}{\partial \tau_f \partial \tau_s \partial \zeta} \left(W_1^{(0)} + W_2^{(0)} \right) \right] \\
&+ D_y \left[\frac{\partial^5}{\partial \xi^2 \partial \zeta^3} \left(\Phi_1^{(1,0)} + \Phi_2^{(1,0)} \right) \right] = 0.
\end{aligned}
\tag{4.26}
$$

Employing the Cauchy-Riemann identities (2.16) for a plane harmonic function and substituting into the boundary conditions (4.26), we may establish that

$$
\begin{aligned}
&(D_1-\lambda_1^2 D_y)\frac{\partial^4\Phi_1^{(1,0)}}{\partial\xi^4}+(D_1-\lambda_2^2 D_y)\frac{\partial^4\Phi_2^{(1,0)}}{\partial\xi^4}=\frac{D_1}{\gamma^2}\left[\frac{1}{\lambda_1^2}\frac{\partial^2 W_1^{(0)}}{\partial\tau_f\tau_s}+\frac{1}{\lambda_2^2}\frac{\partial^2 W_2^{(0)}}{\partial\tau_f\tau_s}\right]-\frac{D_x}{p}\frac{\partial^2 M}{\partial\xi^2}\\
&(D_1+4D_{xy})\ \left[\lambda_1\frac{\partial^4\Phi_1^{(1,0)}}{\partial\xi^4}+\lambda_2\frac{\partial^4\Phi_2^{(1,0)}}{\partial\xi^4}\right]=\left[\frac{1}{\gamma^2}\frac{\partial^2}{\partial\tau_f\tau_s}\left(\lambda_1 W_1^{(0)}+\lambda_2 W_2^{(0)}\right)\right]+D_y\\
&\qquad\qquad\qquad\qquad\qquad\qquad\qquad\left[\lambda_1^3\frac{\partial^4\Phi_1^{(1,0)}}{\partial\xi^4}+\frac{\lambda_2^3\partial^4\Phi_2^{(1,0)}}{\partial\xi^4}\right].
\end{aligned}
\tag{4.27}
$$

From the solvability of equation (4.21), and after some transformations, we have

$$
\sum_{j=1}^{2}\left(\lambda_j^2(D_1+4D_{xy})-D_1\right)\left[1-\frac{D_1-\lambda_i^2 D_y}{D_1-\lambda_j^2 D_y}\right]\frac{\partial^2 W_j^{(0)}}{\partial\tau_f\partial\tau_s}=\gamma^2\lambda_1\left[(D_1+4D_{xy})+\lambda_1^2 D_y\right]\frac{D_x}{p}\frac{\partial^2 M}{\partial\xi^2},
\tag{4.28}
$$

where $1\leq i\neq j\leqslant 2$.

Now we use the representation of the wave field in terms of a single harmonic function, expressing the deflection W on the edge ζ as

$$
W^{(0)}=\left(1-\frac{D_1-\lambda_1^2 D_y}{D_1-\lambda_2^2 D_y}\right)W_1^{(0)}(\xi,0,t).
\tag{4.29}
$$

Finally, using formula (3.32), we obtain from (4.28), that

$$
\frac{\partial^2 W^{(0)}}{\partial\tau_f\partial\tau_s}=\frac{QD_x}{2p}\frac{\partial^2 M}{\partial\xi^2}
\tag{4.30}
$$

where Q is a material constant depending on D_x, D_y, D_1 and D_{xy} with E and ν as

$$
Q=\frac{\gamma^2\lambda_1\left[(D_1+4D_{xy})+\lambda_1^2 D_y\right]}{A_1-A_2},\quad A_i=\left[\lambda_i(D_1+4D_{xy})-D_1\right]\left[1-\frac{D_1-\lambda_i^2 D_y}{D_1-\lambda_j^2 D_y}\right].
\tag{4.31}
$$

As will be shown later, the coefficient Q is rather important, appearing in the right hand side of a parabolic equation on the edge, see (4.35).

It may be shown that Q could be expressed in simplified form as

$$Q = \frac{\chi\,(\chi + D_1)}{D_y(\chi + 2D_{xy})}, \tag{4.32}$$

with

$$\chi = \sqrt{D_x D_y (1 - \gamma^4)}.$$

In Figs.4.1-4.3 behaviour of the coefficient Q (4.32) on the material parameters is illustrated, with the values of material parameters given in captions.

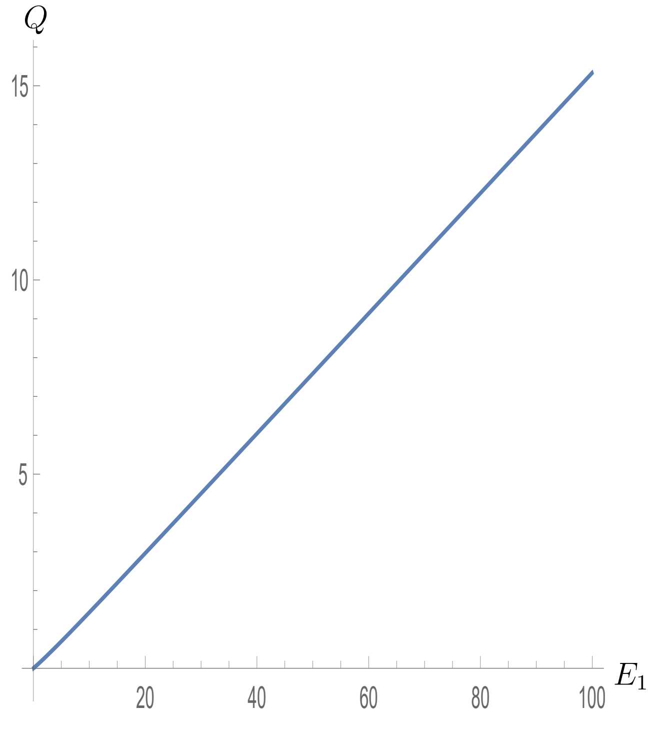

Figure 4.1: The coefficient Q vs. the material constant E_1, GPa for $E_2 = 18.1$GPa, $\nu_1 = 0.25, h = 0.1m$.

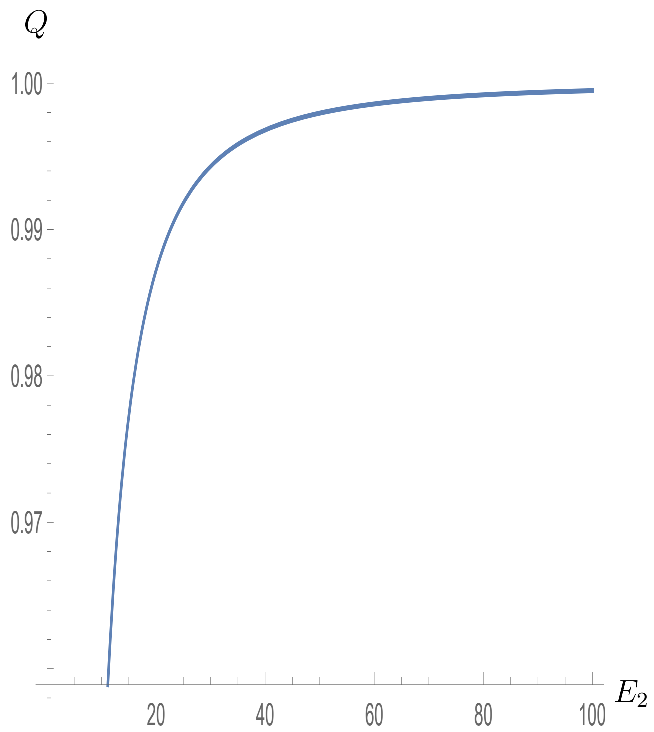

Figure 4.2: The coefficient Q vs. the material constant E_2, GPa for $E_1 = 54.2$GPa, $\nu_1 = 0.25, h = 0.1m$.

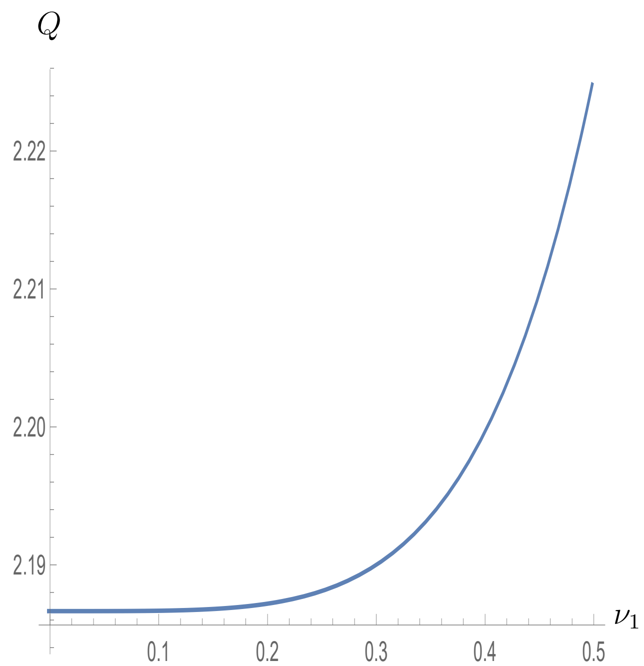

Figure 4.3: The coefficient Q vs. the material constant ν_1 for $E_1 = 54.2$GPa, $E_2 = 18.1$GPa, $h = 0.1m$.

.

As may be seen from all Figs. 4.1-4.3, the coefficient Q is an increasing function of E_1, E_2 and ν_1. We also note that Fig 4.3 is rather similar to Fig 2.3 for an isotropic plate.

Applying the leading-order approximation

$$W \approx \frac{h^2 P}{\epsilon D_x} W^{(0)}, \tag{4.33}$$

and using the relation (3.23), equation (4.30) can be transformed to a parabolic equation at the edge

$$D_x \gamma^4 \frac{\partial^4 W}{\partial \xi^4} + \frac{\partial^2 W}{\partial \tau^2} + 2\epsilon \frac{\partial^2 W^{(0)}}{\partial \tau_f \partial \tau_s} + \beta W = Q \frac{\partial^2 M}{\partial \xi^2}. \tag{4.34}$$

Returning back to the original coordinates x, y and t, (4.34) takes the form of a parabolic beam-like equation along the edge $y = 0$, namely

$$D_x \gamma^4 \frac{\partial^4 W}{\partial x^4} + 2\rho h \frac{\partial^2 W}{\partial t^2} + \beta W = Q \frac{\partial^2 M}{\partial x^2}. \tag{4.35}$$

Thus, for the bending edge wave excited by the given bending moment M the wave field at $y = 0$ is governed by a parabolic equation (4.35).

The decay over the interior is described by the elliptic equation

$$\frac{\partial^2 W_1}{\partial y^2} + \lambda_1^2 \frac{\partial^2 W_1}{\partial x^2} = 0, \tag{4.36}$$

with the resulting deflection W found from (3.34).

As a result, we have a simpler formulation for a scaled Laplace equation, not a bi-harmonic one. Thus, we established a dual parabolic-elliptic nature of the studied wave, with the solution of the parabolic equation (4.35) serving as a boundaru value for elliptic equation (4.36).

(b) Shear force

A similar formulation may be derived for the second type of boundary conditions (4.20), now with $M = 0$, $N \neq 0$, corresponding to a shear force excitation

$$\begin{aligned} & D_1 \frac{\partial^2 W}{\partial \xi^2} + D_y \frac{\partial^2 W}{\partial \zeta^2} = 0, \\ & (D_1 + 4D_{xy}) \frac{\partial^3 W}{\partial \xi^2 \partial \zeta} + D_y \frac{\partial^3 W}{\partial \zeta^3} = \frac{h^3 D_x}{p} N. \end{aligned} \tag{4.37}$$

The analysis is rather similar to that presented in the previous subsection. The dispersion relation follows from the leading order boundary conditions, with the following system obtained at the next order

$$\begin{aligned} & D_1 \frac{\partial^2 W_1^{(1)}}{\partial \xi^2} + D_1 \frac{\partial^2 W_2^{(1)}}{\partial \xi^2} + D_y \frac{\partial^2 W_1^{(1)}}{\partial \zeta^2} + D_y \frac{\partial^2 W_2^{(1)}}{\partial \zeta^2} = 0, \\ & (D_1 + 4D_{xy}) \frac{\partial^3 W_1^{(1)}}{\partial \xi^2 \partial \zeta} + (D_1 + 4D_{xy}) \frac{\partial^3 W_2^{(1)}}{\partial \xi^2 \partial \zeta} \\ & + D_y \frac{\partial^3 W_1^{(1)}}{\partial \zeta^3} + D_y \frac{\partial^3 W_2^{(1)}}{\partial \zeta^3} = \frac{h^2 D_x}{P} N. \end{aligned} \tag{4.38}$$

Substituting solution (4.19) into (4.37), we deduce

$$\begin{aligned} & D_1 \left[\frac{\partial^4}{\partial \xi^4} \left(W_1^{(1)} + W_2^{(1)} \right) \right] + D_y \left[\frac{\partial^4}{\partial \xi^2 \partial \zeta^2} \left(\Phi_1^{(1,0)} + \Phi_2^{(1,0)} \right) \right] = 0, \\ & (D_1 + 4D_{xy}) \left[\frac{\partial^5}{\partial \xi^4 \partial \zeta} \left(\Phi_1^{(1,0)} + \Phi_2^{(1,0)} \right) - \frac{1}{\gamma^2} \frac{\partial^3}{\partial \tau_f \partial \tau_s \partial \zeta} \left(W_1^{(0)} + W_2^{(0)} \right) \right] + \\ & D_y \left[\frac{\partial^5}{\partial \xi^2 \partial \zeta^3} \left(\Phi_1^{(1,0)} + \Phi_2^{(1,0)} \right) \right] = \frac{h^3 D_x}{p} \frac{\partial^2 N}{\partial \xi^2}. \end{aligned} \tag{4.39}$$

It worth notice that this system does not lead to a parabolic beam equation for the deflection W. Instead it provides an equation for the rotation angle $\theta = \dfrac{\partial W}{\partial y}$ evaluated at the edge y =0, namely

$$D_x \gamma^4 \frac{\partial^4 \theta}{\partial x^4} + 2\rho h \frac{\partial^2 \theta}{\partial t^2} + \beta W = Q \frac{\partial^2 N}{\partial x^2}, \tag{4.40}$$

with the constant Q defined in (4.32).

The resulting explicit model for the shear edge force is similar to that obtained in respect of a bending moment. It contains the elliptic equation

$$\frac{\partial^2 \theta_i}{\partial y^2} + \lambda_2^2 \frac{\partial^2 \theta_i}{\partial x^2} = 0. \tag{4.41}$$

Thus, for the bending edge moment excitation the parabolic-elliptic model is comprised of (4.35) and (4.36), whereas in case of the shear force excitation, the explicit formulation for bending edge wave consists of an elliptic equation (4.40) and a parabolic equation (4.41).

4.2 Implementation of the model

Consider now model examples for illustrating the implementation of the formulation developed in above section, in particular, including near-resonant excitation and moving loads.

4.2.1 Comparison with exact solution

Let us consider the problem of moment excitation having the governing equation (3.1), subject to boundary condition (3.27). Then, by applying the Laplace transform to (3.22) with respect to scaled time τ, and Fourier integral transform with respect to longitudinal variable ξ, we have

$$D_y \frac{d^4 W^{FL}}{d\eta^4} - 2Hp^2 \frac{d^2 W^{FL}}{d\eta^2} + D_x \left(p^4 + s^2 + \beta\right) W^{FL} = 0, \tag{4.42}$$

where p and s are the parameters of Fourier and Laplace transforms, respectively, and W^{FL} the transformed deflection.

For decaying solution of (4.42) we require

$$W^{FL} = C_1 e^{-\mu_1 \eta} + C_2 e^{-\mu_2 \eta}, \tag{4.43}$$

where C_1 and C_2 are arbitrary constants, and

$$\mu_1^2 + \mu_2^2 = \frac{2Hp^2}{D_y}, \quad \mu_1^2 \mu_2^2 = \frac{D_x p^4 - s^2 + \beta}{D_y}. \tag{4.44}$$

Then the boundary conditions (3.27) are transformed to

$$\begin{aligned} D_y \frac{\partial^2 W^{FL}}{\partial \eta^2} - D_1 p^2 W^{FL} &= -M_0^{FL}, \\ D_y \frac{\partial^3 W^F}{\partial \eta^3} - (D_1 + 4D_{xy}) p^2 \frac{\partial W^F}{\partial \eta} &= 0, \end{aligned} \tag{4.45}$$

where M^{FL} is the transformed moment M.

On substituting the solution (4.43) into the boundary conditions (3.27), it is possible to determine the constants C_1 and C_2. The result for the transformed deflection W^{FL} may be expressed as

$$W^{FL} = \frac{\Delta_1}{\Delta} e^{-\mu_1 \eta} + \frac{\Delta_2}{\Delta} e^{-\mu_2 \eta}, \tag{4.46}$$

where

$$\Delta_1 = \begin{vmatrix} -M^{FL} & -D_1 p^2 + D_y \mu_2^2 \\ & \\ 0 & -D_y \mu_2^3 + (D_1 + 4D_{xy})\mu_2 p^2 \end{vmatrix}, \tag{4.47}$$

$$\Delta_2 = \begin{vmatrix} -D_1 p^2 + D_y \mu_1^2 & -M^{FL} \\ & \\ -D_y \mu_1^3 + (D_1 + 4D_{xy})\mu_1 p^2 & 0 \end{vmatrix}, \tag{4.48}$$

and

$$\Delta = \begin{vmatrix} -D_1 p^2 + D_y \mu_1^2 & -D_1 p^2 + D_y \mu_2^2 \\ & \\ -D_y \mu_1^3 + (D_1 + 4D_{xy})\mu_1 p^2 & -D_y \mu_2^3 + (D_1 + 4D_{xy})\mu_2 p^2 \end{vmatrix}. \tag{4.49}$$

Therefore, using the definition (4.44) we establish

$$\Delta_i = (-1^j) M^F \mu_j \left[D_y \mu_j^2 - (D_1 + 4D_{xy}) p^2 \right], i \neq j = 1, 2,$$

and

$$\Delta = (\mu_2 - \mu_1) \left[D_y^2 \mu_1^2 \mu_2^2 - D_y D_1 p^2 (\mu_1^2 + \mu_2^2) + 4 D_y D_{xy} p^2 \mu_1 \mu_2 + p^4 D_1 (D_1 + 4D_{xy}) \right]. \tag{4.50}$$

After some transformations the solution of (4.46) for W^{FL} at the edge $\zeta = 0$ may be found in the form

$$W^{FL} \mid_{\zeta=0} = -\frac{M_0^{FL} (D_1 p^2 + D_y q)}{D_y^2 q^2 + 4 D_y D_{xy} q p^2 - D_1^2 p^4}, \tag{4.51}$$

with

$$q = \mu_1\mu_2 = \sqrt{\frac{D_x}{D_y}p^4(1-\gamma^4)}. \tag{4.52}$$

Note that the pole of the denominator given by

$$s^2 + \beta = -\gamma^4 p^4, \tag{4.53}$$

is associated with the dispersion relation for bending edge wave (3.12).

Approximating the result (4.51) around the pole (4.53), we deduce

$$W^{FL}\,|_{\zeta=0} \approx -\frac{M_0^{FL} p^2 \chi\,(\chi + D_1)}{D_y\,(\chi + 2D_{xy})\,(\beta + D_x\gamma^4 p^4 + s^2)}, \tag{4.54}$$

with

$$\chi = \sqrt{D_x D_y (1-\gamma^4)}\ .$$

which is a transformed solution of the parabolic equation (4.35) rewritten in terms of ξ and τ. Thus, it is concluded that the presented parabolic-elliptic models (4.35) and (4.46) capture the contribution of the bending edge wave field to overall dynamics response.

4.2.2 Near-resonant excitation

Let us consider inhomogeneous boundary conditions and prescribe the edge bending moment in the form of time-harmonic sinusoidal form

$$M = Ae^{-i(kx-\omega t)}, \tag{4.55}$$

with no modified shear force assumed.

This loading allows a particular form of solution of the plate bending equation (3.1), subject to the inhomogeneous boundary conditions (1.24), which can be given as

$$W(x, y, t) = F(y)e^{-i(kx-\omega t)}. \tag{4.56}$$

As a result, the secular equation for the function $F(y)$ is given by

$$\frac{d^4F}{dy^4} - \frac{2D_1 + 4D_{xy}}{D_y}k^2\frac{d^2F}{dy^2} + \left(\frac{D_xk^4 + \beta - 2\rho h\omega^2}{D_yk^4}\right)F = 0. \tag{4.57}$$

The solution of (4.57) is conventionally expressed as a sum of two decaying exponents, i.e.

$$F(y) = \sum_{j=1}^{2} C_j e^{-k\chi_j}, \tag{4.58}$$

with

$$\chi_1^2 + \chi_2^2 = \frac{2D_1 + 4D_{xy}}{D_y}, \quad \chi_1^2\chi_2^2 = \frac{D_xk^4 + \beta - 2\rho h\omega^2}{D_yk^4}. \tag{4.59}$$

It may be easily verified that the attenuation orders χ_j satisfy the dispersion relation (3.12), provided that the χ_j coincide with λ_j.

The arbitrary constants C_1 and C_2 are determined from the boundary conditions (4.20) as

$$C_1 = \frac{\Delta_1^*}{\Delta^*} \quad \text{and} \quad C_2 = \frac{\Delta_2^*}{\Delta^*},$$

where

$$\Delta_j^* = (-1^j)M\ \chi_j\left[D_y\chi_j^2\ - (D_1 + 4D_{xy})k^2\right],$$

and

$$\Delta^* = (\chi_2 - \chi_1)\left[Dy^2\chi_1^2\chi_2^2 - D_y D_1 k^2(\chi_1^2 + \chi_2^2) + 4D_y D_{xy} k^2 \chi_1\chi_2 + k^4 D_1(D_1 + 4D_{xy})\right].$$

The exact solution at the edge is then given by

$$W(x,0,t) = -\frac{A}{D_x k^2}\frac{D_1 k^2 + D_y q}{D_y^2\chi_1^2\chi_2^2 + 4D_y D_{xy}\chi_1\chi_2 - D_1^2}. \tag{4.60}$$

Let us now compare the last formula with that obtained from the approximate formulation derived in (4.35) for the case of edge moment excitation. The related particular solution of equation(4.35) is given by

$$W(x,0,t) = -\frac{AQk^2}{D_x k^4\gamma^4 + \beta - 2\rho h\omega^2}e^{i(kx-\omega t)}, \tag{4.61}$$

with Q defined in (4.32).

It is clear that both exact and approximate formulae (4.60) and (4.61), respectively, display resonant behaviour, provided that the frequency ω and the wave number k satisfy the dispersion relation (3.12).

We will now compare solutions (4.60) and (4.61) when the frequency of the excitation is close to that of the bending edge wave.

Consider a frequency perturbation of the form

$$\omega = \omega_0 + \epsilon\omega_1, \tag{4.62}$$

where

$$\omega_0 = \sqrt{\frac{D_x k^4\gamma^4 + \beta}{2\rho h}},$$

is a eigenfrequency, see (3.12).

As before, we operate with the same type of motion evolving in slow time $\tau = \epsilon t$, which is in line with the asymptotic theory presented in section 4.2.

In view of (4.62) and considering the bending moment evolve in slow time as

$$m(\xi, \tau_f, \tau_s) = \frac{\partial^2 m}{\partial \tau_f \partial \tau_s}, \tag{4.63}$$

satisfying the beam-like equation.

The form of the near-resonant excitation (4.55) gives

$$m = Ae^{ih\left(k\chi_j + (\omega_0 \tau_f + \omega_1 \tau_s)\right)}, \tag{4.64}$$

the simplest example of behaviour (4.61). First, we obtain

$$\chi_1^2 \chi_2^2 = \sqrt{\frac{D_x k^4 + \beta - 2\rho h \omega^2}{D_y k^4}} \approx \lambda_1 \lambda_2 - \frac{2\rho h}{D_x k^4} \frac{\epsilon \omega_0 + \omega_1}{\lambda_1 \lambda_2}. \tag{4.65}$$

On substituting the particular solution (4.60) and using the dispersion relation (3.12), we arrive at

$$\begin{aligned} W(x,0,t) &= -\frac{A}{D_x k^2} \frac{D_1 k^2 + D_y \lambda_1 \lambda_2}{\left[D_y^2 \lambda_1^2 \lambda_2^2 + 4 D_y D_{xy} \lambda_1 \lambda_2 - D_1^2\right] - \dfrac{4\rho h \epsilon \omega_0 \omega_1}{D_x k}} \\ &= \frac{A k^2 \chi \left(\chi + D_1\right)}{4\rho h \epsilon \omega_0 \omega_1 \left(D_y (\chi + 2D_{xy})\right)} = \frac{AQk^2}{4\rho h \epsilon \omega_0 \omega_1}. \end{aligned} \tag{4.66}$$

Thus, this expression coincides with the leading order behaviour of the approximation solution (4.61), indeed we have

$$W(x,0,t) = \frac{AQk^2}{\left[D_x k^4 \gamma^4 + \beta - 2\rho h \omega\right] - 4\rho h \epsilon \omega_0 \omega_1} = \frac{AQk^2}{4\rho h \epsilon \omega_0 \omega_1} \tag{4.67}$$

which matches with (4.66).

4.2.3 Edge moving load

In this subsection we present another related problem, namely, steady-state motion of a bending edge moment and the associated field of the bending edge wave on an orthotropic Kirchhoff plate resting on the Winkler foundation see Fig 4.4.

Due to range of validity of the model we focus on the near-resonant regime. Beam-like behaviour on the edge is revealed, which might be expected from the parabolic-elliptic model derived in the subsection 4.1.

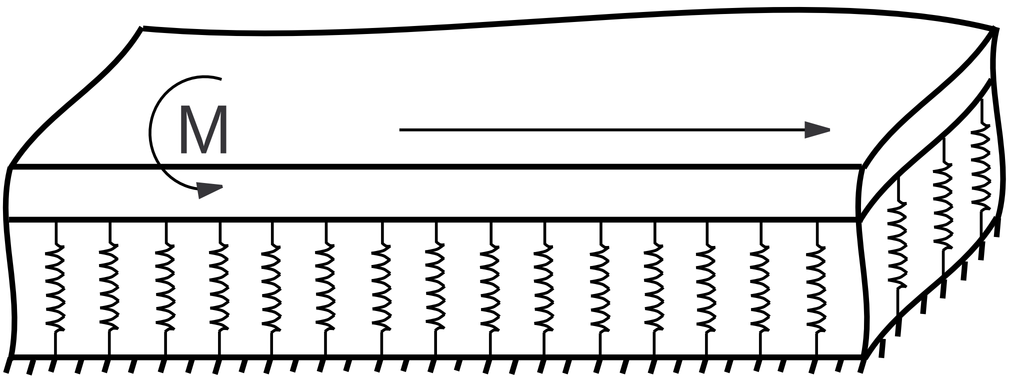

Figure 4.4: Moving along the edge of the plate.

Let us replace the first boundary condition in (1.23) by

$$D_1 \frac{\partial^2 W}{\partial x^2} + D_y \frac{\partial^2 W}{\partial y^2} = -M_0 \delta(x - vt), \tag{4.68}$$

corresponding to a point moment of amplitude M_0 moving along the edge of the plate at a constant speed v. Let us transform to the moving coordinate system $(\xi, y) = (x - vt, y)$.

On applying the Fourier transform with respect to ξ in equation (3.1) and conditions (4.68) , we obtain the following ODE for the transformed deflection W^F

$$D_y \frac{d^4 W^F}{dy^4} - 2Hk^2 \frac{d^2 W^F}{dy^2} + \left(D_x k^4 - 2\rho h v^2 k^2 + \beta\right) W^F = 0, \tag{4.69}$$

subject to the boundary conditions at the edge $y = 0$

$$\begin{aligned} D_y \frac{\partial^2 W^F}{\partial y^2} - D_1 k^2 W^F &= -M_0, \\ D_y \frac{\partial^3 W^F}{\partial y^3} - (D_1 + 4D_{xy}) k^2 \frac{\partial^3 W^F}{\partial y} &= 0, \end{aligned} \tag{4.70}$$

where k is the Fourier parameter.

The decaying solution of (4.69) is given by

$$W^F = C_1 e^{-\mu_1 y} + C_2 e^{-\mu_2 y} \tag{4.71}$$

where C_1 and C_2 are arbitrary constants, and

$$\mu_1^2 + \mu_2^2 = \frac{2Hk^2}{D_y}, \qquad \mu_1^2 \mu_2^2 = \frac{D_x k^4 - 2\rho h v^2 k^2 + \beta}{D_y}. \tag{4.72}$$

On inserting the solution (4.71) into the transformed boundary conditions (4.68), the coefficients C_1 and C_2 may be determined. The solution for W^F at the edge $y = 0$ is then given by

$$W^F\big|_{y=0} = -\frac{M_0^F \left(D_1 k^2 + D_y q\right)}{D_y^2 q^2 + 4 D_y D_{xy} q k^2 - D_1^2 k^4}, \tag{4.73}$$

with $q = \mu_1 \mu_2$, which may be easily rewritten as

$$W^F\big|_{y=0} = -\frac{M_0^F \left(D_1 k^2 + D_y q\right)}{\left(D_y q + 2D_{xy} k^2\right)^2 - \left(D_1^2 + 4D_{xy}^2\right) k^4} \tag{4.74}$$

with

$$\sqrt{D_1^2 + 4D_{xy}^2} - 2D_{xy} = \sqrt{D_x D_y (1-\gamma^4)}.$$

Rearranging (4.74), we have

$$W^F\big|_{y=0} = -\frac{M^F\left(D_1 k^2 + D_y q\right)\left(D_y q + (\sqrt{D_1^2 + 4D_{xy}^2} - 2D_{xy})k^2\right)}{\left(D_y q - k^2(\sqrt{D_1^2 + 4D_{xy}^2} - 2D_{xy})\right)\left(D_y q + k^2(\sqrt{D_1^2 + 4D_{xy}^2} + 2D_{xy})\right)} \tag{4.75}$$

which implies

$$W^F\big|_{y=0} = -\frac{M^F\left(D_1 k^2 + D_y q\right)\left(D_y q + \sqrt{D_x D_y (1-\gamma^4)}k^2\right)}{D_y\left(D_x \gamma^4 k^4 - 2\rho h \nu^2 k^2 + \beta\right)\left(D_y q + k^2(\sqrt{D_1^2 + 4D_{xy}^2} \pm 2D_{xy})\right)}. \tag{4.76}$$

The last formula may be re-written in terms of the dimensionless wave number K and phase speed V as

$$K = \frac{k}{\gamma}\sqrt{\frac{\beta}{D_x}}, \qquad v = \frac{\gamma\sqrt[4]{\beta D_x}}{\sqrt{2\rho h}}V, \tag{4.77}$$

as

$$W^F\big|_{y=0} \approx -\frac{P}{\beta\left(K^4 - V^2K^2 + 1\right)}, \tag{4.78}$$

where

$$P = \sqrt{\frac{\beta^3}{D_y \gamma^4}}\,\frac{M\left(Q + \chi_1 K^2\right)\left(Q + \sqrt{1-\gamma^4}K^2\right)}{\left(Q + \left(\sqrt{1-\gamma^4} + 4\chi_2\right)K^2\right)}, \tag{4.79}$$

with

$$Q = \sqrt{K^4 - \gamma^4\left(K^2V^2 - 1\right)}, \qquad \chi_1 = \frac{D_1}{\sqrt{D_x D_y}}, \qquad \chi_2 = \frac{D_{xy}}{\sqrt{D_x D_y}}. \tag{4.80}$$

It is clear from (4.74) that $V = \sqrt{2}$ corresponds to the resonant speed, confirming the expectations of the section 3.2 Moreover, it may be shown that in the vicinity of the critical values $K = 1$ and $V = \sqrt{2}$ the resulting transformed deflection (4.78) corresponds to the moving load problem for an elastically supported beam specified by

$$D_x \gamma^4 \frac{\partial^4 W}{\partial x^4} + 2\rho h \frac{\partial^2 W}{\partial t^2} + \beta W = P^* \delta(x - \nu t), \tag{4.81}$$

with $P^* = P\big|_{K=1, V=\sqrt{2}}$.

It may be easily verified that in case of a near-resonant excitation, when $M = M_0 \delta(x - vt)$, the Fourier transform of the deflection governed along the edge by (4.35), coincides with that obtained in the previous section, see (4.35), where $P = P^*$.

Thus, parabolic-elliptic model for the bending edge wave on an orthotropic Kirchhff plate resting on the Winkler foundation is derived. It includes the elliptic equation (4.41) and parabolic equation (4.35). The model was illustrated for several cases of loading. In addition, the obtained constant Q_k see (4.32), was studied numerically for different values of the material parameters in order to investigate the effect of anisotropy on propagation of bending edge waves in a Kirchhoff plate resting on a Winkler foundation.

Chapter 5

Effect of inhomogeneous Winkler-Fuss foundation

In the present chapter we extend the results for bending edge wave Kaplunov et al. (2014), to account for the effect of an inhomogeneous Winkler foundation. The periodic Winkler foundation has been studied in a number of contributions, see e.g. Jedrysiak (2003). We also mention related works for corrugated surfaces, see Asfar and Hawwa (1995), Nayfeh and Hawwa (1998) and Hawwa and Asfar (2008), motivated in particular by frequency-filtering applications. The analysis is carried out for both isotropic and orthotropic plates. A multi-scale approach is performed to study the resonant frequencies, as well as the region of wave numbers allowing decaying solution.

5.1 Isotropic plate

In this section we consider bending edge waves, propagating in a semi-infinite isotropic elastic plate resting on an inhomogeneous Winkler foundation .

5.1.1 Statement of the problem

Consider a semi-infinite isotropic elastic plate of thickness $2h$ occupying the domain $-\infty < x < \infty$, $0 \leqslant y < \infty$, $-h \leqslant z \leqslant h$, resting on an inhomogeneous Winkler foundation, see Fig.5.1, with the foundation domain given by $-\infty < x < \infty$,

$0 < y < \infty, 2h \leqslant z < \infty$,

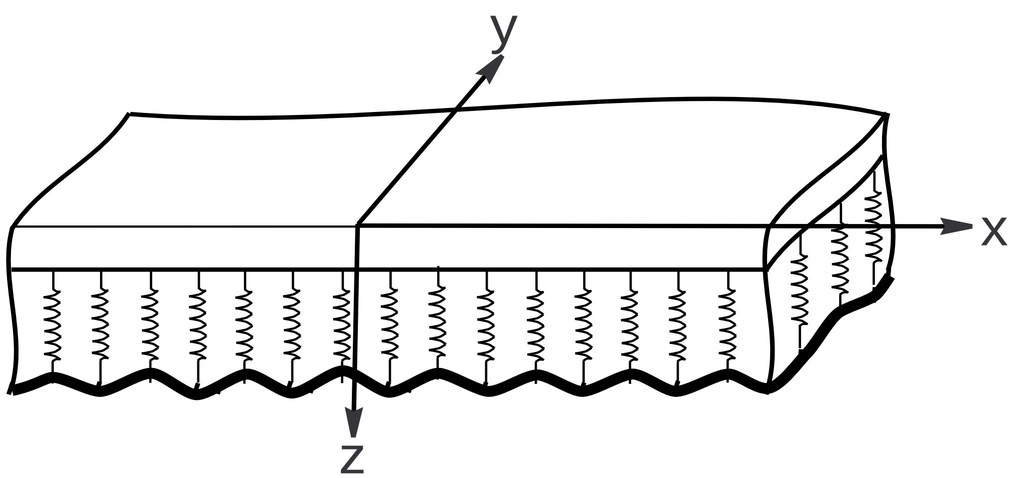

Figure 5.1: Thin elastic plate on a periodic Winkler foundation.

having a periodic modulus of subgrade reaction in the form

$$\beta = \beta_0[1 + \epsilon \sin(k_g x)], \tag{5.1}$$

where β_0 is the average Winkler modules and k_g is the wave number associated with the sinusoidal variation of stiffness of the foundation. Within the framework of the classical Kirchhoff theory, the equation of bending motion in a thin elastic plate, supported by a Winkler foundation, is given by

$$\frac{\partial^4 W}{\partial x^4} + 2\frac{\partial^4 W}{\partial x^2 \partial y^2} + \frac{\partial^4 W}{\partial y^4} + \varphi^4 \frac{\partial^2 W}{\partial t^2} + \gamma_0[1 + \epsilon \sin(k_g x)]W = 0, \tag{5.2}$$

where $\varphi^4 = \dfrac{2\rho h}{D}$ and $\gamma_0 = \dfrac{\beta_0}{D}$.

The boundary conditions at $y = 0$ are taken in the standard form (1.24).

5.1.2 Perturbation procedure

Let us expand the deflection W into asymptotic series as

$$W = W^{(0)} + \epsilon W^{(1)} + \ldots . \tag{5.3}$$

The leading order problem is given by

$$\Delta^2 W^{(0)} + \varphi^4 \frac{\partial^2 W^{(0)}}{\partial t^2} + \gamma W^{(0)} = 0. \tag{5.4}$$

The solution of (5.4) is then expressed as a sum of two decaying exponents, yielding

$$W^{(0)} = \sum_{j=1}^{2} A_j \cos(kx - \omega t) e^{-\lambda_j y}. \tag{5.5}$$

Here k and ω denote wave number and frequency, respectively.

The dispersion relation for the bending edge wave on a semi-infinite Kirchhoff plate supported by a Winkler foundation has the form

$$Dk^4\chi^4 = 2\rho h\omega^2 - \beta_0, \tag{5.6}$$

where c is a well-known constant appearing first in Konenkov (1961), see (2.7), and the attenuation coefficients are given by

$$\lambda_j = k\sqrt{1 + (-1)^j \chi^2}.$$

It should be noted that in view of (5.5) the first boundary condition in (1.24) implies a relation between the constants A_j, i.e.

$$A_2 = \frac{\lambda_1^2 - \nu k^2}{\lambda_2^2 - \nu k^2}\, A_1 = \alpha_0 A_1 \tag{5.7}$$

with

$$\alpha_0 = \frac{1 - \chi^2 - \nu}{1 + \chi^2 - \nu}, \tag{5.8}$$

therefore the leading order solution may be expressed through a single constant, say A_1 as

$$W^{(0)} = A_1 \left(e^{-\lambda_1 y} + \alpha_0 e^{-\lambda_2 y}\right) \cos\left(kx - \omega t\right). \tag{5.9}$$

At the next order, we obtain from (5.2)

$$\frac{\partial^4 W^{(1)}}{\partial x^4} + 2\frac{\partial^4 W^{(1)}}{\partial x^2 \partial y^2} + \frac{\partial^4 W^{(1)}}{\partial y^4} + \gamma W_1 + \varphi^4 \frac{\partial^2 W^{(1)}}{\partial t^2} = -\gamma \sin(k_g x) W^{(0)}, \tag{5.10}$$

subject to boundary conditions at $y = 0$ given by

$$\begin{aligned} &\frac{\partial^2 W^{(1)}}{\partial y^2} + \nu \frac{\partial^2 W^{(1)}}{\partial x^2} = 0, \\ &\frac{\partial^3 W^{(1)}}{\partial y^3} + (2-\nu) \frac{\partial^3 W^{(1)}}{\partial x^2 \partial y} = 0. \end{aligned} \tag{5.11}$$

Equation (5.10) may be written as

$$\begin{aligned} &\frac{\partial^4 W^{(1)}}{\partial x^4} + 2\frac{\partial^4 W^{(1)}}{\partial x^2 \partial y^2} + \frac{\partial^4 W^{(1)}}{\partial y^4} + \gamma W_1 + \varphi^4 \frac{\partial^2 W^{(1)}}{\partial t^2} \\ &\qquad = -\gamma \sin(k_g x) A_j \cos(kx - \omega t) e^{-\lambda_j y} \\ &\qquad = \frac{\gamma A_1}{2} [\sin(k_g - k)x - \omega t) - \sin(k_g + k)x - \omega t)] \left(e^{-\lambda_1 y} + \alpha_0 e^{-} \lambda_2 y\right), \end{aligned} \tag{5.12}$$

implying the following representation corresponding to the two terms in the right hand side as

$$W^{(1)} = W_1^{(1)} + W_2^{(1)}.$$

Let us first deal with the terms in the right hand side associated with $\sin\left[(k_g - k)x - \omega t)\right]$. The corresponding particular solution is sought for in the form

$$W_1^{(1)} = F_1(y) \sin\left((k_g - k)x - \omega t)\right). \tag{5.13}$$

Hence, from (5.12) we deduce an equation for the function F, namely

$$\frac{d^4 F_1}{dy^4} - 2\left(k - k_g\right)^2 \frac{d^4 F_1}{dy^2} + \left[\left((k - k_g\right)^4 - \kappa^4 \omega^2 + \gamma\right] F_1 = \frac{\gamma A_1}{2} \left(e^{-\lambda_1 y} + \alpha_0 e^{-\lambda_2 y}\right). \tag{5.14}$$

The related characteristic equation for (5.14) is

$$m^4 - 2\left(k - k_g\right)^2 m^2 + \left((k - k_g)^4 - \chi^4 k^4\right) = 0, \tag{5.15}$$

from which

$$m_j^2 = (k - k_g)^2 + (-1)^j \chi^2 k^2, \qquad j = 1, 2. \tag{5.16}$$

The decay condition at $y \to \infty$ implies $m_j^2 > 0$, which is satisfied automatically for $j = 2$, and infers the restriction on the ratio of wave numbers for $j = 1$, namely

$$\frac{k_g}{k} \in (0; 1 - \chi) \cup (1 + \chi; \infty). \tag{5.17}$$

Indeed, consider several options for the root m_1^2. It is obvious that if $m_1^2 > 0$, then the positive value of m_1 will provide the exponentially decaying solution. At the same time, if $m_1^2 = 0$ or $m_1^2 < 0$ then the solution $e^{m_1 y}$ will correspond to radiation.

Note that the Bragg resonance, for more details see Brillouin (1953), associated with $k_g = 2k$ is very close to the boundary interval, $1 + \chi \approx 1.99$.

As will be shown later, one of the non-Bragg resonances that we obtain is within the region (5.17), and another one falls outside of the region (5.17), and is associated with radiation.

Thus, in case of $m_j > 0$ $(j = 1, 2)$, the decaying solution of (5.14) is given by

$$F_1(y) = C_1 e^{-m_1 y} + C_2 e^{-m_2 y} + \alpha_1 e^{-\lambda_1 y} + \alpha_0 \alpha_2 e^{-\lambda_2 y}, \tag{5.18}$$

where

$$\alpha_j = \frac{\gamma_1 A_1}{2\left((\lambda_j^2 - (k - kg)^2 - \chi^4 k^4\right)}, \qquad j = 1, 2. \tag{5.19}$$

The values of C_1 and C_2 may now found from the boundary conditions (5.11).

Indeed, on substituting (5.13) with (5.19) into the boundary conditions (5.11), we result in a system of linear equations, which can be presented in a matrix form as

$$\begin{pmatrix} m_1^2 - \nu(k_g-k)^2 & m_2^2 - \nu(k_g-k)^2 \\ \\ m_1\left((2-\nu)(k_g-k)^2 - m_1^2\right) & m_2\left((2-\nu)(k_g-k)^2 - m_2^2\right) \end{pmatrix} \begin{pmatrix} C_1 \\ \\ C_2 \end{pmatrix} \tag{5.20}$$

$$= \alpha_1 A_1 \begin{pmatrix} \lambda_1^2 - \alpha_0\lambda_2^2 + (1+\alpha_0)\nu(k_g-k)^2 \\ \\ \lambda_1^3 - \alpha_0\lambda_2^3 + ((\lambda_1 - \alpha_0\lambda_2)(2-\nu)(k_g-k)^2 \end{pmatrix}.$$

It is possible to determine the constants C_1 and C_2 from above system (5.20), as

$$C_1 = \frac{\Delta_1}{\Delta}, \qquad C_2 = \frac{\Delta_2}{\Delta}, \tag{5.21}$$

where

$$\Delta = \begin{vmatrix} m_1^2 - \nu(k_g-k)^2 & m_2^2 - \nu(k_g-k)^2 \\ \\ m_1\left((2-\nu)(k_g-k)^2 - m_1^2\right) & m_2\left((2-\nu)(k_g-k)^2 - m_2^2\right) \end{vmatrix},$$

$$= (m_1 - m_2)\left[m_1^2 m_2^2 + 2m_1 m_2 (k_g-k)^2(1-\nu) - \nu^2(k_g-k)^4\right]$$

and

$$\Delta_1 = \alpha_1 A_1 \begin{vmatrix} \lambda_1^2 - \alpha_0\lambda_2^2 + (1+\alpha_0)\nu(k_g-k)^2 & m_1^2 - \nu(k_g-k)^2 \\ \\ \lambda_2^3 + (\lambda_1 - \alpha_0\lambda_2)(2-\nu)(k_g-k)^2 & m_2\left((2-\nu)(k_g-k)^2 - m_2^2\right), \end{vmatrix},$$

$$\Delta_2 = \alpha_1 A_1 \begin{vmatrix} m_1^2 - \nu(k_g-k)^2 & \lambda_1^2 - \alpha_0\lambda_2^2 + (1+\alpha_0)\nu(k_g-k)^2 \\ \\ m_2^2 - \nu(k_g-k)^2 & \lambda_2^3 + (\lambda_1 - \alpha_0\lambda_2)(2-\nu)(k_g-k)^2 \end{vmatrix}.$$

Substituting solution (5.16) in (5.21), we have from $\Delta = 0$

$$k^4(1-2\chi^2) - 2k^2(k_g-k)^2(1-\chi^2) + (k_g-k)^4 = 0, \tag{5.22}$$

providing the resonant values

$$r_B = \frac{k_g}{k} = \frac{1}{2} \quad , \quad r_{nB_1} = \frac{k_g}{k} = \frac{\sqrt{2\chi^2+1}-1}{2\chi^2}. \tag{5.23}$$

The first value $k = 2k_g$ is a well-known Bragg resonance, see Brillouin (1953). The second value is seemingly a new result , which we will report to as a non-Bragg resonance.

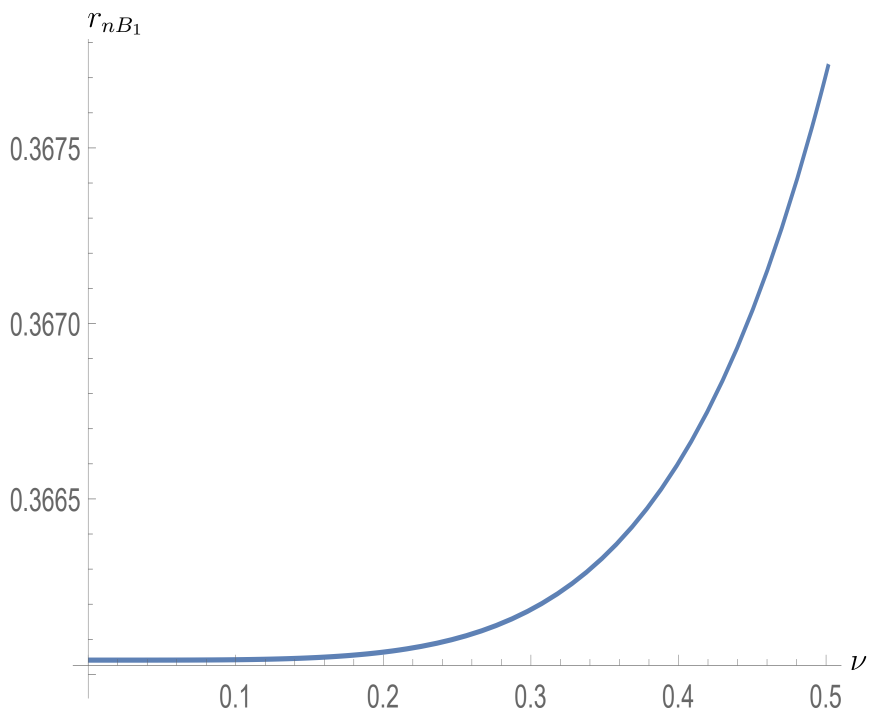

Figure 5.2: Non-Bragg resonant value r_{nB_1} versus the Poisson's ratio ν.

The Fig. 5.2 illustrates dependence of the non-Bragg resonant value r_{nB_1} on the Poisson's ratio. Since χ is close to unity, this non-Bragg resonance happens approximately at $k \sim 0.37k_g$, which belongs to the interval (5.17) allowing decaying solutions. Similarly, for the terms associated with $\sin(k_g + k)x - \omega t$, we have

$$W_2^{(1)} = F_2(y) \sin\left((k_g + k)x - \omega t\right), \tag{5.24}$$

for which

$$\frac{d^4F_2}{dx^4} - 2\left(k+k_g\right)^2 \frac{d^4F_2}{dx^2} + \left[\left((k+k_g\right)^4 - \kappa^4\omega^2 + \gamma\right] F_2 = -\frac{\gamma A_2}{2}\left(e^{-\lambda_1 y} + \alpha_0 e^{-\lambda_2 y}\right), \quad (5.25)$$

hence, the attenuation orders are

$$m_j^2 = (k+k_g)^2 + (-1)^j \chi^2 k^2, \qquad j = 3, 4, \quad (5.26)$$

both allowing decaying solution.

The solution of (5.25) is found as

$$F_2(y) = C_3 e^{-m_3 y} + C_4 e^{-m_4 y} + \alpha_1 e^{-\lambda_1 y} + \alpha_0 \alpha_2 e^{-\lambda_2 y}, \quad (5.27)$$

where

$$\alpha_j = \frac{\gamma A_2}{2\left((\lambda_j^2 - (k+k_g)^2 - \chi^4 k^4\right)}, \qquad j = 1, 2. \quad (5.28)$$

The values of C_3 and C_4 once again can be found from the boundary conditions (4.9), using the Cramer's rule as

$$C_3 = \frac{\Delta_3}{\Delta}, \qquad C_4 = \frac{\Delta_4}{\Delta}, \quad (5.29)$$

where

$$\Delta = \begin{vmatrix} m_1^2 - \nu(k_g+k)^2, & m_2^2 - \nu(k_g+k)^2 \\ m_1\left((2-\nu)(k_g+k)^2 - m_1^2\right), & m_2\left((2-\nu)(k_g+k)^2 - m_2^2\right) \end{vmatrix},$$

$$= (m_1 - m_2)\left[m_1^2 m_2^2 + 2m_1 m_2 (k_g + k)^2 (1-\nu) - \nu^2 (k_g + k)^4\right]$$

and

$$\Delta_3 = \alpha_1 A_1 \begin{vmatrix} \lambda_1^2 - \alpha_0 \lambda_2^2 + (1+\alpha_0)\nu(k_g+k)^2 & m_1^2 - \nu(k_g+k)^2 \\ \lambda_2^3 + (\lambda_1 - \alpha_0\lambda_2)(2-\nu)(k_g+k)^2 & m_2\left((2-\nu)(k_g+k)^2 - m_2^2\right), \end{vmatrix},$$

$$\Delta_4 = \alpha_1 A_1 \begin{vmatrix} m_1^2 - \nu(k_g+k)^2 & \lambda_1^2 - \alpha_0 \lambda_2^2 + (1+\alpha_0)\nu(k_g+k)^2 \\ m_2^2 - \nu(k_g+k)^2 & \lambda_2^3 + (\lambda_1 - \alpha_0\lambda_2)(2-\nu)(k_g+k)^2 \end{vmatrix}.$$

After some algebraic manipulations we establish from $\Delta = 0$

$$k^4(1-2\chi^2) - 2k^2(k_g+k)^2(1-\chi^2) + (k_g+k)^4 = 0, \tag{5.30}$$

with the only positive resonant value being

$$r_{nB_2} = \frac{k_g}{k} = \frac{1+\sqrt{2\chi^2+1}}{2\chi^2}, \tag{5.31}$$

which is again a non-Bragg resonance. Other roots have a negative value, and therefore, have no physical meaning.

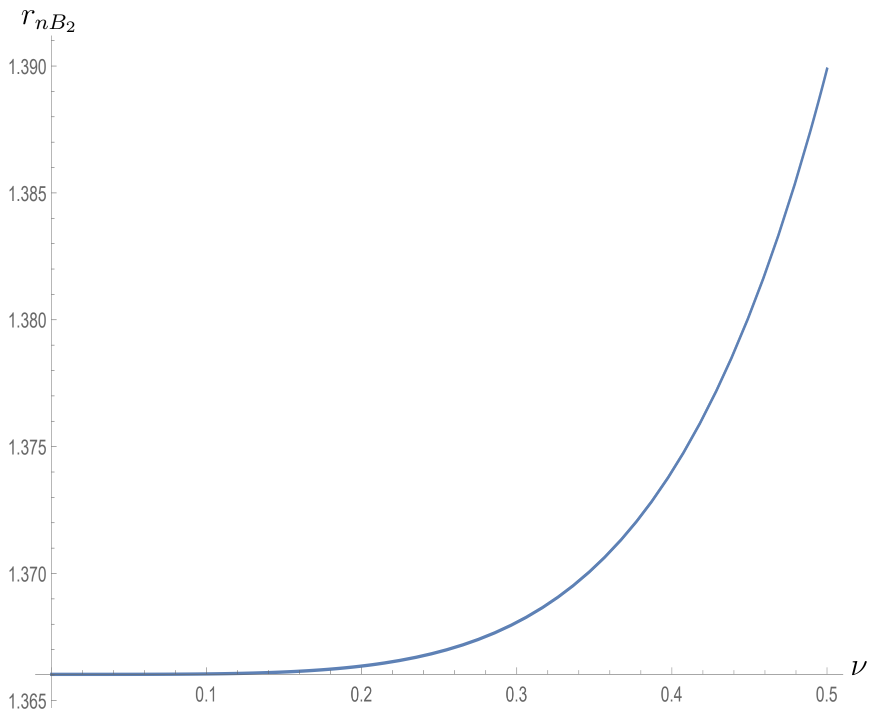

Figure 5.3: The resonant value r_{nB_2} versus the Poisson's ratio ν.

The Fig.5.3 illustrates dependence of the resonant value (5.31) on Poisson's ratio, showing that the value is around $r_{nB_2} \approx 1.38$, which is outside of the region (5.18), being associated with radiation.

In the following Fig 5.4, a typical variation of the function $F_1(y)$ at $y = 0$ on the dimensionless parameter $\dfrac{k}{k_g}$ is presented, with both resonances (5.23) and (5.31) clearly observed.

Let us now study the next order approximation, which follows from (5.2) as

$$\frac{\partial^4 W^{(2)}}{\partial x^4} + 2\frac{\partial^4 W^{(2)}}{\partial x^2 \partial y^2} + \frac{\partial^4 W^{(2)}}{\partial y^4} + \gamma W^{(2)} + \kappa^4 \frac{\partial^2 W^{(2)}}{\partial t^2} = -\gamma \sin(k_g x) W^{(1)}. \tag{5.32}$$

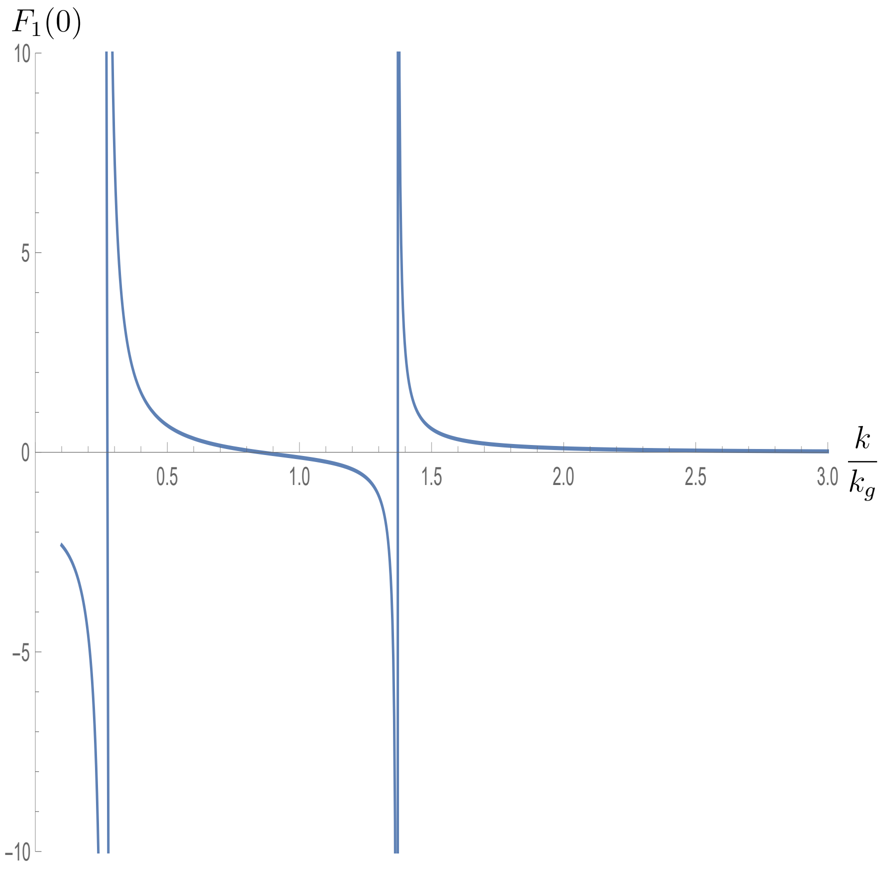

Figure 5.4: Dependence of $F_1(y)$ at $y = 0$ on the dimensionless parameter $\frac{k}{k_g}$

.

The boundary conditions at $y = 0$ are

$$\begin{aligned} \frac{\partial^2 W^{(2)}}{\partial y^2} + \nu \frac{\partial^2 W^{(2)}}{\partial x^2} &= 0, \\ \frac{\partial^3 W^{(2)}}{\partial y^3} + (2-\nu) \frac{\partial^3 W^{(2)}}{\partial x^2 \partial y} &= 0. \end{aligned} \tag{5.33}$$

The right hand side of equation (5.32) can be rewritten as

$$\begin{aligned} &\frac{\partial^4 W^{(2)}}{\partial x^4} + 2\frac{\partial^4 W^{(2)}}{\partial x^2 \partial y^2} + \frac{\partial^4 W^{(2)}}{\partial y^4} + \gamma W^{(2)} + \kappa^4 \frac{\partial^2 W^{(2)}}{\partial t^2} = \\ &-\gamma \sin(k_g x) \left[F_1(y) \sin\left((k_g - k)x - \omega t\right) + F_2(y) \sin\left((k_g + k)x - \omega t\right) \right]. \end{aligned} \tag{5.34}$$

The solution can again be decomposed as

$$W^{(2)} = W_1^{(2)} + W_2^{(2)} \tag{5.35}$$

where

$$W_1^{(2)} = F_1(y)\cos\left((k-2k_g)x-\omega t\right) - F_2(y)\cos(-kx+\omega t), \tag{5.36}$$

and

$$W_2^{(2)} = F_3(y)\cos\left((k+2k_g)x-\omega t\right) - F_4(y)\cos(kx+\omega t). \tag{5.37}$$

The analysis is rather similar to that presented in first order. The $F_1(y)$, the related characteristic equation for (5.34) may be given by

$$m^4 - 2\left(k-2k_g\right)^2 m^2 + \left((k-2k_g)^4 - \chi^4 k^4\right) = 0, \tag{5.38}$$

from which

$$m_j^2 = (k-2k_g)^2 + (-1)^j \chi^2 k^2, \qquad j = 1, 2. \tag{5.39}$$

Substituting the solution (5.36) into the boundary conditions (5.33), it is possible to determine the constants C_1 and C_2.

After some algebraic manipulations we establish

$$\Delta = k^4(1-2\chi^2) - 2k^2(2k_g+k)^2(1-\chi^2) + (k_g+k)^4, \tag{5.40}$$

which has the roots as $\dfrac{k_g}{k} = \pm 1$, see Fig.4, which is higher-order Bragg-resonance, see e.g. Yu and Howard (2010).

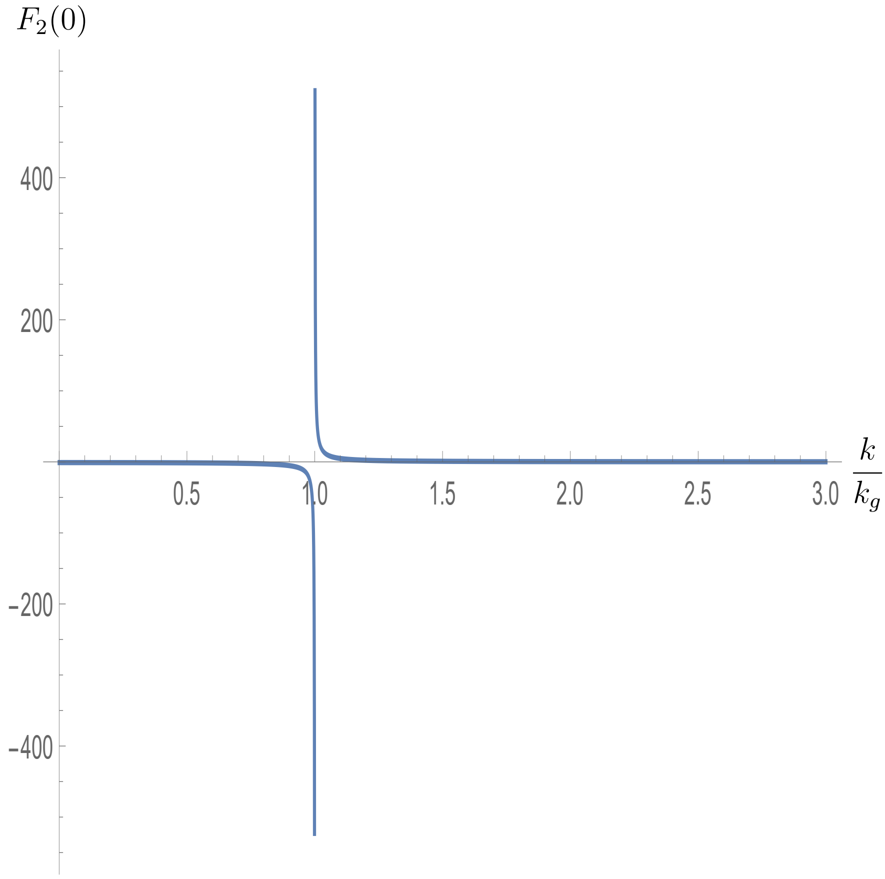

Figure 5.5: Dependence of $F_2(y)$ at $y = 0$ on the dimensionless parameter $\dfrac{k}{k_g}$.

5.2 Orthotropic plate

In this section we investigate a homogeneous edge wave propagating along the edge of a semi-infinite orthotropic plate resting on an inhomogeneous Winkler foundation.

5.2.1 Formulation the problem

Consider a semi-infinite orthotropic elastic plate of thickness $2h$, supported by an inhomogeneous Winkler foundation, occupying the domain $-\infty < x < \infty$, $0 \leqslant y < \infty$, $-h \leqslant z \leqslant h$, resting on an inhomogeneous Winkler foundation, see Fig.5.1, with the foundation domain given by $-\infty < x < \infty, 0 < y < \infty, 2h \leqslant z < \infty$. As introduced in above section the foundation is having a periodic modulus of subgrade reaction as (5.1), the equation of motion is given by

$$D_x \frac{\partial^4 W}{\partial x^4} + 2H \frac{\partial^4 W}{\partial x^2 \partial y^2} + D_y \frac{\partial^4 W}{\partial y^4} + \varphi_o^4 \frac{\partial^2 W}{\partial t^2} + \gamma[1 + \epsilon \sin(k_g x)]W = 0, \tag{5.41}$$

where $\varphi_o^4 = \dfrac{2\rho h}{D_x}$ and the boundary conditions at $y = 0$ are taken in the form (1.23).

5.2.2 Perturbation scheme

A perturbation procedure similar to that in previous section for isotropic direction leads to expansion of the deflection W as

$$W = W^{(0)} + \epsilon W^{(1)} + \dots . \tag{5.42}$$

At leading order we have

$$D_x \frac{\partial^4 W^{(0)}}{\partial x^4} + 2H \frac{\partial^4 W^{(0)}}{\partial x^2 \partial y^2} + D_y \frac{\partial^4 W^{(0)}}{\partial y^4} + \varphi_o^4 \frac{\partial^2 W^{(0)}}{\partial t^2} + \gamma W^{(0)} = 0. \tag{5.43}$$

The solution of (5.41) is then given by a combination of harmonic functions, yielding

$$W^{(0)} = \sum_{j=1}^{2} B_j \cos(kx - \omega t) e^{-\lambda_j y}, \tag{5.44}$$

where k and ω denote wave number and frequency, respectively.

The dispersion relation for the bending edge wave on a semi-infinite orthotropic plate supported by a Winkler foundation has the form (3.12).

At next order we deduce

$$D_x \frac{\partial^4 W^{(1)}}{\partial x^4} + 2H \frac{\partial^4 W^{(1)}}{\partial x^2 \partial y^2} + D_y \frac{\partial^4 W^{(0)}}{\partial y^4} + \varphi_o^4 \frac{\partial^2 W^{(1)}}{\partial t^2} + \gamma W^{(1)} = -\gamma \sin(k_g x) W^{(0)}, \tag{5.45}$$

accompanied by the boundary condition at $y = 0$ given by

$$\begin{aligned} &D_1 \frac{\partial^2 W^{(1)}}{\partial x^2} + D_y \frac{\partial^2 W^{(1)}}{\partial y^2} = 0, \\ &(D_1 + 4D_{xy}) \frac{\partial^3 W^{(1)}}{\partial x^2 \partial y} + D_y \frac{\partial^3 W^{(1)}}{\partial y^3} = 0. \end{aligned} \tag{5.46}$$

Equation (5.45) can be re-cast in the form

$$\begin{aligned} D_x \frac{\partial^4 W^{(1)}}{\partial x^4} + 2H \frac{\partial^4 W^{(1)}}{\partial x^2 \partial y^2} + D_y \frac{\partial^4 W^{(0)}}{\partial y^4} + \varphi_o^4 \frac{\partial^2 W^{(1)}}{\partial t^2} + \gamma W^{(1)} = \\ -\gamma \sin(k_g x) \cos(kx - \omega t) \sum_{j=1}^{2} B_j e^{-\lambda_j y}, \end{aligned} \tag{5.47}$$

with

$$W^{(1)} = W_1^{(1)} + W_2^{(1)}.$$

The analysis is rather similar to that provided in isotropic case. Let us first consider the following solution

$$W_1^{(1)} = F_1(y) \sin\left((k_g - k)x - \omega t\right), \tag{5.48}$$

associated with $\sin((k-k_g)x-\omega t)$.

Hence, equation (5.47) is transformed into a secular equation for the function F_1, namely

$$\frac{d^4F_1}{dy^4}-\frac{2H\left(k-k_g\right)^2}{D_y}\frac{d^2F_1}{dy^2}+\frac{\left[D_x(k-k_g)^4-\varphi_o^4\omega^2+\gamma\right]}{D_y}F_1= \\ \frac{\gamma B_1}{2}\left(e^{-\lambda_1 y}+\alpha_0 e^{-\lambda_2 y}\right), \tag{5.49}$$

The related characteristic equation is

$$m^4-\frac{2H\left(k-k_g\right)^2}{D_y}m^2+\frac{\left[(D_x(k-k_g)^4-\gamma^4k^4\right]}{D_y}=0, \tag{5.50}$$

from which

$$m_j^2=\frac{2H\left(k-k_g\right)^2}{D_y}+(-1)^j\frac{\kappa(k-k_g)^4}{2} \quad \text{and} \quad \kappa=2\sqrt{\frac{H^2}{D_y^2}-\left(\frac{D_x}{D_y}-\gamma^4\right)}, \tag{5.51}$$

where γ is introduced in (3.32), and known from Norris (1994).

The solution of (5.49), decaying away from the edge $y=0$, is then given by

$$F_1(y)=C_1e^{-m_1y}+C_2e^{-m_2y}+\alpha_1e^{-\lambda_1y}+\alpha_0\alpha_2e^{-\lambda_2y}, \tag{5.52}$$

The values of C_1 and C_2 can be found from the boundary conditions (1.23).

The substitution of the solution (5.52) into the boundary conditions (5.46). This leads to a system of linear equations for unknowns C_1 and C_2, can be written in a matrix form as

$$\begin{pmatrix} -D_1(k_g-k)^2+D_ym_1^2, & -D_1(k_g-k)^2+D_ym_2^2 \\ -D_ym_1^3+(D_1+4D_{xy})m_1(k_g-k)^2, & -D_ym_2^3+(D_1+4D_{xy})m_2(k_g-k)^2 \end{pmatrix}\begin{pmatrix} C_1 \\ C_2 \end{pmatrix} \tag{5.53}$$

$$= \alpha_1 B_1 \begin{pmatrix} (\lambda_1^2 - \alpha_0\lambda_2^2)\, D_y + D_1(1+\alpha_0)(k_g-k)^2 \\ \\ (\lambda_1^3 - \alpha_0\lambda_2^3)\, D_y + (D_1+4D_{xy})((\lambda_1-\alpha_0\lambda_2)(k_g-k)^2 \end{pmatrix}.$$

The values of C_1 and C_2 can be found from the boundary conditions (1.23), which can be expressed in the form

$$C_1 = \frac{\Delta_1}{\Delta}, \qquad C_2 = \frac{\Delta_2}{\Delta}, \tag{5.54}$$

where

$$\Delta = \begin{vmatrix} -D_1(k_g-k)^2 + D_y m_1^2 & -D_1(k_g-k)^2 + D_y m_2^2 \\ \\ -D_y m_1^3 + (D_1+4D_{xy})m_1(k_g-k)^2 & -D_y m_2^3 + (D_1+4D_{xy})m_2(k_g-k)^2 \end{vmatrix}, \tag{5.55}$$

and

$$\Delta_1 = \alpha_1 B_1 \begin{vmatrix} (\lambda_1^2 - \alpha_0\lambda_2^2)\, D_y + D_1(1+\alpha_0)(k_g-k)^2 & -D_1(k_g-k)^2 + D_y m_1^2 \\ \\ (\lambda_1^3 - \alpha_0\lambda_2^3)\, D_y + (D_1+4D_{xy})((\lambda_1-\alpha_0\lambda_2)(k_g-k)^2 & -D_1(k_g-k)^2 + D_y m_2^2 \end{vmatrix}, \tag{5.56}$$

$$\Delta_2 = \alpha_1 B_1 \begin{vmatrix} (\lambda_1^2 - \alpha_0\lambda_2^2)\, D_y + D_1(1+\alpha_0)(k_g-k)^2 & -D_1(k_g-k)^2 + D_y m_2^2 \\ \\ -D_1(k_g-k)^2 + D_y m_2^2 & (\lambda_1^3 - \alpha_0\lambda_2^3)\, D_y + (D_1+4D_{xy})((\lambda_1-\alpha_0\lambda_2)(k_g-k)^2 \end{vmatrix}. \tag{5.57}$$

It may be shown that $\Delta = 0$

$$D_y^2 q^2 + 4D_y D_{xy} q (k_g-k)^2 - D_1^2 (k_g-k)^4 = 0, \tag{5.58}$$

where $q = m_1 m_2$, which may be factorised as

$$\left(D_y q - (k_g - k)^2(\sqrt{D_1^2 + 4D_{xy}^2} - 2D_{xy})\right)\left(D_y q + (k_g - k)^2(\sqrt{D_1^2 + 4D_{xy}^2} + 2D_{xy})\right) = 0, \tag{5.59}$$

from which

$$D_y q \chi_0 - \chi_0^2 (k_g - k)^2 = 0, \tag{5.60}$$

therefore the resonant values is

$$\frac{k_g}{k} = 1 - \frac{\chi_0}{D_x(1 - \gamma^4)} \tag{5.61}$$

where $\chi_0 = \sqrt{D_1^2 + 4D_{xy}^2} + 2D_{xy}$.

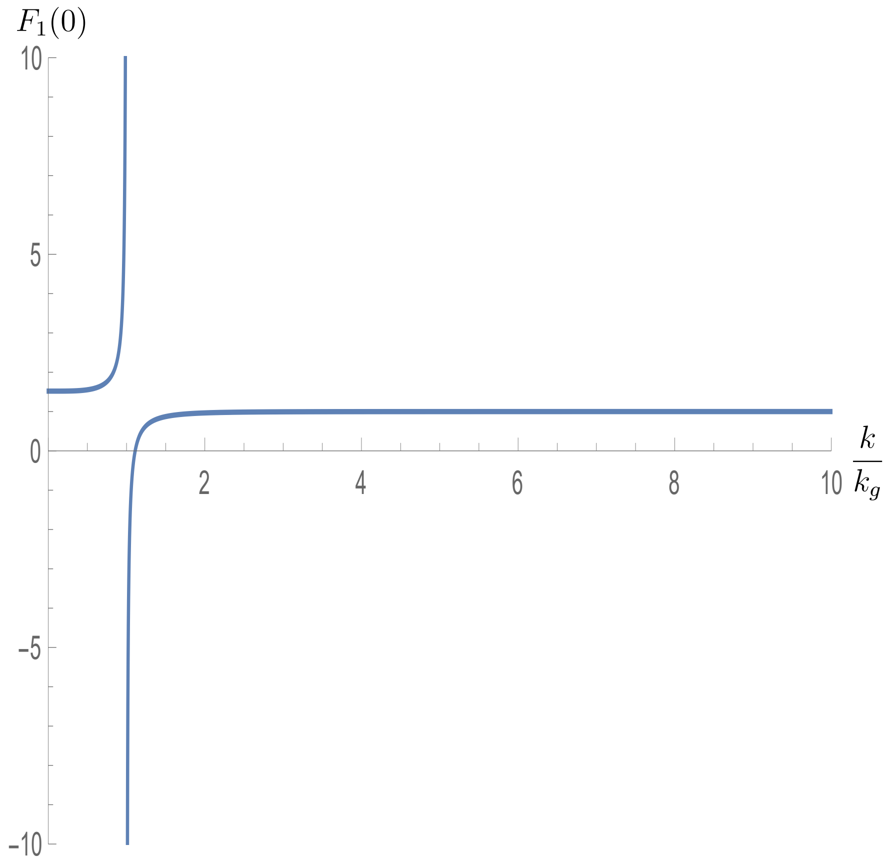

Figure 5.6: Dependence of $F_1(y)$ for $y = 0$ on k/k_g.

The dependence of the function $F_1(y)$ at $y = 0$ on the dimensionless parameter k_g/k is shown in Fig.5.6 for $E_1 = 54.2GPa, E_2 = 18.1GPa$ and $\nu_1 = \nu_2 = 0.25$

Similarly, for term $W_2^{(1)}$ associated with $\sin((k + k_g)x - \omega t)$, we have

$$W_2^{(1)} = F_2(y) \sin\left[(k_g + k)x - \omega t)\right]. \tag{5.62}$$

The equation of motion (5.47) is transformed to

$$\begin{aligned} \frac{d^4 F_2}{dy^4} - \frac{2H\left(k + k_g\right)^2}{D_y}\frac{d^4 F_2}{dy^2} + \frac{\left[D_x(k + k_g)^4 - \varphi^4\omega^2 + \gamma\right]}{D_y} F_2 = \\ \frac{\gamma B_2}{2}\left(e^{-\lambda_1 y} + \alpha_0 e^{-\lambda_2 y}\right), \end{aligned} \tag{5.63}$$

hence, the attenuation orders are

$$m_j^2 = \frac{2H\left(k + k_g\right)^2}{D_y} + (-1)^j \frac{\kappa(k + k_g)^4}{2} \quad \text{and} \quad \kappa = 2\sqrt{\frac{H^2}{D_y^2} - \left(\frac{D_x}{D_y} - \gamma^4\right)}. \tag{5.64}$$

The decaying solution is given by

$$F_2(y) = C_3 e^{-m_1 y} + C_4 e^{-m_2 y} + \alpha_1 e^{-\lambda_1 y} + \alpha_0 \alpha_2 e^{-\lambda_2 y}, \tag{5.65}$$

where

$$C_3 = \frac{\Delta_3}{\Delta}, \qquad C_4 = \frac{\Delta_4}{\Delta}, \tag{5.66}$$

with

$$\Delta = \begin{vmatrix} -D_1(k + k_g)^2 + D_y m_1^2 & -D_1(k + k_g)^2 + D_y m_2^2 \\ & \\ -D_y m_1^3 + (D_1 + 4D_{xy})m_1(k + k_g)^2 & -D_y m_2^3 + (D_1 + 4D_{xy})m_2(k + k_g)^2 \end{vmatrix}. \tag{5.67}$$

The resonant values follow from

$$D_y^2 q^2 + 4D_y D_{xy} q(k_g+k)^2 - D_1^2(k_g+k)^4 = 0. \tag{5.68}$$

$$\Delta = \left(D_y q - (k_g+k)^2(\sqrt{D_1^2+4D_{xy}^2} - 2D_{xy})\right)\left(D_y q + (k_g+k)^2(\sqrt{D_1^2+4D_{xy}^2} + 2D_{xy})\right), \tag{5.69}$$

also

$$\Delta_3 = \alpha_1 B_1 \begin{vmatrix} (\lambda_1^2 - \alpha_0\lambda_2^2)\,D_y + D_1(1+\alpha_0)(k+k_g)^2 & -D_1(k_g+k)^2 + D_y m_1^2 \\ (\lambda_1^3 - \alpha_0\lambda_2^3)\,D_y + (D_1+4D_{xy})((\lambda_1-\alpha_0\lambda_2)(k_g+k)^2 & -D_1(k_g+k)^2 + D_y m_2^2 \end{vmatrix}, \tag{5.70}$$

$$\Delta_4 = \alpha_1 B_1 \begin{vmatrix} (\lambda_1^2 - \alpha_0\lambda_2^2)\,D_y + D_1(1+\alpha_0)(k_g+k)^2 & -D_1(k_g+k)^2 + D_y m_2^2 \\ -D_1(k_g+k)^2 + D_y m_2^2 & (\lambda_1^3 - \alpha_0\lambda_2^3)\,D_y + (D_1+4D_{xy})((\lambda_1-\alpha_0\lambda_2)(k_g+k)^2 \end{vmatrix}. \tag{5.71}$$

Then, after some transformation we have Δ on the following form

$$\Delta = D_y q \chi_0 + \chi_0^2(k_g+k)^2. \tag{5.72}$$

The related resonant value is explicit

$$\frac{k_g}{k} = 1 + \frac{\chi_0}{D_x(1-\gamma^4)}. \tag{5.73}$$

The dependence of the function $F_2(y)$ for $y=0$ on the dimensionless parameter k_g/k is shown in Fig.5.7 for $E_1 = 54.2GPa, E_2 = 18.1GPa$ and $\nu_1 = \nu_2 = 0.25$, with resonant value (5.37) clearly seen.

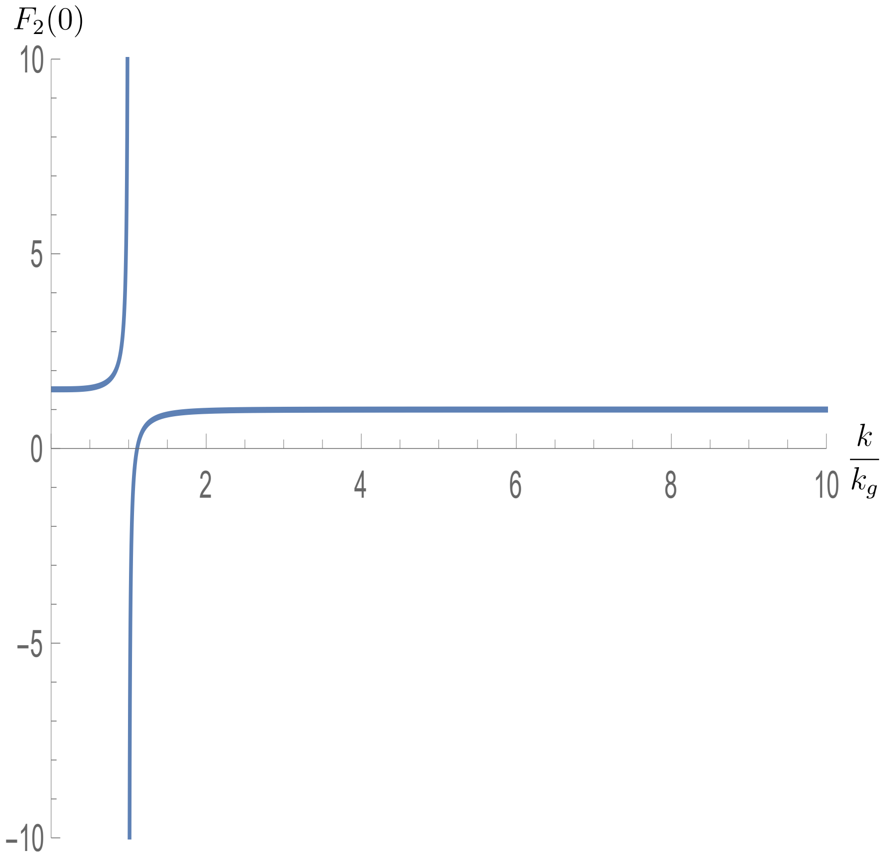

Figure 5.7: Dependence of $F_2(y)$ at $y = 0$ on k/k_g.

Thus, we have investigated the effect of inhomogeneous Winkler-Fuss foundation with periodic stiffness on propagation of bending edge waves on isotropic and orthotropic plates. This study was mostly focussed on the analysis of resonant frequencies, revealing both expected Bragg resonant values, as well as novel non-Bragg resonant frequencies. Further development may include attempts of generalisation of the eigensolution and explicit models for the bending edge wave.

Conclusion

In this thesis, the propagation of the bending edge wave in a semi-infinite orthotropic Kirchhoff plate supported by a Winkler-Fuss foundation is considered. The consideration is carried out for the case of principle directions of orthotropy along the coordinate axis. First, the conventional profile of a sinusoidal shape is investigated, and the dispersion relation is derived. The analysis of the dispersion relation reveals similar features to that of an isotropic plate considered in Kaplunov et al. (2014), including the cutt-off frequencey and the local minimum of the phase velocity, coinciding with the value of the group velocity, corresponding to the critical speed of the moving load. Then, the sinusoidal displacement profile is generalised to that in terms of an arbitrary plane harmonic function.

Then, the derived eigensolution is perturbed in slow-time, leading to a parabolic-elliptic model for the bending edge wave, excited by the bending edge moment and modified shear force, extracting the contribution of the wave to the overall dynamic response, thus generalising the results of Kaplunov et al. (2016). The derived formulation is implemented to a number of dynamic problems, including the impulse edge loading, internal sources the near-resonant regimes of the and moving loads.

In the last Chapter 5 the results of Kaplunov et al. (2014) are extended in a different direction, incorporating the effect of inhomogeneity of the foundation, considering more specifically a periodic modules of subgrade reaction. The classical Bragg resonances are found, as well as novel non-Bragg resonant frequencies.

The possible future developments of the methodology include, in particular, implementation of advanced foundation models, see e.g. Kaplunov and Nobili (2015), as well as refined plate models, see Zakharov (2004). Another possible direction is related to considering more general anisotropy, see e.g. Thompson et al. (2002). Moreover, we note a less trivial extension to interfacial localized waves, curved plates and shells see Zilbergleit and Suslova (1983), edge waves on curved platessee Cherednichenko (2007), and edge waves in thin elastic shell, see e.g. Kaplunov et al. (2000) and Fu and Kaplunov (2012). Another challenge is connected with crack propagation problems, see Nobili et al. (2014) and Nobili et al. (2017).

References

J.D. Achenbach. Wave propagation in elastic solids, 16. North-Holland Publishing Co, 1973.

L.A. Aghalovyan. Asymptotic theory for anisotropic plates and shells. World Scientific Publishing, 376, 2015.

L. A. Aghalovyan and M. L. Aghalovyan. On asymptotic theory of beams, plates and shells. Curved and Layered Structures, 3(1), 2016.

Alexandrov, V.M.: Contact problems on soft and rigid coatings of an elastic half-plane. Mech. Solids 45(1), 34-40, 2010.

S. Althobaiti, J. Kaplunov and D. A. Prikazchikov. An edge moving load on an orthotropic plate resting on a Winkler foundation, X International Conference on Structural Dynamics, Procedia Engineering, 199, 2579-2584, 2017.

S. Althobaiti and D. A. Prikazchikov. Edge bending waves on an orthotropic elastic plate resting on the WinklerFuss foundation, Proceedings of the National Academy of

Sciences of Armenia, Mechanics, 69(1), 16-24, 2016.

S. A.Ambartsumyan and M. V. Belubekyan. On bending waves localized along the edge of a plate. International Applied Mechanics, 30(2), pp. 135-140, 1994.

O. R. Asfar and M. A. Hawwa. Filtering of Rayleigh surface waves by means of periodic corrugations. Modal Analysis, 1(1), 5-14, 1995.

M. Belubekyan, K. Ghazaryan, P. Marzocca and C. Cormier. Localised bending waves in a rib-reinforced elastic orthotropic plate. Journal of Applied Mechanics, 74, 169-171, 2007.

M. Belubekyan, K. Ghazaryan and P. Marzocca. Localised membrane vibration of cylindrical shells. The Journal of the Acoustical Society of America, 141, 3, 1947-1952, 2017.

F.M. Borodich. The Hertz-type and adhesive contact problems for depth-sensing indentation. In Advances in Applied Mechanics, 47, 225-366, 2014.

L. Brillouin, Wave Propagation in Periodic Structures, Dover, New York, 1953.

P. Chadwick. Surface and interfacial waves of arbitrary form in isotropic elastic media, Journal of Elasticity, 6, 73-80, 1976.

J. Chamuel. Flexural edge waves along free and immersed elastic waveguides. In Review of Progress in Quantitative Nondestructive Evaluation, 129-136. Springer, Boston, MA, 1997.

K. Cherednichenko. An asymptotic expansion of the boundary-layer type for flexural waves along the curved edge of a Kirchoff-Love elastic plate, Journal of Mathematical Sciences, 6, 142, 2007.

T.H. Courtney. Mechanical behavior of materials. McGraw-Hill, New York, 1990.

R. V. Craster, L. M. Joseph, and J. Kaplunov. Long-wave asymptotic theories: The connection between functionally graded waveguides and periodic media. Wave Motion, 51(4), 581-588, 2014.

H. Dai, J. Kaplunov, D.A. Prikazchikov. A long-wave model for the surface elastic wave in a coated half-space. Proceedings of the Royal Society of London A: Mathematical, Physical and Engineering Sciences, A 466(2122), 3097-3116, 2010.

M. Destrade and Y. B. Fu. A wave near the edge of a circular disk, The Open Acoustics Journal, 1, 15-18, 2008.

M. Destrade, Y. B. Fu and A. Nobili. Edge wrinkling in elastically supported prestressed incompressible isotropic plates. Proceedings of the Royal Society of London A: Mathematical, Physical and Engineering Sciences, 472(2193), 20160410, 2016.

S.C. Dutta and R. Roy. A critical review on idealization and modeling for interaction among soil-foundation-structure system. Computers and structures. 80(2021), 1579-1594, 2002.

N.Ege, B. Erbas and D. A. Prikazchikov. On the 3D Rayleigh wave field on an elastic half-space subject to tangential surface loads. ZAMM-Journal of Applied Mathematics and

Mechanics/Zeitschrift fur Angewandte Mathematik und Mechanik, 95(12), 15581565, 2015.

I. Elishakoff, J. Kaplunov and E. Nolde. Celebrating the centenary of Timoshenko's study of effects of shear deformation and rotary inertia. Applied Mechanics Reviews, 67(6), 060802, (2015).

B. Erbas, J. Kaplunov and D. A. Prikazchikov. The Rayleigh wave field in mixed problems for a half-plane. IMA Journal of Applied Mathematics, 78, 1078-1086, 2013.

B. Erbas, J. Kaplunov and D. A. Prikazchikov and O. Sahin. The near-resonant regimes of a moving load in a three-dimensional problem for a coated elastic half-space. Mathematics and Mechanics of Solids, 22, 89-100, 2017.

S. A. Epshtein, F. M. Borodich and S. J. Bull.Evaluation of elastic modulus and hardness of highly inhomogeneous materials by nanoindentation. Applied Physics A, 119(1), 325-335, 2015.

D. V. Evans and R.Porter. Flexural waves on a pinned semi-infinite thin elastic plate. Wave Motion, 45(6), 745-757, 2008.

F. Feng, Z. Shen, and J. Shen. Edge waves in a 3D plate: Two solutions based on plate mode matching. Mathematics and Mechanics of Solids, 22(11), 2065-2074, 2017.

L. Filon. On an approximate solution for the bending of a beam of rectangular cross-section under any system of load, with special reference to points of concentrated or discontinuous loading. Philosophical Transactions of the Royal Society of London seies A, 201, 63-155, 1903.

K. O. Friedrichs and R. F. Dressler. A boundary-layer theory for elastic plates. Communications on Pure and Applied Mathematics, 14(1), 1-33, 1961.

F. G. Friedlander. On the total reflection of plane waves. The Quarterly Journal of Mechanics and Applied Mathematics. 1, 376-384, 1948.

L. Fryba. History of Winkler foundation. Vehicle system dynamics, 24(1), 712, 1995.

Y.B. Fu. Existence and uniqueness of edge waves in a generally anisotropic elastic plate.

J. Yu and L. N. Howard. On higher order Bragg resonance of water waves by bottom corrugations. Journal of Fluid Mechanics, 659, 484-504, 2010. Quarterly Journal of Mechanics and Applied Mathematics. 56, 605-616, 2003.

Y.B. Fu and D.W. Brookes. Edge waves in asymmetrically laminated plates. Journal of Mechanics and Physics of Solids, 54, 1-21, 2006.

Y.B. Fu and J. Kaplunov. Analysis of localised edge vibrations of cylindrical shells using the Stroh formalism. Mathematics and Mechanics of Solids, 17, 59-66, 2012.

A. L. Goldenveizer, J. D. Kaplunov, and E. V. Nolde. Asymptotic analysis and improvements of Timoshenko-Reissner-type theories of plates and shells. Mechanics of Solids, 25, 126-139, 1990.

A. L. Goldenveizer, J. D. Kaplunov, and E. V. Nolde. On Timoshenko-Reissner type theories of plates and shells. International Journal of Solids and Structures, 30(5): 675-694, 1993.

K. Graff. Wave motion in elastic solids, Dover edition. New York: Dover Publications Inc., 1991.

D. Gridin, R. V. Craster, and A. T. I. Adamou. Correction for Gridin et al., Trapped modes in curved elastic plates. Proceedings of the Royal Society of London A: Mathematical, Physical and Engineering Sciences, 461(2064), 4057-4061, 2005.

L.G. Gulgazaryan G.R. Gulgazaryan and D. L. Srapionyan. Localized vibrations of a thin-walled structure consisted of orthotropic elastic non-closed cylindrical shells with free and rigid-clamped edge generators. Journal of Applied Mathematics and Mechanics, 2012.

R. Gunda, S. M. Vijayakar, R. Singh and J. E. Farstad. Harmonic Greens functions of a semi-infinite plate with clamped or free edges. The Journal of the Acoustical Society of America, 103(2), 888-899, (1998).

M. A.Hawwa and O. R. Asfar. Mechanical-wave filtering in a periodically corrugated elastic plate. Journal of Vibration and Acoustics, 118(1), 16-20, 2008.

M. Hetenyi. Beams on Elastic Foundation. The University of Michigan Press, Ann Arbor, 1946.

H.Hunt. Types of rail roughness and the selection of vibration isolation measures. In

Noise and Vibration Mitigation for Rail Transportation Systems. 99, 341-347 , 2008.

A.Y. Ishlinskii. On a limiting process in the theory of the stability of elastic rectangular plates. Doklady Akademii Nauk SSSR 95(3), 477-479, 1954.

J. Jedrysiak. The length-scale effect in the buckling of thin periodic plates resting on a periodic Winkler foundation. Meccanica, 38(4), 435-4, 2003.

R.M. Jones. Mechanics of composite materials. Philadelphia, Taylor and Francis, 519, 1999.

J. D. Kaplunov. Long-wave vibrations of a thin-walled body with fixed faces. The Quarterly Journal of Mechanics and Applied Mathematics, 48(3), 311-327, 1995.

J. D. Kaplunov and D. G. Markushevich. Plane vibrations and radiation of an elastic layer lying on a liquid half-space. Wave Motion, 17(3), 199 -211, 1993.

J. Kaplunov and A. Nobili. The edge waves on a Kirchhoff plate bilaterally supported by a two-parameter elastic foundation, Journal of Vibration and Control, 23(12), 2014-2022, 2015.

J. D. Kaplunov and E. V. Nolde. Long-wave vibrations of a nearly incompress- ible isotropic plate with fixed faces. The Quarterly Journal of Mechanics and Applied Mathematics, 55(3), 345-356, 2002.

J. D. Kaplunov, E. V. Nolde, and G. A. Rogerson. A low-frequency model for dy- namic motion in pre-stressed incompressible elastic structures. Proceedings of the Royal Society of London A: Mathematical, Physical and Engineering Sciences, 456, 2589-2610, 2000.

J. D. Kaplunov, E. V. Nolde, and G. A. Rogerson. Short wave motion in a pre- stressed incompressible elastic plate. IMA Journal of Applied Mathematics, 67(4):383, 2002.

J. Kaplunov, E.V. Nolde and D. A. Prikazchikov. A revisit to the moving load problem using an asymptotic model for the Rayleigh wave. Wave Motion, 47, 440-451, 2010.

J. Kaplunov and D. A. Prikazchikov. Explicit models for surface, interfacial and edge waves, Dynamic Localization Phenomena in Elasticity, Acoustics and Electromagnetism, Springer-Verlag, 547, 73-114, 2013.

J. Kaplunov and D. A. Prikazchikov. Asymptotic theory for Rayleigh and Rayleigh-type waves. In Advances in applied mechanics, 50, 1-106, 2017.

J. Kaplunov, D.A. Prikazchikov, and G.A. Rogerson. Edge vibration of a prestressed semi-infinite strip with traction-free edge and mixed face boundary conditions. Zeitschrift fur Angewandte Mathematik und Physik (ZAMP), 55(4), 701-719, 2004.

J. Kaplunov, D. A. Prikazchikov and G. Rogerson. On three-dimensional edge waves in semi-infinite isotropic plates subject to mixed face boundary conditions. The Journal of the Acoustical Society of America, 118(5), 2975-2983, 2005.

J. Kaplunov, D. A. Prikazchikov and G. Rogerson. Edge bending wave on a thin elastic plate resting on a Winkler foundation. Proceedings of the Royal Society of London A:

Mathematical, Physical and Engineering Sciences, 472(2190), 20160178, 2016.

J. Kaplunov, D. A. Prikazchikov, G. Rogerson and M. Lashab, The edge wave on an elastically supported Kirchhoff plate. Journal of the Acoustical Society of America, 136, 1487-1490, 2014.

J. Kaplunov, D. A. Prikazchikov and L. A. Prikazchikova. Dispersion of elastic waves in a strongly inhomogeneous three-layered plate. International Journal of Solids and Structures, 113, 169-179, 2017.

J. Kaplunov, D. A. Prikazchikov and L. Sultanova. Justification and refinement of Winkler-Fuss hypothesis. Zeitschrift fur Angewandte Mathematik und Physik, 69(3), 80, 2018.

J. Kaplunov, D. A. Prikazchikov, B. Erbas and O. Sahin. On a 3D moving load problem for an elastic half space. Wave motion, 50(8), 1229-1238, 2013.

J. D. Kaplunov, L. Yu. Kossovitch, and E. V. Nolde. Dynamics of thin walled elastic bodies. Academic Press, 1998.

J. D. Kaplunov, L. Yu. Kossovitch, and E. V. Nolde. Free localised vibratio ns of a semi-innite cylindrical shell. Journal of Acoustical Society of America, 107, 1383-1393, 2000.

J. D. Kaplunov, L. Yu. Kossovich, and G. A. Rogerson. Direct asymptotic integration of the equations of transversely isotropic elasticity for a plate near cut-off frequencies. The Quarterly Journal of Mechanics and Applied Mathematics, 53(2), 323-341, 2000.

J. Kaplunov and M. Wilde. Edge and interfacial vibrations in elastic shells of revolution. Zeitschrift fr angewandte Mathematik und Physik ZAMP. 51(4), 530-549, 2000.

J. D. Kaplunov, G. A. Rogerson, and P. E. Tovstik. Localized vibration in elastic structures with slowly varying thickness. The Quarterly Journal of Mechanics and Applied Mathematics, 58(4), 645-664, 2005.

J. Kaplunov, A. Zakharov and D. A. Prikazchikov. Explicit models for elastic and piezoelastic surface waves. IMA Journal of Applied Mathematics, 71, 768-782, 2006.

A.D. Kerr. Elastic and viscoelastic foundation models. Kerr, A.D., 1964. Elastic and viscoelastic foundation models. Journal of Applied Mechanics, 31(3), 491-498, 1964.

L.A. Khajiyeva, D. A. Prikazchikov and L.A. Prikazchikova. Hyperbolic-elliptic model for surface wave in a pre-stressed incompressible elastic half-space. Mechanics Research Communications, 92, 49-53, 2018.

R. Kienzler. On consistent plate theories. Archive of Applied Mechanics, 72(4-5), 229-247, 2002.

G. Kirchhoff. Uber das gleichewicht und die bewegung einer elastischen scheibe. Journal Furdie Reine und Angewandte Mathematik Crelle's Journal, 40-51, 1850.

A. P. Kiselev and D. F. Parker. Omni-directional Rayleigh, Stoneley and Schlte waves with general time dependence. Proceedings of the Royal Society A: Mathematical, Physical and Engineering Sciences, 466(2120), 2241-2258, 2010.

A. P. Kiselev and G. A. Rogerson. Laterally dependent surface waves in an elastic medium with a general depth dependence. Wave Motion, 46(8), 539-547, 2009.

Yu. K. Konenkov. A Rayleigh-type flexural wave, Soviet Physics-Acoustics, 6, 122-123, 1960.

L. Yu. Kossovich. Non-stationary problems in theory of thin elastic shells, 1986.

E. Kossovich. PhD thesis, Brunel University, UK, 2011.

A.A. Kryshynska. Flexural edge waves in semi-infinite elastic plates. Journal of Sound and Vibration, 330, 1964-1976, 2011.

V.I. Kuznetsov. Elastic Foundation, Elastic Foundations. Gosstroiizdat, Moscow, 1952.

J. B. Lawrie and J. D. Kaplunov, Edge waves and resonance on elastic structures: An overview, Journal of Mathematics and Mechanics of Solids, 17, 4-16, 2011.

P. Liu, Y. W. Zhang and H. J. Gao, Interior and edge elastic waves in graphene. J. Appl. Mech. 80 (4), 040901, 2013.

Lu. P. Chen, H.B. Lee, and C. Lu, Further studies on edge waves in anisotropic elastic plates. International Journal of Solids and Structures, 44, 2192-2208, 2007.

D.S. Liyanapathirana and H.G. Poulo. Pseudostatic approach for seismic analysis of piles in liquefying soil. Journal of Geotechnical and Geoenvironmental Engineering. 131(12), 1480-1487, 2005.

M. Lutianov and G. A. Rogerson. Long wave motion in layered elastic media. International Journal of Engineering Science, 48(12), 1856-1871, 2010.

R.M. Martynyak, I.A. Prokopyshyn and I.I. Prokopyshyn. Contact of elastic bodies with nonlinear Winkler surface layers. Journal of Mathematical Sciences. 205(4), 535-553, 2015.

J. McCoy and R.D. Mindlin. Extensional waves along the edge of an elastic plate. Journal of Applied Mechanics, 30(1):7578, 1963.

A. Milanese, P. Marzocca, M. Belubekyan and K. Ghazaryan. Effect of the stiffness and inertia of a rib reinforcement on localized bending waves in semi-infinite strips. International Journal of Solids and Structures, 46(10), 2126-2135, 2009.

R. D. Mindlin. An introduction to the mathematical theory of vibrations of elastic plates. Fort Monmouth, New Jersey: U.S. Army Signal Corps Eng. Lab. A monograph. (1955).

M. Morvaridi, G.Carta and M. Brun. Platonic crystal with low-frequency locally-resonant spiral structures: wave trapping, transmission amplification, shielding and edge waves. Journal of the Mechanics and Physics of Solids, 121, 496-516, 2018.

B.G. Muravskii. Mechanics of Non-Homogeneous and Anisotropic Foundations. Springer-Verlag, Berlin, 2012.

A. H.Nayfeh and M. A. Hawwa. Interaction of surface gravity waves on a nonuniformly periodic seabed. Physics of Fluids, 6(1), 209-213, 1994.

S. Nikolaou, G. Mylonakis, G. Gazetas and T. Tazoh. Kinematic pile bending during earthquakes: analysis and field measurements. Geotechnique. 51(5), 425-440, 2001.

A. Nobili, E. Radi and L. Lanzoni. A cracked infinite Kirchhoff plate supported by a two-parameter elastic foundation. Journal of the European Ceramic Society, 34(11), 2737-2744, 2014.

A. Nobili, E. Radi and L. Lanzoni. Flexural edge waves generated by steady-state propagation of a loaded rectilinear crack in an elastically supported thin plate. Proceedings of the Royal Society A: Mathematical, Physical and Engineering Sciences, 473(2204), 20170265, 2017.

A. Nobili and D.A. Prikazchikov. Explicit formulation for the Rayleigh wave field induced by surface stresses in an orthorhombic half-plane. European Journal of Mechanics-A/Solids, 70, 86-94, 2018.

E. V. Nolde, L. A. Prikazchikova and G. A. Rogerson. Dispersion of small amplitude waves in a pre-stressed, compressible elastic plate. Journal of Elasticity, 75(1), 1-29, 2004.

A.N.Norris. Flexural edge waves. Journal of Sound and Vibration. 171, 571-573, 1994.

A.N.Norris and I.D. Abrahams. On the existence of flexural edge waves on submerged elastic plates. Proceedings of the Royal Society of London. Series A: Mathematical, Physical and Engineering Sciences, 456, 1559-1582, 2000.

A.N. Norris, V.V. Krylov and I.D. Abrahams. Flexural edge waves and comments on A new bending wave solution for the classical plate equation, Journal of the Acoustical Society of America, 107(3), 1781-1784, 2000.

J. Oliver, F. Press and M. Ewing. Two-dimensional model seismology. Geophysics, 19(2), 202-219, 1954.

V. Pagneux. Complex resonance and localized vibrations at the edge of a semiinfinite elastic cylinder. Mathematics and Mechanics of Solids, 17(1), 17-26, 2011.

R. K. Pal and M. Ruzzene. Edge waves in plates with resonators: an elastic analogue of the quantum valley Hall effect. New Journal of Physics, 19(2), 025001, 2017.

D. Parker and A. Kiselev. Rayleigh waves having generalised lateral dependence. The Quarterly Journal of Mechanics and Applied Mathematics, 62, 19-30, 2009.

D. Parker. The Stroh formalism for elastic surface waves of general profile. Proc. R. Soc. A, 469(2160), 20130301, 2013.

P.L. Pasternak. On a New Method of Analysis of an Elastic Foundation by Means of Two Foundation Constants (in Russian). Gosudarstvennoe Izdatelstvo Literaturi po Stroitelstvu i Arkhitekture, Moscow, 1954.

A. V. Pichugin and G. A. Rogerson. A two-dimensional model for extensional motion of a pre-stressed incompressible elastic layer near cut-off frequencies. IMA Journal of Applied Mathematics, 66(4), 357, 2001.

A. V. Pichugin and G. A. Rogerson. Anti-symmetric motion of a pre-stressed in- compressible elastic layer near shear resonance. Journal of Engineering Mathematics, 42(2), 181-202, 2002.

A. V. Pichugin and G. A. Rogerson. Extensional edge waves in pre-stressedincompressible plates. Mathematics and Mechanics of Solids, 17(1), 27-42, 2012.

G.T.Piliposian, M.V. Belubekyan, and K.B. Ghazaryan. Localized bending waves in a transversely isotropic plate. Journal of Sound and Vibration, 329, 3596-3605, 2010.

D.A. Prikazchikov. Rayleigh waves of arbitrary profile in anisotropic media. Mechanics Research Communications, 50, 83-86, 2013.

A.P. Prudnikov, Y.A. Brichkov and O.I. Marichev. Integrals and series. Gordon and Breach, New-York, 1986.

L. Rayleigh, On waves propagated along the plane surface of an elastic solid, Proceedings of the London Mathematical Society, 17 (253), 4-11, 1885.

J.N. Reddy. Theory and analysis of elastic plates and shells, CRC press, 2006.

E.Reissner. On the derivation of the theory of thin elastic shells. Journal of Mathematics and Physics, 43, pp. 263-277, 1964.

G. A. Rogerson, I. V. Kirillova, and Ya. A. Parfenova. Boundary Layers Near the Reflected and Transmitted Dilatational Wave Fronts in a Composite Cylindrical Shell, In Theories of Plates and Shells. Springer Berlin Heidelberg, Berlin, Heidelberg, 193-200, 2004.

G. A. Rogerson and L. A. Prikazchikova. Generalisations of long wave theories for pre-stressed compressible elastic plates. International Journal of Non-Linear Mechanics, 44(5), 520-529, 2009.

I.Roitberg, D. Vassiliev and T. Weidl. Edge resonance in an elastic semi-strip. Quarterly Journal of Mechanics and Applied Mathematics 51(1), 1-13, 1998.

M. Yu. Ryazantseva and F. K. Antonov. Harmonic running waves in sandwich plates. International Journal of Engineering Science, 59, 184-192, 2012.

A. Selvadurai. Elastic Analysis of Soil-Foundation Interaction. Developments in Geotechnical Engineering, 17, Elsevier, 1979.

E. A. G. Shaw, On the resonant vibrations of thick barium titanate disks. Journal of the Acoustical Society of America, 28, 38-50, 1956.

A.K. Singh, A. Lakshman and A. Chattopadhyay. The plane waves at the edge of a uniformly pre-stressed ber-reinforced plate, Journal of vibration and control, 22(10), 2530-2541, 2014.

B. K. Sinha, Some remarks on propagation characteristics of ridge for acoustic waves at low frequencies, Journal of the Acoustical Society of America, 56, 16-18, 1974.

R. Sinclair and R.W.B. Stephens. Velocity dispersion of waves propagating along the edge of a plate. Acustica, 24(3), 160-165, 1971.

S. Timoshenko and S. Woinowsky-Krieger. Theory of plates and shells. A McGraw-Hill Classic Textbook Reissue. McGraw-Hill Book Company, 1987.

S. Timoshenko. Method of analysis of statistical and dynamical stresses in rail. In Proceedings of second international congress for applied mechanics, Zurich, 12-17, 1926.

S. Timoshenko. Vibration problems in engineering. New York: D. Van Nostrand Company, Inc. (1938).

E.C. Titchmarch. The theory of functions. 2nd Ed., Oxford University Press, Oxford, UK, 1939.

P. J Torvik,. Refection of wave trains in semi-infinite plate. Journal of the Acoustical Society of America. 41, 346-353, 1967.

I. Thompson and I.D. Abrahams. Diffraction of flexural waves by cracks in orthotropic thin elastic plates. I Formal solution. Proceedings of the Royal Society of London, A, 461, 3413-3436, 2005.

I. Thompson, I.D. Abrahams and A.N. Norris. On the existence of flexural edge waves on this orthotropic plates. Journal of the Acoustical Society of America, 112, 1756-1765, 2002.

R. N. Thurston and J. McKenna. Flexural acoustic waves along the edge of a plate, IEEE Transactions on Sonics and Ultrasonics, 21, 296-297, 1974.

V.Z. Vlasov and U.N. Leontiev. Technical Theory of Analysis of Foundations on an Elastic Base. MISI Sbornik Trudov, 14, 1966.

Y. H. Wang, L. G. Tham and Y. K. Cheung. Beams and plates on elastic foundations: a review. Progress in Structural Engineering and Materials, 7(4), 174-182, 2005.

E. Winkler, Die Lehre von der Elasticitaet und Festigkeit mit besondere Ruecksicht auf ihre Anwendung in der Technik, fuer polytechnische Schuhlen, Bauakademien, Ingenieure, Maschienenbauer, Architecten, etc., H. Dominicus, Prague, 1867.

L. Yang, K. Yu, Y. Wu, R. Zhao and S. Liu. Topological spin-Hall edge states of flexural wave in perforated metamaterial plates. Journal of Physics D: Applied Physics, 51(32), 325302, 2017.

C.S. Yim and A.K. Chopra. Earthquake response of structures with partial uplift on Winkler foundation. Earthquake engineering and structural dynamics. 12(2), 263-281, 1984.

D.D. Zakharov. Konenkov's waves in anisotropic layered plates. Acoustical Physics, 48, 171-175, 2002.

D.D. Zakharov. Analysis of the acoustical edge bending mode in a plate using refined asymptotics. Journal of Acoustical Society of America, 116 (4), 872-878, 2004.

D.D. Zakharov and W. Becker. Rayleigh type bending waves in anisotropic media. Journal of Sound and Vibration, 261, 805-818, 2003.

V.Zernov, and J. Kaplunov, Three dimensional edge-waves in plates. Proceedings of the Royal Society A: Mathematical, Physical and Engineering Sciences, 301-318, 2008.

A.S. Zilbergleit and A.B. Suslova. Contact flexural waves in thin plates. Soviet Physics -Acoustics, 29, 108-111, 1983.